



Calcium phosphate nanoparticles as carriers of nucleic acids

Dissertation

Zur Erlangung des akademischen Grades

eines

Doktors der Naturwissenschaften

– Dr. rer. nat. –

vorgelegt von

Anna Kovtun

aus Kharkiv / Ukraine

Institut für Anorganische Chemie

der

Universität Duisburg-Essen

Essen 2009

Dedicated to my parents and my wonderful friend Olga

Die vorliegende Arbeit wurde im Zeitraum von April 2006 bis September 2009 am Institut für Anorganische Chemie, Arbeitskreis Prof. Dr. Matthias Epple, der Universität Duisburg-Essen durchgeführt.

- | | |
|---------------|---------------------------|
| 1. Gutachter: | Prof. Dr. M. Epple |
| 2. Gutachter: | Prof. Dr. C. Schmuck |
| 3. Gutachter: | Prof. Dr. W. E. G. Müller |
| Vorsitzender: | Prof. Dr. B. Siebers |

Tag der mündlichen Prüfung: 26.05.2010

List of contents

| | |
|--|----|
| 1 Introduction | 8 |
| 2 Theoretical background | 10 |
| 2.1 Nucleic acids | 10 |
| 2.1.1 Chemical structure of desoxyribonucleic acid (DNA) | 10 |
| 2.1.2 Chemical structure of ribonucleic acid (RNA) | 11 |
| 2.1.3 Biological role of nucleic acids..... | 13 |
| 2.2 Mechanism of RNA interference | 13 |
| 2.3 Oligonucleotides for the maturation of dendritic cells | 16 |
| 2.4 Transfection..... | 17 |
| 2.5 Calcium phosphate nanoparticles as carriers of nucleic acids..... | 19 |
| 2.6 Colloid stability and DLVO theory..... | 22 |
| 3 Materials and Methods | 24 |
| 3.1 Applied materials for cell culture experiments | 24 |
| 3.1.1 Cell culture solutions/antibiotics..... | 24 |
| 3.1.2 Chemicals..... | 24 |
| 3.1.3 Instruments..... | 24 |
| 3.1.4 Applied consumables und kits | 25 |
| 3.2 Molecular-biological methods | 25 |
| 3.2.1 Preparation of plasmid DNA from bacterial culture..... | 25 |
| 3.3 Cell culture methods and experimental procedures | 26 |
| 3.3.1 Cultivation of secondary cell lines..... | 27 |
| 3.3.2 Cryoconservation of cells | 27 |
| 3.3.3 Defrosting of cells..... | 28 |
| 3.3.4 Fluorescence microscopy..... | 28 |
| 3.3.5 Preparation of calcium phosphate nanoparticles substituted with Al ³⁺ and Mg ²⁺ | 28 |

| | |
|--|----|
| 3.3.6 Cell transfection | 29 |
| 3.3.7 Calculation of transfection efficiency of magnesium- or aluminum-substituted calcium phosphate nanoparticles | 31 |
| 3.3.8 Ca-imaging using Fura-2AM..... | 32 |
| 3.3.9 Staining of cells with propidium iodide..... | 32 |
| 3.3.10 Toxicity tests | 33 |
| 3.3.11 Experiments with radioactive ^{45}Ca | 33 |
| 3.3.12 Preparation of cell lysates | 36 |
| 3.3.13 Determination of the protein concentration | 36 |
| 3.3.14 Preparation of metal surfaces coated with calcium phosphate/PEI/DNA-nanoparticles..... | 37 |
| 3.3.15 Transfection from metal surfaces..... | 37 |
| 3.3.16 Cell fixation..... | 39 |
| 3.3.17 Flow cytometry of NIH3T3 cells..... | 39 |
| 3.3.18 Preparation of multi-shell calcium phosphate nanoparticles functionalized with siRNA..... | 40 |
| 3.3.19 Preparation of calcium phosphate nanoparticles functionalized with CpG and Poly(I:C) | 40 |
| 3.3.20 Preparation of calcium phosphate nanoparticles functionalized with shRNA..... | 41 |
| 3.4 Physicochemical methods | 42 |
| 3.4.1 Dynamic light scattering | 42 |
| 3.4.2 Zeta potential measurements..... | 42 |
| 3.4.3 Scanning electron microscopy (SEM) | 43 |
| 3.4.4 Transmission electron microscopy (TEM) | 44 |
| 4 Results and Discussion | 45 |
| 4.1 Calcium phosphate nanoparticles substituted with Al^{3+} and Mg^{2+} | 45 |
| 4.1.1 Synthesis and characterization of calcium phosphate substituted with Al^{3+} and Mg^{2+} | 45 |

| | |
|--|-----|
| 4.1.2 Transfection with calcium phosphate nanoparticles substituted with Al ³⁺ and Mg ²⁺ | 55 |
| 4.1.3 Conclusion | 57 |
| 4.2 Tracking of the intracellular calcium level during the transfection of cells | 59 |
| 4.2.1 Marking of nanoparticles with ⁴⁵ Ca ²⁺ | 59 |
| 4.2.2 Monitoring of the internal calcium level using the calcium-sensitive dye Fura-2 | 70 |
| 4.2.3 Conclusion | 80 |
| 4.3 Calcium phosphate nanoparticles functionalized with siRNA against EGFP | 81 |
| 4.3.1 Synthesis and characterization of siRNA-functionalized calcium phosphate nanoparticles | 81 |
| 4.3.2 Gene silencing on HeLa-EGFP cells by siRNA-functionalized calcium phosphate nanoparticles | 83 |
| 4.3.3 Conclusion | 89 |
| 4.4 Calcium phosphate nanoparticles functionalized with shRNAs | 90 |
| 4.4.1 Synthesis and characterization of the nanoparticles functionalized with shRNAs | 90 |
| 4.4.2 Gene silencing using calcium phosphate nanoparticles functionalized with shRNAs | 93 |
| 4.4.3 Conclusion | 99 |
| 4.5 Functionalization of nanoparticles with oligonucleotides for the activation of dendritic cells | 100 |
| 4.5.1 Synthesis and characterization of the nanoparticles functionalized with Poly(I:C) and CpG | 100 |
| 4.5.2 Activation of dendritic cells using nanoparticles functionalized with Poly(I:C) and CpG | 102 |
| 4.5.3 Conclusion | 105 |
| 4.6 Surface-mediated transfection with DNA-functionalized calcium phosphate nanoparticles | 106 |

| | |
|---|-----|
| 4.6.1 Preparation of electrophoretically coated titanium substrates | 106 |
| 4.6.2 Surface-mediated transfection of cells..... | 108 |
| 4.6.3 Conclusion | 119 |
| 5 Summary..... | 120 |
| 6 Literature | 122 |
| 7 Appendix | 133 |
| 7.1 List of abbreviations..... | 133 |
| 7.2 Publications | 135 |
| 7.2.1 Regular papers in refereed journals | 135 |
| 7.2.2 Other publications | 136 |
| 7.3 Presentations and posters | 138 |
| 7.4 Patents | 144 |
| 7.5 Awards | 145 |
| 7.6 Curriculum vitae..... | 146 |
| Acknowledgments | 147 |

1 Introduction

For many centuries people were trying to understand the basic mechanisms of nature and to use them for curing of diseases. Nowadays nanotechnology is one of the modern and promising areas for solving a huge variety of problems in healthcare and in medicine as well as in technology. Nanotechnology works with objects of size up to 1 μm , thus manipulating on a dimension much smaller than living cells. It is already widely used in medicine and molecular biology, *e.g.* in diagnostics, drug delivery, cell sorting, production of stable cell lines and transgenic animals.

One of the most advantageous areas is the application of nanoparticles as carriers of drugs and nucleic acids into cells thus acquiring new cell properties: synthesis of a failing or a completely new protein, inhibition of gene expression, breaking of the immune tolerance against viral or bacterial antigens. However, although this seems quite easy, scientists still face many challenges. Some carriers are very effective but immunogenic and cancerogenic, others are not so toxic but show very low efficiency. So it is always a problem of choice, of finding an optimal balance between drawbacks and advantages.

We were interested in the synthesis and application of non-toxic and potentially very effective nanoparticles. Thus, we chose calcium phosphate as a core material for our gene delivery system. In this study we produced calcium phosphate nanoparticles functionalized with nucleic acids (DNA and RNA) and tested them on cell cultures. The first chapter deals with the synthesis of nanoparticles with different additives and under different conditions in order to achieve smaller nanoparticles able to bind DNA.

However, the toxicity needed further investigation. As it is well known, the intracellular calcium level is quite low and its increase can disturb many processes, *e.g.* muscle contraction or intracellular signaling pathways, thus causing cell death. So we explicitly studied the changes of the intracellular

calcium level via application of $^{45}\text{Ca}^{2+}$ and the marker of ionic calcium Fura-2. We also analyzed the vitality of the cells transfected by different methods.

The next step was to protect the DNA against intracellular cleavage by nucleases; therefore we synthesized multi-shell nanoparticles and functionalized them with oligonucleotides to achieve an effective gene silencing. By using oligonucleotides, we could also stimulate immune cells and break the tolerance against previously undetectable antigens.

Our next step was to localize the application of nanoparticles. Therefore we coated metal surfaces by electrophoresis, achieving not systemic but local transfection. This could possibly be used for bone defects healing, stimulating bone growth by covering the implants.

2 Theoretical background

2.1 Nucleic acids

Nucleic acids are organic macromolecules maintaining the storage and transfer of hereditary information in living cells and viruses. The nucleic acids can be divided into two main groups depending on the type of the sugar: desoxyribonucleic acids (DNA) and ribonucleic acids (RNA).

DNA contains information about the aminoacidic sequences of the proteins in all living cells and most viruses and thereby serves for long-term information storage.

RNA works as a transfer molecule, delivering the information from the nuclear DNA to the place of protein synthesis, or delivering single amino acids to the ribosomes providing the short-term information storage.

2.1.1 Chemical structure of desoxyribonucleic acid (DNA)

DNA is a polymeric biomolecule consisting of monomers called nucleotides. Each nucleotide consists of a pentose (desoxyribose), a phosphoric acid residue and a nucleic base. The DNA molecule forms a double helix.^[1-3] In such a helix, the sugar and the nucleic bases are turned inward.^[4] The bases hold the chains together due to the formation of two or three hydrogen bonds, depending on the type of the base.

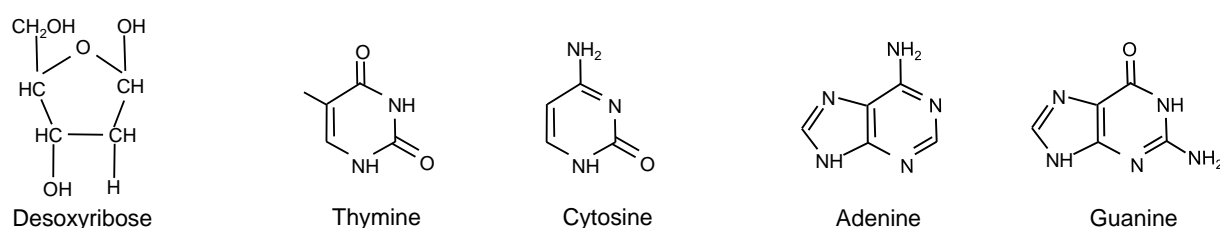


Figure 2.1.1.1: Sugar and nucleic bases in DNA.

The nucleic bases are paired not randomly, but in a predefined order. There are two types of bases: purines (adenine and guanine) and pyrimidines (thymine and cytosine) as shown in Figure 2.1.1.1.^[5-7] According to Chargaff's rules, in DNA thymine always binds to adenine, guanine to cytosine and *vice versa*. The bases are paired due to the hydrogen bonds to form Watson-Crick base pairs.^[1]

Monomers of the nucleic acid are used in the cell not only as a structural unit of DNA, but also in some cofactors and as a signaling or as an energy-efficient molecule.^[8,9]

Due to a great amount of information contained in DNA, it is a very large molecule; therefore it must be packed inside the cell. In living organisms DNA is present mostly in two forms: As a circular molecule in prokaryotic cells and as chromosomes in eukaryotes. Because the interest of this work is human gene therapy, we will focus on the structure of the eukaryotic DNA.

First, the chains of DNA form a double helix. Then this helix is wrapped around special packaging proteins (histones), moulding a simple circular unit called nucleosome.^[3] The nucleosome beads form compact fibrils with a diameter of about 100 Å. These fibrils form a helix where one turn comprises about 3-6 nucleosomes. Afterwards this complex helix is organized in loop-structures of thick fibrils. The ends of the loops are fixed on a chromosome backbone. The following condensation can proceed due to the spiralization of loops and backbone structures, and the diameter of the final chromosome is about 2 µm.

2.1.2 Chemical structure of ribonucleic acid (RNA)

The RNA nucleotides have structural differences comparing to DNA. Here ribose replaces deoxyribose as sugar and uracil replaces thymine.^[10] RNA is transcribed on the DNA matrix by enzymes and must be further processed. RNA serves as the template for translation of the genetic information into the proteins and transferring the single amino acids to the ribosome to form proteins.

RNA consists of four different bases: Adenine, guanine, cytosine, and uracil. The first three are the same as those of DNA, but uracil replaces thymine.^[11]

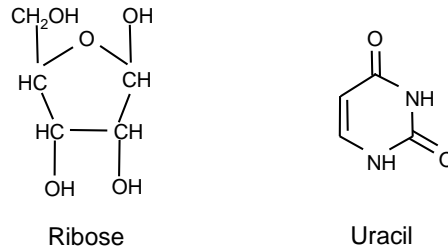


Figure 2.1.2.1: Chemical structure of ribose and uracil.

RNA usually is a single-stranded molecule and has a short nucleotide chain. Double-stranded RNA molecules were found only in viruses. There are several different types of RNA: mRNA, tRNA, rRNA.^[10]

Messenger RNA (mRNA) carries information from DNA to the ribosome where protein synthesis occurs. mRNA is transcribed from DNA, proceeded and transferred from the nucleus into the cytoplasm, where it bounds to the ribosomes.

Transfer RNA (tRNA) is a small RNA containing about 74-93 nucleotides that transports a specific amino acid to a place of protein synthesis. It has binding sites for amino acids on one side and an anticodon region that binds to a specific sequence on the mRNA chain on the other side.

Ribosomal RNA (rRNA) is a structural component of the ribosomes.

The other types of RNA are so-called non-coding RNA or "RNA genes" (sometimes referred to as small RNA) which encode RNA that is not translated into the proteins. These are siRNAs (small interfering RNA), miRNAs (microRNA) and shRNAs (short hairpin RNA). In the eukaryotes they also act as triggers to initiate the process of RNA interference and to regulate gene expression.^[12-15]

2.1.3 Biological role of nucleic acids

The central dogma of molecular biology^[12,16] postulates that all genetic information is realized in the same definite way:



All inherited and individual information about the organism is stored in the genome. In eukaryotic cells the genome is present mainly in the nucleus. All processes of transcription and replication occur under the close regulation of enzymes and packaging proteins.

The sequences of nucleic bases in DNA encode the sequences of amino acids in proteins. In such a way DNA encodes all the mechanisms of development of every organism. Each amino acid is coded by three nucleotides forming triplet codons. There are $4^3=64$ possible combinations of the nucleotides. The genetic code is redundant, *i.e.* each amino acid is encoded by more than one codon. This characteristic of the genetic code makes it more stable to the changes induced by point mutations of DNA.

2.2 Mechanism of RNA interference

The mechanism of RNA interference (or RNA silencing) was first described by Fire and Mello in the late 1990s.^[17] They found that the interaction between mRNAs and specific double-stranded RNAs can lead to the cleavage of the initial mRNA. So, RNA interference (RNAi) is a process of sequence-specific post-transcriptional gene silencing initiated by double-stranded siRNA (so-called small interfering RNA). In many organisms the RNA silencing mechanism is a part of the immune response against RNA-containing viruses.^[18]

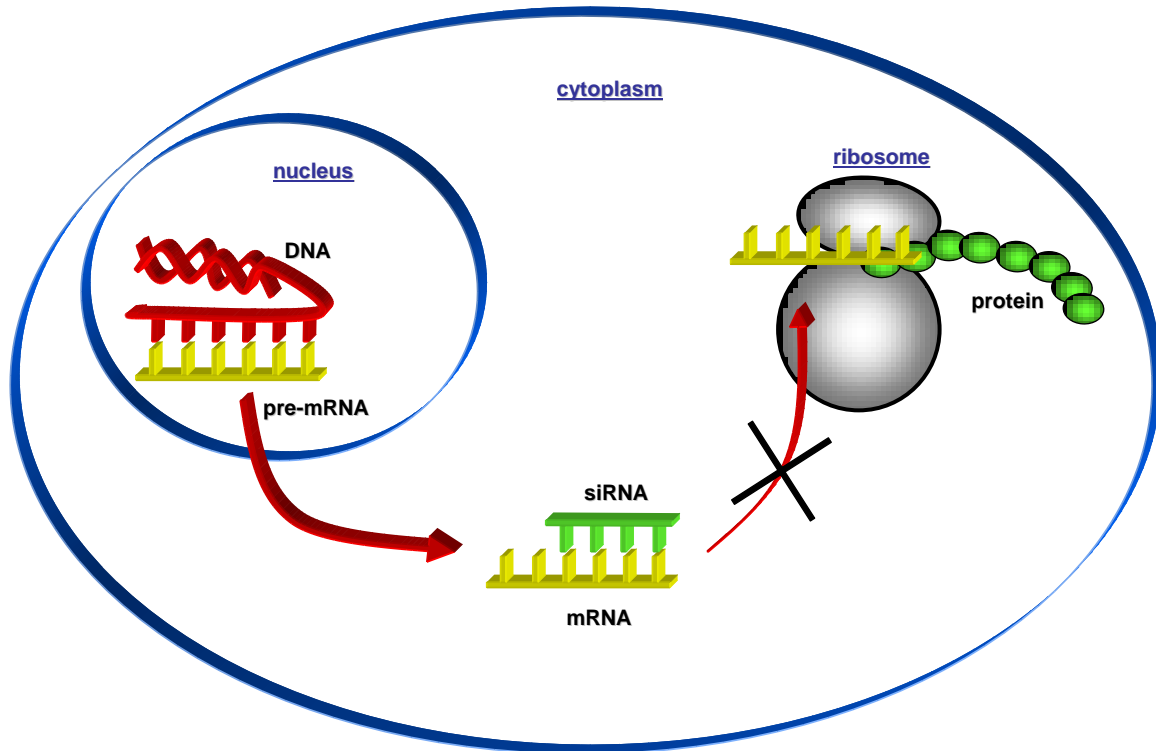


Figure 2.2.1: Schematic representation of gene silencing mechanism.

Different types of double-stranded RNAs from *Arabidopsis thaliana*, Trypanosomes, *Drosophila*, *C. elegans* and different mammals were investigated,^[12,14] showing the differences in some steps of gene silencing, but the principle of the process remains unchanged. In mammals, the long siRNA-precursor is processed inside the cell by the specific RNase III-type endonuclease (called Dicer) into small functional fragments of siRNA duplexes, which are around 21 bp, of which 19 nucleotides form a helix and 2 nucleotides on each of 3' ends are unpaired (Figures 2.2.1 and 2.2.2). The point is that only short RNA duplexes can be used without evoking of a nonspecific immune response by interferons, which usually leads to shutdown of protein synthesis and global RNA degradation.^[12,13,19]

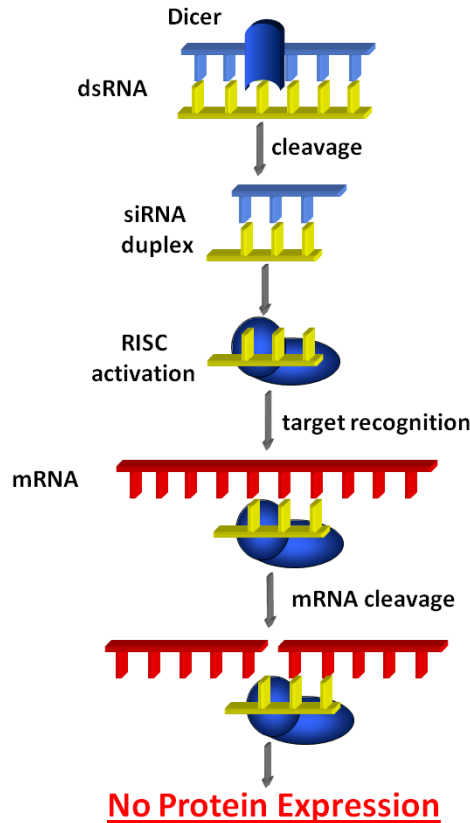


Figure 2.2.2: Schema of gene silencing by siRNA: Double stranded RNA, consisting of sense and anti-sense strands, is cleaved by Dicer to produce siRNA duplexes. These siRNAs will incorporate into a RISC complex and will be unwound by its helicase activity. Then the antisense strand of siRNA hybridizes to mRNA which afterwards will be cleaved.

The following maturation of siRNA includes the formation of the complex between the RNA duplex and the proteins, including proteins of the Argonaute family (Ago2) and subsequent transient association with Dicer. These complexes of ribonucleoprotein particles are afterwards rearranged into the so-called RNA-induced silencing complex (RISC) with different molecular mass, *e.g.* for humans it is between 130 and 160 kDa.^[20,21] The further unwinding of the siRNA strands results in the formation of activated RISCs. These activated RISCs then bind to complementary or near complementary target mRNA

molecules leading to their cleavage. That leads to the inhibition of protein synthesis – gene silencing.

shRNA (short hairpin) is one of the predecessors of siRNA. shRNA is called so due to its structure: Sense and antisense strands are bound together via small ~9-nt loop. It is usually introduced into the cell as a vector, which is then transcribed by cellular RNA polymerase III to shRNA which is then cleaved to siRNA. This process may give outstanding possibilities for the inherited inhibition of proteins.

Nowadays the application of dsRNA as a direct intervention for the treatment of human diseases remains one of the great challenges. RNAi is investigated first of all as a potential immune-type surveillance mechanism against viruses for mammals.^[22] Previously, the above described effect was already shown to take place in the cells of some invertebrates, such as *C. elegans* and *Drosophila*.^[12]^[23] This technology is also widely applied for pathway and gene functions analysis,^[24,25] and for identification and validation of new drug targets for many diseases including cancer.^[26]

2.3 Oligonucleotides for the maturation of dendritic cells

Another function of nucleic acids is an indirect influence on the cell development not through the control of protein synthesis but through specific receptor-mediated recognition and activation of the signaling mechanisms. Some oligonucleotides are known to be present also in microbial DNA, thus recognized by the immune system and leading to activation and maturation of B-cells and dendritic cells.^[27] This activation leads to immune response against microbial antigens.

One of the immunostimulatory oligonucleotides are so-called CpG fragments with an increased density of C and G nucleotides.^[27,28] The other type of such stimulatory nucleic acids are poly(inosinic acid)-poly(cytidylic acid).^[29] They

both are known to be able to mimic the ability of microbial DNA to activate the innate immune system.^[27,28,30-33] They induce the maturation of dendritic cells,^[34,35] thus breaking the tolerance and activating the immune system against previously undetectable antigens.^[36] These responses can be detected via the secretion of specific proteins by cells, *e.g.* interleukins (IL-6 and 12), IFN- α (interferon), CD-80 and CD-86.^[28,29,37]

2.4 Transfection

The method of introduction of foreign nucleic acids (DNA or RNA) into eukaryotic cells is called transfection. Such an introduction leads to the regulation of the desirable protein synthesis, *e.g.* production of a failing protein, blocking of the overexpression, acquiring new cell properties or replacement of a defect protein. Thus, the application of the technique allows the production of new cell lines as well as the potential treatment of a wide variety of diseases.

However, during the transfection the nucleic acid must overcome many barriers (cell and nuclear membranes) and also escape the degradation by the cytoplasmatic endonucleases.^[38,39] Therefore, the development of an efficient transfection technique meets many difficulties and among them the low efficiency of some methods and high toxicity of others. That is why the development of efficient and safe transfection methods is a great challenge in gene therapy.

To introduce the nucleic acid into the cell, special carriers are usually needed. Transfection systems may be divided into two main groups: viral and non-viral techniques.^[40]

1. Viral gene delivery systems.

Virus-based gene delivery systems are the most effective transfection technique. They are based on viral ability to infect cells. These techniques are applied for more than 50 years using adenoviruses,^[36,41-43] retroviruses,^[44-46] and other

viruses.^[31,47,48] However, these methods have potential disadvantages, *e.g.* immunogenicity, inflammatory response, and carcinogenicity, thus promoting the development of alternative delivery systems. Moreover, although viral particles can easily penetrate into the cell, even impaired viruses remain potentially dangerous because of the threat of the recreation of the highly infectious wild-type viruses.^[40]

Thus, different non-viral transfection techniques were developed and tested although they have a much lower efficiency than virus-based systems.

2. Nonviral gene delivery systems can be divided into two subgroups: physical and chemical methods.

- Physical methods are microinjection^[49,50] and electroporation.^[51-53] However, by microinjection one can transfect only a single cell at a time, but not many, *i.e.* this method cannot be used for large numbers of cells and for *in vivo* experiments. As for the electroporation, in order to achieve the successful transfection it requires an optimization of many parameters for every cell type, such as the voltage or the length of the pulse.

- The chemical methods of nucleic acid delivery include different agents able to form a complex with DNA and transport it inside the cell. These carriers can be divided into three groups: cationic compounds, recombinant proteins and inorganic nanoparticles.

Cationic compounds include a variety of cationic lipids,^[54-62] and polymers, *e.g.* poly(ethylene imine),^[63] poly(methacrylic acid), poly(vinylpyrrolidone),^[64] and poly(lactic-*co*-glycolic acid).^[65] The cationic lipids decrease the negative charge of the DNA, thus facilitating its transport through a negatively charged cell membrane.

Recombinant proteins are used as carriers and also as nuclear localization sequences. They may include polylysine or polyarginine segments for sufficient

charge. Moreover, protamines or histones may bind DNA to protect it from the degradation by nucleases.^[66-70]

Inorganic nanoparticles consist of different elements: gold,^[71-74] silver,^[75,76] magnetite,^[77-79] silica,^[80] carbon,^[81] manganese phosphate^[82] and calcium phosphate. The great advantage of the calcium phosphate transfection method is that it provides a higher biocompatibility than other types of nanoparticles.

The standard calcium phosphate transfection method was introduced by Graham and van der Eb in early 1970s.^[83] Here calcium phosphate spontaneously forms complexes with DNA *in situ*. Usually these complexes consist of DNA backbone and “beards” of calcium phosphate crystals on in, and calcium phosphate particles with inorganic core and nucleic acid as a shell. But such a method has definite drawbacks such as polydispersity of the particles, little control of the experimentalist over their size and morphology, non-physiological pH of the dispersion and short storage time.

Thus, in spite of the fact that the inorganic nanoparticles cannot compete with viral methods or liposomes in high transfection efficiency, they have often a low toxicity, easy and low-cost preparation and good storage stability.

2.5 Calcium phosphate nanoparticles as carriers of nucleic acids

Calcium and phosphorus are very important inorganic components of biological hard tissues, *e.g.* bones and teeth.^[84] They are also included in the regulation of many processes, such as the transfer of intracellular signals (where calcium ions act as mediators) or maintenance of salt balance of organism.

As minerals, calcium phosphates form large crystals, but their biological formation often leads to nanocrystals because it takes place under mild conditions.^[85] Also these calcium phosphates often include different additives such as sodium, magnesium or carbonate. An important parameter for the formation of different calcium phosphates is also the molar Ca/P ratio and

solubility. Most types of calcium phosphates are only partially soluble in water or insoluble at all, but they can all be dissolved in acids.^[84]

Thus, calcium phosphate possesses very important properties for the application to living objects: It is biocompatible due to its chemical nature and thus biodegradable.

As carriers of nucleic acids, calcium phosphate nanoparticles have been widely used for more than 35 years. The precipitation occurs *in situ* and includes a subsequent mixing of calcium chloride solution, DNA and phosphate-buffered saline solution. This results in the formation of polydisperse nano- and microparticles of calcium phosphate and DNA.^[42,83,86-90] This dispersion is added to a cell suspension, and the nanoparticles are taken up by cells.^[91]

The interaction between calcium phosphate and nucleic acid occurs presumably due to the affinity of calcium to the phosphate backbone in nucleic acids (Figure 2.5.1),^[91-94] thus making the nucleotide sequence of the nucleic acid unimportant, but taking into account its length.^[95]

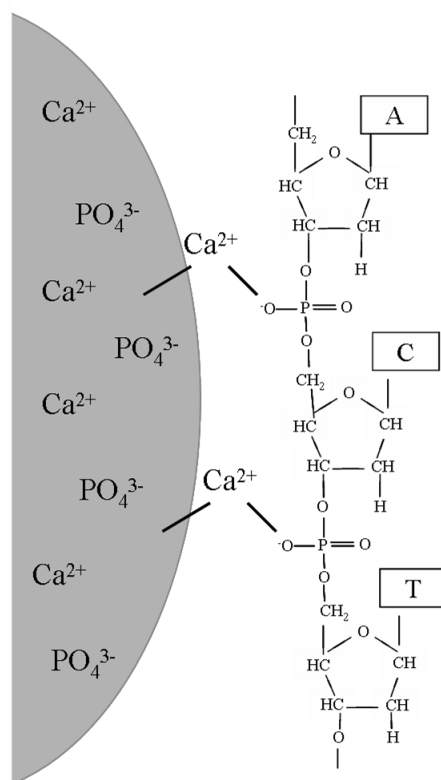


Figure 2.5.1: Schematic model of the interaction between the surface of a calcium phosphate nanoparticle and a nucleic acid.^[91]

To have more control over the precipitation of calcium phosphate and, therefore, over the particle morphology and size, many ways of synthesis were developed. Bisht *et al.* prepared calcium phosphate nanoparticles in microemulsion, thus precipitation takes place only in an aqueous core of the microemulsion droplets.^[96] These particles had a size of 30-40 nm but rapidly aggregated with time. Fu and co-workers used calcium phosphate/DNA precipitates together with porous collagen spheres to transfect different cell lines.^[97] These particles had a size of 50-200 nm and could effectively transfect cells. They could be stored for approx. 5 days, but with a loss of efficiency. Olton *et al.* prepared monodisperse calcium phosphate nanoparticles with a typical diameter of 25-50 nm by precipitation in the presence of DNA and found a most efficient transfection.^[98] Sokolova *et al.* prepared calcium phosphate nanoparticles by

rapid precipitation of calcium and phosphate, followed by an immediate functionalization with DNA^[99] or oligonucleotides.^[95] These particles typically have a size of 80 nm and form stable colloidal solutions. To protect DNA against degradation in the cytoplasm by endonucleases the additional shells of calcium and phosphate were used to encapsulate DNA and to protect it on its way to the nucleus.^[100]

2.6 Colloid stability and DLVO theory

A colloid is a system which consists of a dispersed phase distributed throughout a dispersion medium.^[101,102] The dimension of the disperse phase lies in the range of 1 nm to 1 μm . The most important properties of colloidal systems are the following:

- Large ratio of the specific surface area to the volume of the dispersed particles;
- Particle-particle interactions;
- Volume effects compete with interfacial effects;
- Adsorption of charged molecules on the surface.

The colloid as well as the dispersant may be present in solid, liquid or gaseous form. The examples of colloidal systems are smoke, milk or glass.^[101,103,104]

The particles in a colloid are almost always electrically charged. This charge on the particle is balanced by the opposite charge in the surrounding fluid. Ions are adsorbed on colloidal particles, where they form the partly rigid, partly diffuse electrostatic double layer, leading to the so-called zeta potential, *i.e.* the difference in electrical potential between the dense layer of ions surrounding the particle and the bulk of the suspended fluid.^[105]

A colloidal dispersion may be stable or unstable towards aggregation. This will depend on the balance of the repulsive and attractive forces that exist between the particles. The DLVO theory (developed by Derjaguin, Landau, Verwey and Overbeek) states that the stability of a particle in solution depends on the total

interaction energy, which is the sum of the attractive van der Waals force and the repulsive force that arise when the diffuse double layers around the two particles overlap.^[102]

Theoretically, monodisperse colloidal systems should not aggregate. However, it is very difficult to prepare really monodisperse colloids.

There are two general mechanisms for the stabilization of colloids: electrostatic repulsion between the electrical double layer and steric stabilization. The electrostatic stabilization occurs due to ions or charged molecules adsorbed on the particle surface as discussed above.

The steric stabilizing mechanism includes the adsorption of protective agents (often polymeric) on the particle surface. Such molecules do not have to carry an electrical charge but must have a relatively low solubility in the dispersion medium and a high tendency to adsorb onto the particle surface which improves the stability of the colloid by the imposition of a barrier to a close particle approach.

In our case the nucleic acids lead to both ways of stabilization: The DNA molecule gives steric stabilization and simultaneously provides electrostatic stability due to the negatively charged phosphate backbone.^[91]

3 Materials and Methods

3.1 Applied materials for cell culture experiments

3.1.1 Cell culture solutions/antibiotics

| | |
|-------------------------|---------------------------|
| DMEM | PAA |
| FCS | PAA, Biochrom |
| Glutamine | Gibco BRL/Invitrogen |
| HEPES | Biomol |
| Penicillin/Streptomycin | Gibco BRL/Invitrogen, PAA |
| RPMI 1640 | PAA |
| L15 | PAA |
| Trypsine | Gibco BRL/Invitrogen |
| Geneticin (G418) | Gibco BRL |
| Propidium iodide | Fluka |
| DAPI | Fluka |
| Fura-2AM | Invitrogen |
| MTT | Sigma |
| DMSO | JT Baker |
| BM Cyclin | PAA |

3.1.2 Chemicals

| | |
|----------------------|---|
| Ampicillin | Biomol |
| Ethanol | JT Baker |
| Yeast extract | Roth |
| Pepton hydrolysate | Roth |
| SDS | Biomol |
| NaCl | JT Baker |
| Scintillation liquid | Rotiszint eco Plus for hydrophilic samples, Carl Roth |
| Poly-L-ornithine | Sigma |
| Triton X 100 | AppliChem |
| PMSF | Acros |
| Paraformaldehyde | Janssen Chimika |

3.1.3 Instruments

| | |
|-------------------|---|
| Incubator | Heraeus |
| Microscopes | Olympus IX51 Olympus IX 81 Olympus CK 2 |
| Laminar flow hood | Heraeus |

| | |
|-------------------------------|---|
| Thermomixer | Eppendorf |
| Centrifuges | Eppendorf 5415C (Minifuge) Heraeus Megafuge 1.0R Sorvall Superspeed RC2-B |
| ELISA-Reader | SLT Labinstruments |
| Liquid Scintillation Analyzer | Tri-Carb 2800TR, Perkin Elmer |
| Vortex | Vortex 2 Genie, Scientific Industries |
| Shaker | Certomat [®] H |
| Photometer | UV 1202, Shimadzu |
| Flow cytometer | FACSCalibur [™] , BD-Bioscience CyFlow [®] SL, Partec |

3.1.4 Applied consumables und kits

| | |
|---|----------------------|
| Nucleobond [®] PC 10000 plasmid DNA purification kit (endotoxin- free) | Macherey-Nagel |
| QIAGEN Plasmid Maxi Kit | Qiagen |
| Bio-Rad D _C Protein Assay | Bio-Rad Laboratories |
| Multiwell plates (24-, 6-wells) | TPP |
| Polyfect [®] | Qiagen |
| Flasks 75 cm ³ | Nunc, TPP |
| 35 mm glass-bottom dishes | MatTek Corporation |
| 35 mm dishes | Nunc |

3.2 Molecular-biological methods

3.2.1 Preparation of plasmid DNA from bacterial culture

All work with the intact bacteria was carried out under semi-sterile conditions with autoclaved instruments and solutions.

The preparation of the plasmid DNA for the transfection of the eukaryotic cells was performed with a NucleoBond[®] PC 10000 EF kit and a Qiagen Plasmid Maxi kit. Sterile plasticware and autoclaved glassware were used. 20 ml ampicillin-containing LB-medium was mixed with a bacterial culture and incubated overnight while shaking at 37 °C. Afterwards this bacterial culture was mixed with 2000 mL of the ampicillin-containing LB-medium and incubated once more under the same conditions. The bacteria were centrifuged

in 50 mL-tubes (Megafuge, 4000 rpm, 15 min, 4 °C). The purification of the plasmid DNA was performed according to the manufacturers' recommendation. After the precipitation, the plasmid DNA was placed in sterile endotoxin-free water. The concentration of DNA was determined by UV spectroscopy at $\lambda=260-280$ nm using a photometer UV1202. The solution of DNA was stored at -20 °C.

LB medium:

10 g L⁻¹ Pepton-hydrolysate

10 g L⁻¹ NaCl

5 g L⁻¹ yeast extract

100 µg ml⁻¹ ampicillin

3.3 Cell culture methods and experimental procedures

All cell culture work was carried out with sterile solutions and devices in a laminar flow hood.

The inorganic salts were all of p.a. quality. Ultrapure water (Purelab ultra instrument from ELGA) was used for all preparations.

We used DNA (sodium salt) from salmon testes (16.2 A250 units mg⁻¹ solid; 6.13 % Na) from Sigma and pcDNA3-EGFP purified with a NucleoBond[®] PC 10000 EF kit and Qiagen Plasmid Maxi kit as described above.

siRNA was purchased by Invitrogen (Paisley, UK): sense, 5'-GCAAGCUGACCCUGAAGUUCAU-3'; antisense, 5'-AUGAACUUCAGGGUCAGCUUGC-3'.

CpG was obtained from Eurofins MWG GmbH (Eurofins MWG, Ebersberg, Germany): 5'-TCCATGACGTTCTGACGTT-3'. Poly(I:C) (double-stranded homopolymer) was purchased from Sigma-Aldrich, Germany.

shRNAs were synthesized by the reverse-transcriptase polymerase chain reaction by our collaboration partner Mustapha Oulad-Abdelghai in the *Institut de Génétique et de Biologie Moléculaire et Cellulaire* (IGBMC), *Collège de*

France, Strasbourg Cedex, France. The primer sequences were as follows: Osteopontin (81 bp) CTCAGGCCAGTTGCAGCC and CAAAAGCAAATCACTGCAATTCTC, Osteocalcin (70 bp) GAAGCCCAGCGGTGCA and CACTACCTCGCTGCCCTCC.

3.3.1 Cultivation of secondary cell lines

T24 and NIH3T3 cells were cultivated in RPMI 1640 with 10 % fetal calf serum (FCS), 2 mM glutamine, 100 U mL⁻¹ penicillin, and 100 U mL⁻¹ streptomycin (culture medium) at 37 °C and in humidified atmosphere with 5 % CO₂. HeLa-EGFP cells were cultivated in the DMEM low glucose medium with 10 % FCS, 2 mM glutamine, 100 U mL⁻¹ penicillin, 100 U mL⁻¹ streptomycin and 50 µg mL⁻¹ G418 at 37 °C and in humidified atmosphere with 10 % CO₂.

About once a week the cells were washed twice with PBS (137 mM NaCl, 2.7 mM KCl, 4.3 mM Na₂HPO₄, 1.47 mM KH₂PO₄), then diluted with 1 mL 0.25 % trypsin and centrifuged with 6 mL of the medium containing FCS (Biofuge, 900 rpm, 5 min, 25 °C). Afterwards the supernatant with the rests of the trypsin was removed and the cells were resuspended in the fresh cell culture medium and placed into a new 75 cm³-flask.

| | | |
|-------------------------------------|-------------------------------------|---|
| T24 and NIH3T3 culture medium: | HeLa-EGFP culture medium: | PBS: |
| RPMI 1640 | DMEM low glucose | 137 mM NaCl |
| 10 % FCS | 10 % FCS | 2.7 mM KCl |
| 2 mM glutamine | 2 mM glutamine | 1.44 g L ⁻¹ Na ₂ HPO ₄ |
| 100 U mL ⁻¹ penicillin | 100 U mL ⁻¹ penicillin | 0.24 g L ⁻¹ KH ₂ PO ₄ |
| 100 U mL ⁻¹ streptomycin | 100 U mL ⁻¹ streptomycin | |
| | 50 µg mL ⁻¹ G418 | |

3.3.2 Cryoconservation of cells

For cryoconservation, the cells were washed with PBS, then trypsinized and centrifuged. Afterwards the cells were resuspended in 5 mL of the cell culture

medium, 1 mL was removed, placed into a cryotube (Nunc, Darmstadt, Germany) and mixed with 100 μ L DMSO (dimethyl sulfoxide). Afterwards the cells were slowly cooled down during more than 24 h to -80 °C and then stored in liquid nitrogen.

3.3.3 Defrosting of cells

The cells were defrosted at 37 °C for about two minutes, then in the first 5 min 5 mL of the cell culture medium were added dropwise to avoid an osmotic lysis. Afterwards the cells were centrifuged (Biofuge, 900 rpm, 5 min, 25 °C), and dissolved in fresh cell culture medium with 10 % FCS. After 24 h the medium was exchanged to remove the rests of DMSO.

3.3.4 Fluorescence microscopy

The fluorescence microscopy of EGFP-expressing cells was done by an inverse microscope (Olympus IX 51, Olympus, Hamburg, Germany) on unfixed cells in the cell culture plates with a suitable fluorescent filter.

Fura-2 measurements were carried out on Olympus IX 81 motorized inverted microscope controlled by the Cell^M software (Olympus Soft Imaging Solution, Münster, Germany). During 7 h of experiments, Fura-2 was alternately excited at 340 and 380 nm every 3 min and the emitted fluorescence was detected at >500 nm. The changes of the Fura-2 fluorescence were analyzed offline using the Cell^M software.

3.3.5 Preparation of calcium phosphate nanoparticles substituted with Al^{3+} and Mg^{2+}

Solutions of $\text{Ca}(\text{NO}_3)_2$ with additives ($\text{Mg}(\text{NO}_3)_2$ or AlCl_3) and $(\text{NH}_4)_2\text{HPO}_4$ (3.74 mM) were mixed with a peristaltic pump at the maximum speed. The concentrations of calcium, magnesium and aluminum salts are shown in

Table 4.1.1.1 (Section 4.1). Immediately thereafter the dispersion of calcium phosphate was taken with an Eppendorf pipette and mixed with 0.1, 0.2, 0.5 or 1.0 mL of the DNA solution (from salmon testes; 1 mg mL⁻¹) for each experiment, respectively. The pH of the solutions was adjusted with 0.1 M NaOH to 7.0, 8.0 and 9.0 for each experiment, respectively.

For the transfection we used 0.2 mL of pcDNA3-EGFP solution (1 mg mL⁻¹) per mL of the calcium phosphate dispersion and pH 9 as the optimal parameters for the synthesis of monodisperse nanoparticles.

3.3.6 Cell transfection

The T24 cells were cultivated in RPMI 1640 with 10 % FCS at 37 °C and in humidified atmosphere with 5 % CO₂. Approximately 12 h before the transfection, the cells were trypsinized and seeded in cell culture plates with 5·10⁴ cells per 24-well plate or 10⁵ cells per 35 mm-dish.

pcDNA3-EGFP which encodes the fluorophor protein EGFP (enhanced green fluorescent protein) was purified from *E. coli* using Nucleobond[®] PC 10000 EF kit (Macherey-Nagel, Düren, Germany) or Qiagen Plasmid Maxi kit (Qiagen, Hilden, Germany). The duration of the transfection was 7 h. Afterwards the transfection medium was replaced with the fresh medium. The efficiency of the transfection was measured after approx. 48 h by transmission light microscopy and by fluorescence microscopy.

Transfection with Polyfect[®]

Transfection with the commercial agent Polyfect[®] (Qiagen, Hilden, Germany) was carried out according to the manufacturer's recommendation: 2 µg DNA were dissolved in 100 µL medium without FCS to which 22 µL Polyfect[®] solution were added. 5 min after the mixing, 800 µL of the cell culture medium

(RPMI 1640 with 10 % FCS or L 15) were added. When the transfection was performed in the 24-well plate, 400 μL of fresh cell culture medium and 200 μL of the transfection mixture (0.43 μg DNA) were used per well. When the transfection was performed in 35-mm dishes, 800 μL of fresh cell culture medium and 400 μL of the transfection mixture (0.87 μg DNA) were used per dish. The duration of the transfection was 7 h. After that, the transfection medium was replaced with fresh cell culture medium (RPMI 1640 with 10 % FCS).

Standard calcium phosphate transfection method

The standard transfection with calcium phosphate was carried out as follows: 4 μL aqueous DNA solution (1 mg mL^{-1}) were mixed with 10 μL of 2.5 M CaCl_2 solution. The dispersion was incubated at room temperature for 5 min. The volume of the dispersion was adjusted to 100 μL with water and 100 μL of 2·HBS (2·HBS: 280 mM NaCl, 10 mM KCl, 1.5 mM Na_2HPO_4 , 12 mM dextrose, 50 mM HEPES, $\text{pH}=7.05\pm 0.01$) were added. Afterwards 1 mL of the cell culture medium was added (RPMI 1640 with 10 % FCS or L 15). The culture medium was then removed from the cell culture and the transfection mixture was added. If the transfection was performed in the 24-well plate, 500 μL of the transfection mixture (1.7 μg DNA) were used per well. If the transfection was performed in 35 mm-dishes, 1 mL of the transfection mixture (3.3 μg DNA, 835 μg Ca) was used per dish. The duration of the transfection was 7 h. After that, the transfection medium was replaced with fresh cell culture medium (RPMI 1640 with 10 % FCS).

Transfection with custom-made calcium phosphate nanoparticles

The custom-made calcium phosphate/DNA or magnesium or aluminum substituted calcium phosphate/DNA nanoparticles were used for transfection as

follows: 20 μL of nanoparticle dispersion were mixed with 500 μL medium (RPMI 1640 with 10 % FCS or L 15). Then the cell culture medium was replaced with the transfection mixture. If the transfection was performed in the 24-well plate, 500 μL of the transfection mixture (3.2 μg DNA) were used per well. If the transfection was performed in 35 mm-dishes, 1 mL of the transfection mixture (6.4 μg DNA, 4.2 μg Ca) was used per dish. The duration of the transfection was 7 h. After that, the transfection medium was replaced with fresh cell culture medium (RPMI 1640 with 10 % FCS).

Control experiments using CaCl_2 solution

17 μL of CaCl_2 solution (6.25 mM) were mixed with 1 mL of Leibovitz L15 cell culture medium and then transferred to cells seeded in 35 mm-dishes. After 7 h of incubation the transfection mixture medium was removed and replaced with a fresh cell culture medium (RPMI 1640 containing 10 % FCS) .

Incubation of control cells for Ca^{2+} -imaging

As control we used T24 cells loaded with Fura-2AM and cultivated in the cell culture media (RPMI 1640 or L15 medium, respectively) but without additional calcium or transfection agents.

3.3.7 Calculation of transfection efficiency of magnesium- or aluminum-substituted calcium phosphate nanoparticles

The efficiency of the transfection was studied by transmission light microscopy and by fluorescence microscopy using an IX 51 microscope (Olympus, Hamburg, Germany) at a magnification of 200x. If the transfection was successful and pcDNA3-EGFP was incorporated into the nuclear DNA, the synthesis of the fluorophor protein EGFP took place and the cells showed the

green fluorescence. The transfection efficiency was computed by the ratio of the cells in which EGFP was expressed to the total examined number of cells.

3.3.8 Ca-imaging using Fura-2AM

10^5 T24 cells were seeded on poly-L-ornithine-coated 35mm glass-bottom dishes 24 h before the measurement. The next day, the cells were loaded with Fura-2 by incubating with 1 mL medium which contained 2.5 μ M Fura-2AM (Invitrogen - Molecular Probes, Leiden, the Netherlands) at 37 °C and in humidified atmosphere with 5% CO₂. After 30 min the medium was exchanged by Leibovitz L15 medium whose osmolarity was adjusted to that of the RPMI medium. Furthermore the medium was supplemented by either the standard calcium phosphate transfection mixture, or CaCl₂ solution, or single-shell or triple-shell calcium phosphate nanoparticles.

3.3.9 Staining of cells with propidium iodide

To check whether the cells are damaged we additionally marked them with propidium iodide. 5 μ L of PI solution were mixed with 500 μ L of the RPMI medium and then added to the cell culture. The cells were incubated with this mixture for 30 min at 5 % CO₂. Then the cells were washed twice with PBS and taken for transmission light microscopy and fluorescence microscopy.

3.3.10 Toxicity tests

The T24 cells were seeded 24 h before the experiment in 24-well plates with a cell density of $5 \cdot 10^4$ cells per well. The MTT-assay was performed after the 7 h incubation of cells with different transfection media. The spectrophotometric measurements were carried out 7 h, 24 h and 48 h after the addition of the transfection media to the cells.

First, the MTT-stock-solution (3-(4,5-dimethylthiazol-2-yl)-2,5-diphenyltetrazolium bromide) in PBS (5 mg mL^{-1}) was prepared and afterwards diluted to 1 mg mL^{-1} in the cell culture medium (RPMI 1640 supplemented with 10 % FCS, 2 mM glutamine, 100 U mL^{-1} penicillin, $100 \text{ } \mu\text{g mL}^{-1}$ streptomycin). After the mentioned incubation time, the cell culture medium was replaced with 300 μL of MTT-solution and the cells were incubated for about 1 h at $37 \text{ }^\circ\text{C}$ and 5% CO_2 . Then this solution was removed and replaced with 300 μL DMSO solution. The cells were incubated for 30 more minutes under the conditions described above and afterwards the 50 μL aliquot was taken for spectrophotometric measurements using an ELISA-Reader at $\lambda=560\text{-}600\text{nm}$.

3.3.11 Experiments with radioactive ^{45}Ca

The experiments using ^{45}Ca were performed as follows: 24 h before the transfection the cells were seeded on 35 mm dishes (Nunc, Langensfeld, Germany) with a density of $20 \cdot 10^4$ cells per dish ($5 \cdot 10^4$ in the case of subsequent incubation for a week). We used T24 cells (human bladder carcinoma cell line).

The measurements of radioactivity of the medium and cell lysate were performed after 1 h, 7 h, 48 h, and 1 week of incubation of the cells at $37 \text{ }^\circ\text{C}$ and in humidified atmosphere with 5 % CO_2 .

After 1 h and 7 h of incubation aliquots of the cell culture medium were taken, the rest of the medium was removed, and the cells were three times washed with

PBS. Then 200 μL of lysis buffer (1 % Triton X 100, 10 mM Tris HCl, pH 7.4) were added and mixed with a pipette tip (up and down) 60 times. A 5 μL aliquot was taken to determine the protein concentration, and the rest was taken to measure the radioactivity of the cells.

An aliquot of the cell culture medium and the lysates were mixed with 4 mL of the scintillation liquid (Rotiszint eco Plus for hydrophilic samples, Carl Roth, Karlsruhe, Germany) and then the activity was measured using a Liquid Scintillation Analyzer, Tri-Carb 2800TR.

After 7 h the medium was changed in all residual samples. Half of the samples were washed beforehand three times with PBS to remove ^{45}Ca which could be attached to the cell surface, but had not yet entered the cells. After 48 h and 1 week of incubation, the radioactivity was measured as described above.

Transfection with nanoparticles

Solutions of $\text{CaCl}_2 \cdot 2\text{H}_2\text{O}$ (6.25 mM; Sigma, Steinheim, Germany) and $^{45}\text{CaCl}_2$ (PerkinElmer Life and Analytical Sciences, Boston, MA, USA) were mixed together to a final radioactivity of the mixture 2 MBq mL^{-1} . The overall calcium concentration was still 6.25 mM because the added volume of the ^{45}Ca solution was negligible. Then 250 μL of the CaCl_2 solution (6.25 mM) were rapidly mixed with 250 μL of $(\text{NH}_4)_2\text{HPO}_4$ (3.74 mM) under constant stirring. Then 425 μL of the dispersion were taken with an Eppendorf pipette and transferred into a new plastic vessel. Then 85 μL of the DNA solution (plasmid pcDNA3-EGFP, 1 mg mL^{-1}) were added for the functionalization of the particles. These nanoparticles are denoted "single-shell" in the following.

In order to produce triple-shell nanoparticles, we subsequently added 213 μL of the CaCl_2 solution (6.25 mM, 2 MBq mL^{-1}), 213 μL of $(\text{NH}_4)_2\text{HPO}_4$ (3.74 mM) and 85 μL of pcDNA3-EGFP solution (1 mg mL^{-1}).

40 μL of the nanoparticle dispersion were mixed with 1 mL of the cell culture medium (RPMI 1640 supplemented with 10 % FCS, 2 mM glutamine, 100 U mL^{-1} penicillin, 100 $\mu\text{g mL}^{-1}$ streptomycin) and immediately transferred to the cells. The calculated amount of added Ca was 4.2 μg per 35-mm dish (1 mL).

After 7 h of incubation the transfection mixture was removed and in half of the dishes just replaced with a fresh cell culture medium. In the other half of the dishes, the cells were washed three times with PBS to remove traces of ^{45}Ca , and then fresh medium was added.

Transfection by the standard calcium phosphate method

The transfection was performed according to the standard protocol. 4 μL DNA (plasmid pcDNA3-EGFP, 1 mg mL^{-1}), 10 μL CaCl_2 (2.5 M; final radioactivity 4 MBq mL^{-1}), 86 μL distilled H_2O , 100 μL 2·HBS and 1 mL medium (RPMI 1640) were mixed together. Afterwards the cell culture medium was replaced with 1 mL of this mixture. The calculated amount of Ca added was 835 μg per 35-mm dish (1 mL) containing ^{45}Ca with an activity of 40 kBq mL^{-1} .

After 7 h of incubation the transfection mixture was removed and in half of dishes just replaced with a fresh one. In the other half of the dishes the cells were washed three times with PBS to remove traces of ^{45}Ca and then fresh medium was added.

Control experiments with ^{45}Ca in the medium

17 μL of CaCl_2 solution (6.25 mM, 2 MBq mL^{-1}) were mixed with 1 mL of the cell culture medium and then transferred to cells. The calculated amount of added Ca was 4.2 μg per 35-mm dish (1 mL).

After 7 h of incubation the transfection mixture was removed and in half of dishes just replaced with a fresh one. In the other half of the dishes the cells were washed three times with PBS to remove traces of ^{45}Ca and then fresh medium was added.

3.3.12 Preparation of cell lysates

The cell culture medium was replaced with 100 μL of lysis buffer containing PMSF (1 mM). Then the cells were incubated for 30 min at 4 °C under constant shaking. The lysates were mixed by pipetting and transferred into a 1.5 mL Eppendorf vessel. This step and all subsequent steps were performed on ice at 4 °C. The lysates were centrifuged for 10 min at 14,000 rpm. The clear lysates were transferred into fresh 1.5 mL vessels and stored at -20 °C.

Lysis buffer:

1% Triton X 100

10 mM Tris-HCl

pH 7.4

3.3.13 Determination of the protein concentration

The protein concentration of the lysates (the preparation of the lysates is described in Chapter 3.3.12) was photometrically measured with a Bio-Rad D_C Protein Assay according to the manufacturer's recommendations on an ELISA-Reader, using standard calibration solutions of bovine serum albumin (BSA) (0.05, 0.1, 0.2, 0.4, 0.8, and 1.6 mg mL⁻¹). The measured radioactivity of the cell lysates was then normalized to the protein content of the lysate.

3.3.14 Preparation of metal surfaces coated with calcium phosphate/PEI/DNA-nanoparticles

For the covering of the titanium plates, first, calcium phosphate/PEI nanoparticles were produced. For this, aqueous solutions of $\text{Ca}(\text{NO}_3)_2 \cdot 4\text{H}_2\text{O}$ (19.91 mM) and $(\text{NH}_4)_2\text{HPO}_4$ (11.94 mM) were adjusted to pH 9 with 1.0 M NaOH and then rapidly mixed with a peristaltic pump with a speed of 1.35 mL min^{-1} . Simultaneously to the calcium phosphate solution, the PEI solution (2 g L^{-1} ; Aldrich) was added with a speed of 2.6 mL min^{-1} . Then the nanoparticles were filtered and dried at room temperature.

For the coating of the plates, the nanoparticles were resuspended in 2-propanol (15.4 mg mL^{-1}) via 30 min incubation in the ultrasonic bath. Then, pcDNA3-EGFP solution was added to the concentration of DNA of $1 \mu\text{g mL}^{-1}$.

The titanium plates were coated under the voltage of 50 V for 30 s.

As control, we used titanium plates coated with calcium phosphate/PEI nanoparticles without DNA. This preparation method was the same, only the step of the DNA addition was missing.

3.3.15 Transfection from metal surfaces

NIH3T3 cells were cultivated in RPMI 1640 supplemented with 10 % FCS 2 mM glutamine, 100 U mL^{-1} penicillin and 100 U mL^{-1} streptomycin at $37 \text{ }^\circ\text{C}$ and in humidified atmosphere with 5 % CO_2 .

Just before the transfection, $5 \cdot 10^4$ cells were seeded per well in the 24-well plate onto the pure titanium plates or titanium plates coated with calcium phosphate/PEI and calcium phosphate/PEI/DNA nanoparticles.

A pcDNA3-EGFP which encodes the fluorophor protein EGFP was purified from *E. coli* using the Qiagen Plasmid Maxi kit. The duration of the transfection was 7 h. Afterwards the transfection medium was transferred with fresh medium. The efficiency of the transfection was measured after approx. 48 h of

cell incubation at 37 °C and in humidified atmosphere with 5 % CO₂ by fluorescence microscopy, by FACS measurements and by Western Blot analysis. For these analyses the titanium plates were replaced into fresh 24-well plates (to remove the cells which grew on plastic and not on the titanium plates) and twice washed with PBS.

Transfection from metal surfaces coated with calcium phosphate/PEI/DNA-nanoparticles

The titanium wafers (10·10) mm coated with calcium phosphate/PEI/DNA nanoparticles were placed into the 24-well plates. Then NIH3T3 cells were seeded on the plates and 500 µL of the cell culture medium (RPMI 1640) was added. After 7 h the cell culture medium was replaced with fresh medium.

Transfection from metal surfaces coated with calcium phosphate/PEI-nanoparticles followed by addition of DNA

The titanium plates (10·10) mm coated with calcium phosphate/PEI nanoparticles were placed into the 24-well plate. Then 4 µL of DNA solution (1 mg mL⁻¹) was dripped onto the surface and dried at 37 °C. Afterwards NIH3T3 cells were seeded on the wafers and 500 µL of the cell culture medium (RPMI 1640) was added. After 7 h the cell culture medium was replaced with fresh medium.

Control experiments with titanium plates

As controls we used untransfected NIH3T3 cells, and cells transfected with either Polyfect[®] (as described in 3.3.6), or calcium phosphate/PEI or calcium phosphate/PEI/DNA dispersions. In these cases cells were transfected from the dispersion, but were previously seeded on uncoated titanium plates. The Polyfect[®] transfection protocol is described above.

For further controls, 20 μL calcium phosphate/PEI and calcium phosphate/PEI/DNA isopropanol dispersions were mixed with 500 μL of the cell culture medium and the mixture was transferred to the cells seeded onto uncoated titanium plates.

As another negative control we seeded cells onto the titanium plate coated with calcium phosphate/PEI nanoparticles without addition of DNA. Then 500 μL of the cell culture medium were added.

After 7 h the cell culture medium was replaced with a fresh one (RPMI 1640).

3.3.16 Cell fixation

The titanium plates were transferred into the new 24-well plate and 100 μL of 0.25 % trypsin solution were added. After several minutes 1 mL of RPMI 1640 with FCS was added and the cells were transferred into the 1.5 mL Eppendorf vessel. Then the cells were centrifuged for 3 min at 2000 rpm (Eppendorf 5415C), the supernatant was removed and the cells were resuspended in 100 μL 3 % paraformaldehyde (Janssen Chimika, Belgium), incubated for 10 min at room temperature, washed twice with PBS and centrifuged 3 minutes at 2000 rpm. Then the cells were resuspended in 1 mL of PBS.

3.3.17 Flow cytometry of NIH3T3 cells

Flow cytometry or FACS analysis (fluorescence activated cell sorting) was performed on FACSCaliburTM in collaboration with Prof. Dr. M. Köller at the BG Kliniken Bergmannsheil, and on CyFlow[®] SL at the Chair of Molecular Neurobiochemistry, Ruhr-University of Bochum. The data were analyzed offline using WinMDI 2.9 software.

Flow cytometry is a technique which allows counting and examining microobjects suspended in a stream of fluid (size range of 0.5 μm to 40 μm). Flow cytometry is based on the optical signal of the suspended single cell when

it passes through a laser beam. The cells which contain a fluorescent protein are detected and recorded.

3.3.18 Preparation of multi-shell calcium phosphate nanoparticles functionalized with siRNA

Calcium phosphate nanoparticles were prepared by rapidly pumping an aqueous solution of $\text{Ca}(\text{NO}_3)_2$ (6.25 mM or 18 mM) and an aqueous solution of $(\text{NH}_4)_2\text{HPO}_4$ (3.74 mM or 10.8 mM) into a glass vessel by a peristaltic pump. The pH of both solutions was adjusted to 9 with 0.1 M NaOH. Immediately after mixing, 108.8 μL of the calcium phosphate dispersion was taken with the Eppendorf pipette and rapidly added to 16.2 μL of an aqueous solution of double-stranded small interfering RNA (siRNA, 320 μM) in a sterile Eppendorf vessel. These nanoparticles were denoted "single-shell".

To protect siRNA from the degradation by nucleases, multi-shell calcium phosphate nanoparticles^[100] were prepared. First, single-shell nanoparticles were prepared as described above. Then 54.4 μL of $\text{Ca}(\text{NO}_3)_2$ (6.25 mM or 18 mM, respectively) were added to 125 μL of the above described dispersion of single-shell particles, and 54.4 μL of $(\text{NH}_4)_2\text{HPO}_4$ (3.74 mM or 10.8 mM, respectively) were quickly added. The third layer consisting of siRNA was prepared by adding 16.2 μL of dsRNA (320 μM) to this dispersion. The initial concentration of the double-stranded small interfering RNA (siRNA) used was 320 μM . The resulting concentration of siRNA in these dispersions of nanoparticles was 45 μM .

3.3.19 Preparation of calcium phosphate nanoparticles functionalized with CpG and Poly(I:C)

For the preparation of the oligonucleotide-functionalized calcium phosphate nanoparticles, aqueous solutions of $\text{Ca}(\text{NO}_3)_2 \cdot 4\text{H}_2\text{O}$ (6.25 mM) and $(\text{NH}_4)_2\text{HPO}_4$

(3.74 mM) were adjusted to pH 9 with 0.1 M NaOH and then rapidly mixed via peristaltic pump in a plastic vessel. Immediately thereafter, 1 mL of the mixture was taken with the Eppendorf pipette and mixed with 167 μL of CpG solution (63 μM) or with 2.5 μL of CpG solution (63 μM) and 198 μL Poly(I:C) solution (1 mg mL⁻¹).

3.3.20 Preparation of calcium phosphate nanoparticles functionalized with shRNA

The single- and triple-shell calcium phosphate/shRNA nanoparticles were prepared by the precipitation method as described in Section 3.3.18.^[100] We used two types of shRNA: Spp1 for the silencing of osteopontin expression and Bglap-rs 1 for silencing of osteocalcin expression. The concentrations of shRNA were 0.75 mg mL⁻¹ and 0.83 mg mL⁻¹ for Spp1 and Bglap-rs 1, respectively.

First, aqueous solutions of Ca(NO₃)₂·4H₂O (6.25 mM) and (NH₄)₂HPO₄ (3.74 mM) were adjusted to pH 9 with 0.1 M NaOH and then rapidly mixed with two peristaltic pumps in a plastic vessel. Immediately thereafter, 1 mL of the mixture was taken with the Eppendorf pipette and mixed with 0.1 mg of shRNA dissolved in water. These nanoparticles consisted of a calcium phosphate core and an outer layer of shRNA for electrostatic and steric functionalization and are denoted "single-shell" in the following.

The shRNA was incorporated into the particles, and then 0.5 mL of Ca(NO₃)₂·4H₂O solution (6.25 mM) and 0.5 mL of (NH₄)₂HPO₄ solution (3.74 mM) were added to the dispersed single-shell nanoparticles. Immediately thereafter, we added 0.1 mg of shRNA dissolved in water as an outer layer of the particles (0.75 mg mL⁻¹ and 0.83 mg mL⁻¹ for Spp1 and Bglap-rs 1, respectively). These triple-shell particles consisted of a calcium phosphate core and further layers of shRNA, calcium phosphate and shRNA.

3.4 Physicochemical methods

3.4.1 Dynamic light scattering

Dynamic light scattering (DLS) measurements were carried out with a Zetasizer instrument (NanoZS, Malvern instruments).

Dynamic light scattering was used to determine the size of the particles. For this, two major assumptions were made: The particles have spherical form and they are in Brownian motion.

Shining a monochromatic light beam onto dispersion with spherical particle causes a Doppler shift when the light hits a moving particle, changing the wavelength of the incoming light. This change is related to the size of the particle. It is possible to calculate the distribution of particle sizes and give a description of the particle's motion in the medium, measuring the diffusion coefficient of the particle:

$$D_T = k_B T / 6 \pi \eta R_h$$

D_T : the translation diffusion coefficient

k_B : Boltzmann constant

T : temperature in Kelvin degrees

η : viscosity of the solvent

R_h : hydrodynamic radius.

The radius of the particles can be computed from the formula above.

3.4.2 Zeta potential measurements

The measurements of the zeta potential (ZP) were carried out with a Zetasizer instrument (NanoZS, Malvern instruments).

Zeta potential is the empirical potential on the surface of the particle. It refers to the electrostatic potential generated by the accumulation of ions at the surface of the colloidal particle which is organized into an electrical double-layer consisting of the Stern layer and the diffuse layer.

The zeta potential was calculated by measuring the mobility distribution of a dispersion of charged particles as they are subjected to electric field. The mobility is measured as the velocity of a particle in an applied electric field according to the following equation (the Smoluchowski model was used):

$$B_e = (\varepsilon \zeta f_B / \eta) (\omega r^2 \rho / \eta)$$

B_e : electrophoretic mobility

ε : dielectric constant

ζ : zeta potential

η : viscosity

ω : frequency of the electrical field

r : radius of the particle

ρ : density of the dispersion

f_B : correction factor

3.4.3 Scanning electron microscopy (SEM)

For the SEM observations, an ESEM Quanta 400 microscope with gold-palladium-sputtered samples was used.

The scanning electron microscope produces very high-resolution images of a sample surface which are not possible to be taken by light microscopy because of the higher energy of the electrons. In a scanning electron microscope, the accelerated electrons are focused by the magnetic field into a narrow beam which scans a surface of the sample. The observed image is created by the secondary electron emissions from the sample area so that a contrast-rich 3 D-image can be created.

3.4.4 Transmission electron microscopy (TEM)

TEM observations were performed with a Philips CM 200 FEG instrument on air-dried nanoparticles prepared on carbon-coated copper grids.

The transmission electron microscope is an optical analogue to the conventional light microscope. It is based on the fact that electrons possess a wavelength but at the same time interact with magnetic fields like a point charge. A beam of electrons is applied instead of light, and glass lenses are replaced by magnetic lenses.

A very thin slice of the tested material is exposed to a beam of electrons. Due to the interaction of the electrons with a consistent material structure, a constant fraction of the electrons is transmitted through the sample to the detector. Once a structural imperfection is encountered, the fraction of the transmitted electrons changes.

4 Results and Discussion

4.1 Calcium phosphate nanoparticles substituted with Al³⁺ and Mg²⁺

4.1.1 Synthesis and characterization of calcium phosphate substituted with Al³⁺ and Mg²⁺

Nanoparticles represent a key to a very wide range of problems that can be solved with the help of nanotechnology. One of their possible applications is the use of nanoparticles as carriers for drugs and nucleic acids in molecular biology and medicine.

In the past years many types of nanocarriers of different chemical nature were developed and tested. One of the most promising groups is inorganic nanoparticles.

Inorganic nanoparticles may consist of different elements: gold,^[71] silver,^[75,76] magnetite,^[77-79] silica,^[80] carbon,^[81] manganous phosphate^[82] and calcium phosphate. Among this wide range of materials the calcium phosphates draw our attention due to their special properties: It is a natural biomineral so it possesses outstanding biocompatibility and biodegradability. Also, the originating ions are deeply involved in cell metabolism and can be easily metabolized by cells.

As drug carriers, calcium phosphate nanoparticles have a number of promising properties. They can be dissolved at low pH (around 4), *e.g.* in the lysosomes after the cellular uptake,^[92,106] or in the environment of solid tumors, thereby releasing the incorporated drugs or biomolecules. Their size can be easily controlled by stabilizing agents, such as polymers or nucleic acids. The nanoparticles can be made fluorescing by the incorporation of lanthanide ions,^[107-110] and also act as carriers for different drugs, *e.g.* insulin^[111] and cisplatin.^[112,113] Kester *et al.* produced calcium phosphate nanoparticles functionalized with the anticancer drug ceramide.^[114] Further functionalization of the particles with PEG resulted in the stable particles with a positive surface charge which were easily taken up by the cells.^[115]

As carriers of nucleic acids, calcium phosphate nanoparticles have been used since 1973.^[83] Welzel *et al.* developed a method of controlled precipitation of spherical calcium phosphate nanoparticles functionalized with DNA. Such nanoparticles had a size up to 200 nm with a negative zeta potential up to -30 mV.^[99,116]

In order to obtain smaller nanoparticles we used substitutions of aluminum and magnesium to inhibit the crystal growth. For the synthesis of the nanoparticles we prepared solutions of different composition (Table 4.1.1.1).

The substitution of cations was used to elaborate the influence of the charge and the individual properties of calcium on the precipitation of calcium phosphate nanoparticles. Magnesium has chemical properties very similar to those of calcium and can also partially replace this ion in many crystals.^[117] Therefore, we tried to replace almost all calcium in our samples to see its individual contribution.

Aluminum has a higher charge than calcium which could be good for the adsorption of the negatively charged phosphate groups of DNA on the nanoparticle surface. However, a large amount of aluminum is toxic for cells,^[118] so we only partially substituted calcium with aluminum. In addition, magnesium and aluminum are known to inhibit the growth of calcium phosphate crystals resulting in smaller particles, which can be easier taken up by cells.^[82,117,119-121]

Chowdhury *et al.* successfully incorporated fibronectin and Mg^{2+} into calcium phosphate particles in order to achieve a higher transfection efficiency than the classical precipitation method.^[120] Bhakta and co-workers used magnesium phosphate nanoparticles to transfect HeLa cells and achieved a transfection efficiency comparable to that of Polyfect[®].^[82]

So, in our experiments the calcium ions were partially or fully replaced with alternative cations. We reduced the calcium concentration in solution and

replaced it with adequate concentrations of magnesium or aluminum as shown in Table 4.1.1.1.

Solutions of calcium nitrate with substitutions (magnesium nitrate or aluminum chloride) and diammonium hydrogen phosphate with previously adjusted pH value were mixed with a peristaltic pump at the maximum speed. Immediately thereafter the dispersion of calcium phosphate was taken with an Eppendorf pipette and mixed with a DNA solution (from salmon testes, 1 ml mL⁻¹) for functionalization and stabilization of the nanoparticles.

Table 4.1.1.1: The composition of solutions used for nanoparticle synthesis.

| Sample | Concentration / mM | | | pH | Concentration / mM | pH |
|---------|---------------------|---------------------|---------------------|-----|----------------------------------|----|
| | [Ca ²⁺] | [Mg ²⁺] | [Al ³⁺] | | [PO ₄ ³⁻] | |
| CaP | 6.25 | - | - | 7 | 3.74 | 7 |
| | | | | 8 | | 8 |
| | | | | 9 | | 9 |
| CaMgP-1 | 5.21 | 1.04 | - | 7 | 3.74 | 7 |
| | | | | 8 | | 8 |
| | | | | 9 | | 9 |
| CaMgP-2 | 3.13 | 3.13 | - | 7 | 3.74 | 7 |
| | | | | 8 | | 8 |
| | | | | 9 | | 9 |
| CaMgP-3 | 1.04 | 5.21 | - | 7 | 3.74 | 7 |
| | | | | 8 | | 8 |
| | | | | 9 | | 9 |
| MgP | - | 6.25 | - | 7 | 3.74 | 7 |
| | | | | 8 | | 8 |
| | | | | 9 | | 9 |
| CaAlP-1 | 5.21 | - | 1.04 | 7 | 3.74 | 7 |
| | | | | 7.5 | | 8 |
| | | | | 7.5 | | 9 |
| CaAlP-2 | 4.17 | - | 2.08 | 7 | 3.74 | 7 |
| | | | | 7.5 | | 8 |
| | | | | 7.5 | | 9 |
| CaAlP-3 | 3.13 | - | 3.13 | 7 | 3.74 | 7 |
| | | | | 7.5 | | 8 |
| | | | | 7.5 | | 9 |

In order to find the optimal conditions for the nanoparticles synthesis we used different amounts of DNA for the stabilization of dispersion. We varied the

amount of DNA (1 mg mL^{-1}) per 1 mL of calcium phosphate dispersion: 0.1, 0.2, 0.5 and 1.0 mL of DNA.

We also tested the influence of the pH on the particle precipitation. We adjusted the pH from 7 to 9 in all solutions of inorganic salts with 0.1 M NaOH for each combination of $\text{Ca}^{2+}/\text{Mg}^{2+}$. For experiments with $\text{Ca}^{2+}/\text{Al}^{3+}$ we adjusted the pH from 7 to 7.5, because of the precipitation of aluminum hydroxide at higher pH. The general aim was to obtain small monodisperse nanoparticles because the small particles can more easily penetrate the cell membrane and can be used as a carrier in gene therapy. The schema of nanoparticle preparation is shown in Figure 4.1.1.1.

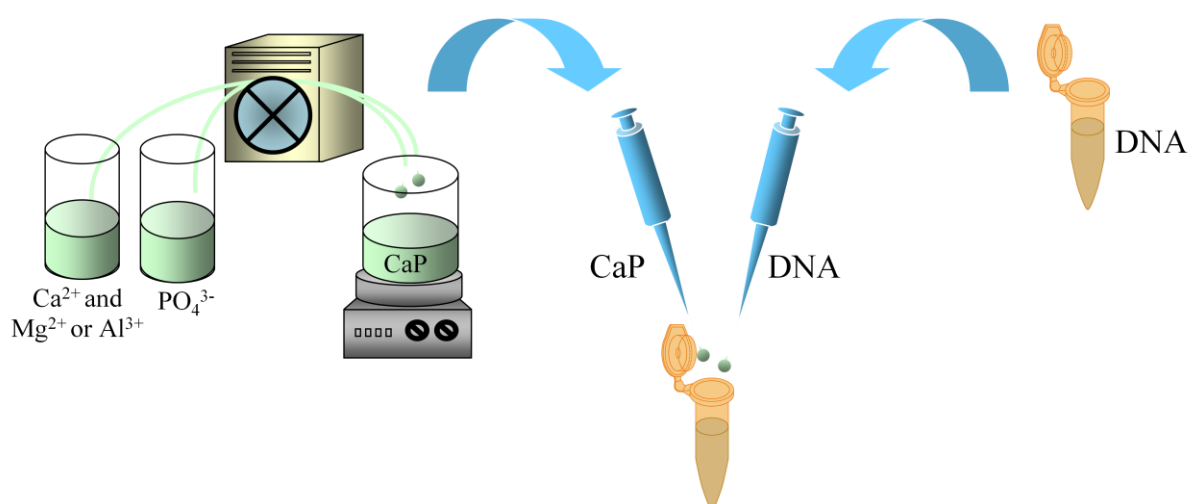


Figure 4.1.1.1: Schematic representation of synthesis of DNA-functionalized calcium phosphate nanoparticles partially or fully substituted with magnesium or aluminum.

All the samples were measured via dynamic light scattering (DLS). At all tested pH values, the nanoparticles functionalized with 0.1 and 1.0 mL of DNA per mL of the calcium phosphate dispersion showed the highest polydispersity index (0.7-1.0) at each pH indicating that the dispersions were not stable. Presumably with 0.1 mL of DNA the concentration of the nucleic acid was too low to

stabilize the nanoparticles, whereas with 1.0 mL DNA the dispersion contains too much organic matrix, so the chains of DNA are “swimming” between the calcium phosphate cores connecting them as one net. At pH 7 in all the samples only the large aggregates were observed. Moreover, in all cases the PDI was between 0.6 and 1.0 which means that data are unreliable because of large measurement error.

At pH 8 also almost all the samples showed large aggregates and PDI 0.5-1.0. The particles also were too polydisperse to be correctly analyzed by Zetasizer.

These data could be explained by the individual properties of the DNA molecules. Comparing to the synthetic polymers, DNA is a very complex molecule whose conformation is strictly determined by the presence of foreign ions and proteins. Even a rather short circular plasmid with approx. 5,000 bp could have different conformation, *i.e.* three-dimensional structure (linear, circular or supercoiled) and, thus, different availability of phosphate groups for a binding. Therefore, interaction of the DNA with calcium phosphate does not have a well-defined geometry. Thus, PDI 1.0 can also be measured even for the pure DNA solution because of the different conformations and cross linking of the DNA chains. It complicated the interpretation of the obtained data. However, when the nanoparticles have more define structure, the PDI can be reduced.

At pH 9 the PDI of the samples was smaller (0.2-1.0) and some data could be taken into account. If we used 0.2 mL of DNA per mL of the calcium phosphate dispersion the PDI was usually between 0.2 and 0.5. In this case we observed not only large aggregates but also the nanoparticles of 120-170 nm. The DLS data are shown in Table 4.1.1.2.

Table 4.1.1.2: Size distribution of the DNA-functionalized calcium phosphate nanoparticles synthesized at pH 9. Dynamic light scattering data show intensity statistics and are presented only for particles smaller than 250 nm. Large aggregates of DNA (>1 μm) were always present.

| Sample | 0.2 mL DNA per mL of calcium phosphate dispersion | | |
|----------------|---|------------------------------|-----|
| | PDI | Size of small particles / nm | % |
| CaP | 0.3 | 174 | 78 |
| | | 28 | 9 |
| CaMgP-1 | 0.4 | 167 | 9 |
| CaMgP-2 | 0.5 | 160 | 9 |
| CaMgP-3 | 0.6 | 155 | 14 |
| MgP | 0.8 | 180 | 62 |
| | | 37 | 38 |
| CaAIP-1 | 0.2 | 123 | 81 |
| CaAIP-2 | 0.5 | 171 | 100 |
| CaAIP-3 | 1.0 | 36 | 100 |

For better control of the precipitation process we tried to produce the nanoparticles at low temperature to slow down the crystal growth and therefore to obtain smaller and more monodisperse particles. For this all solutions were first cooled down to 4 °C and then put into an ice bath as shown in Figure 4.1.1.2.

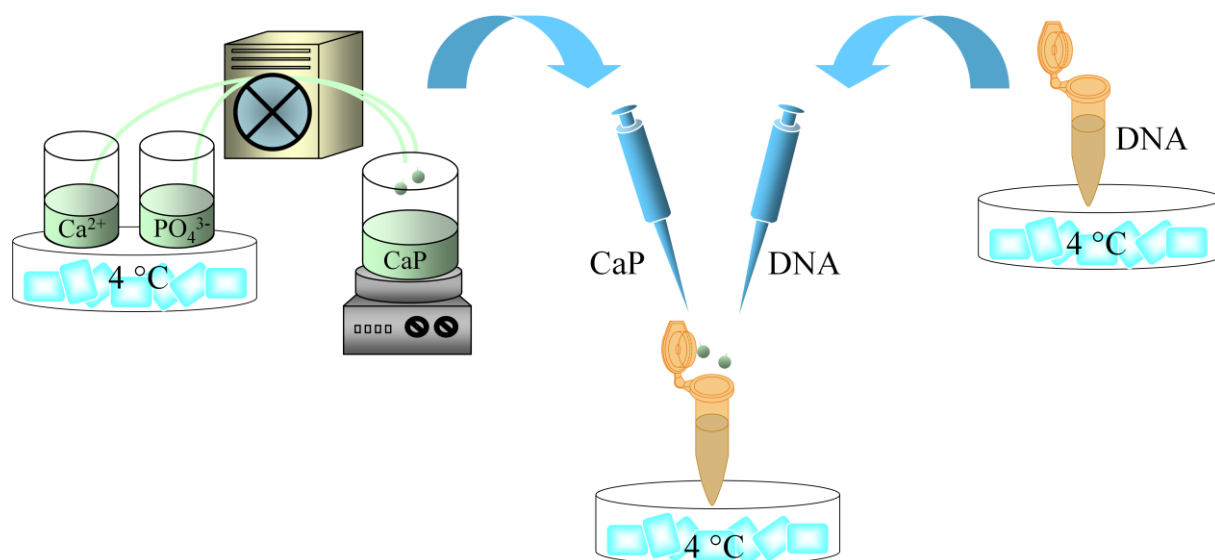


Figure 4.1.1.2: Schematic setup of nanoparticle synthesis at 4 °C.

Solutions of calcium nitrate with substitutions (magnesium nitrate or aluminum chloride) and diammonium hydrogen phosphate were mixed with a peristaltic pump at the maximum speed. Immediately thereafter the dispersion of calcium phosphate was taken with an Eppendorf pipette and mixed with a pre-cooled DNA solution (1 ml mL^{-1}) as shown in Figure 4.1.1.2. We used 0.2 mg of DNA per mL of the calcium phosphate dispersion and pH 9 as the optimal parameters for the synthesis of monodisperse nanoparticles.

The obtained nanoparticles were characterized by scanning electron microscopy and DLS. DLS measurements of all samples showed large aggregates with very high PDI (usually around 0.7). However, the small nanoparticles with a size of 50-120 nm were present in each sample. The zeta potential of all particles was always negative around -30 mV.

To check the DLS data we performed scanning electron microscopy of the particles. It showed a much smaller particle size than that obtained by DLS.

Partially it is due to the fact that DLS measurements show the hydrodynamic radius of the particles whereas electron microscopy shows an inorganic core.

Figure 4.1.1.3 shows SEM images of nanoparticles obtained by precipitation at 4 °C with and without added magnesium. Pure calcium phosphate nanoparticles had a spherical morphology with particle size of 80-100 nm, showing a reduction of particle size with an increase of the magnesium content. However, morphologically defined particles with a size of 30-50 nm were observed only up to a magnesium concentration of 3.13 mM. A further increase of the magnesium content led to the formation of two fractions of poorly defined spherical particles: 150 nm and 15 nm. Pure magnesium phosphate particles show only small particles of approx. 25 nm.

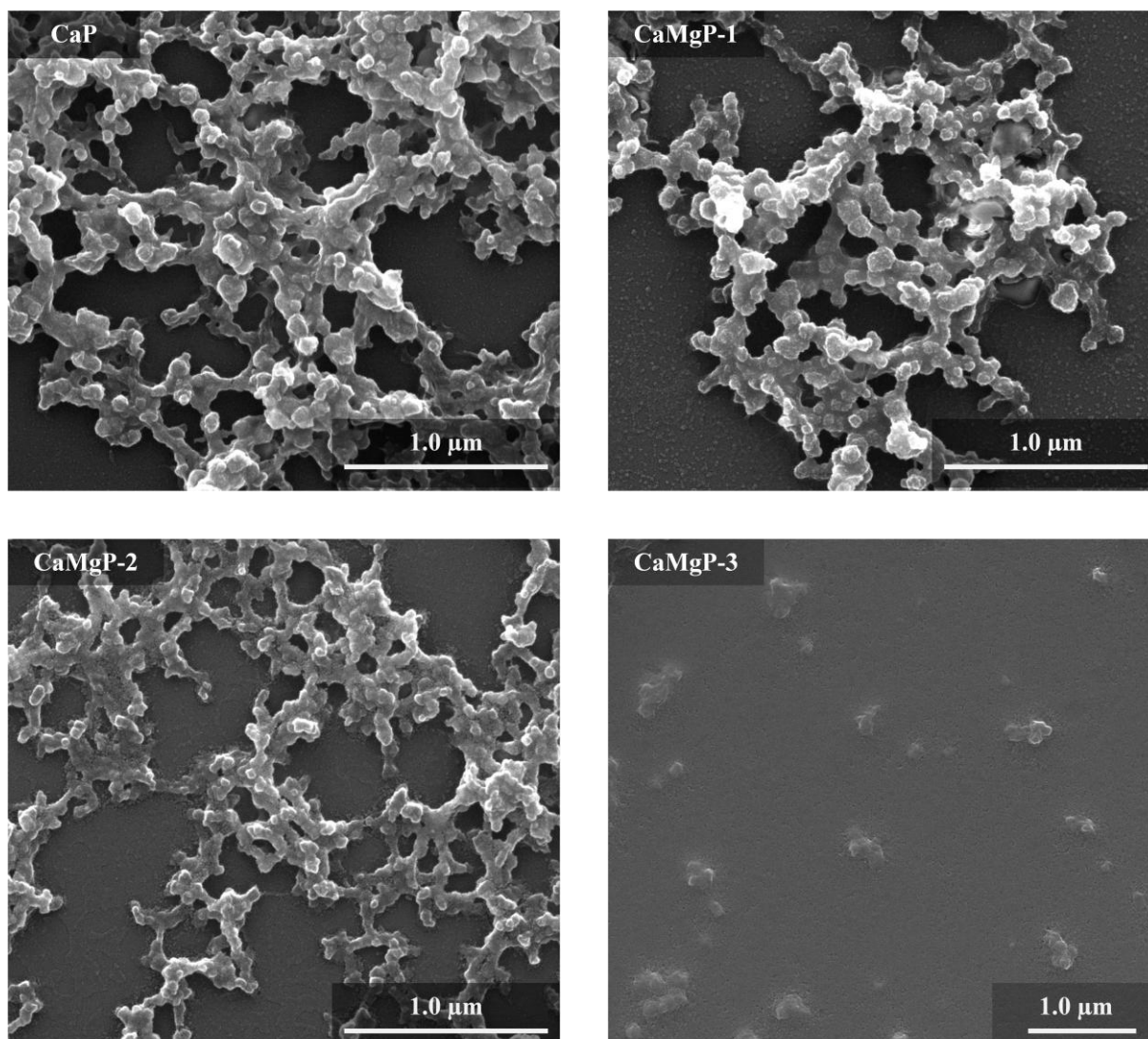


Figure 4.1.1.3: Scanning electron micrographs of calcium phosphate nanoparticles synthesized with and without magnesium additives at 4 °C. We performed the nanoparticle synthesis at pH 9 and used 0.2 mg of DNA per mL of the calcium phosphate dispersion.

The nanoparticles synthesized with aluminum substitutions showed the same tendencies (Figure 4.1.1.4). The particles with low aluminum content showed two different morphologies: Needle-like structures and small spherical particles with a size around 20 nm. The subsequent increase of aluminum content resulted

in small monodisperse but very poorly defined spherical particles with a size around 20 nm.

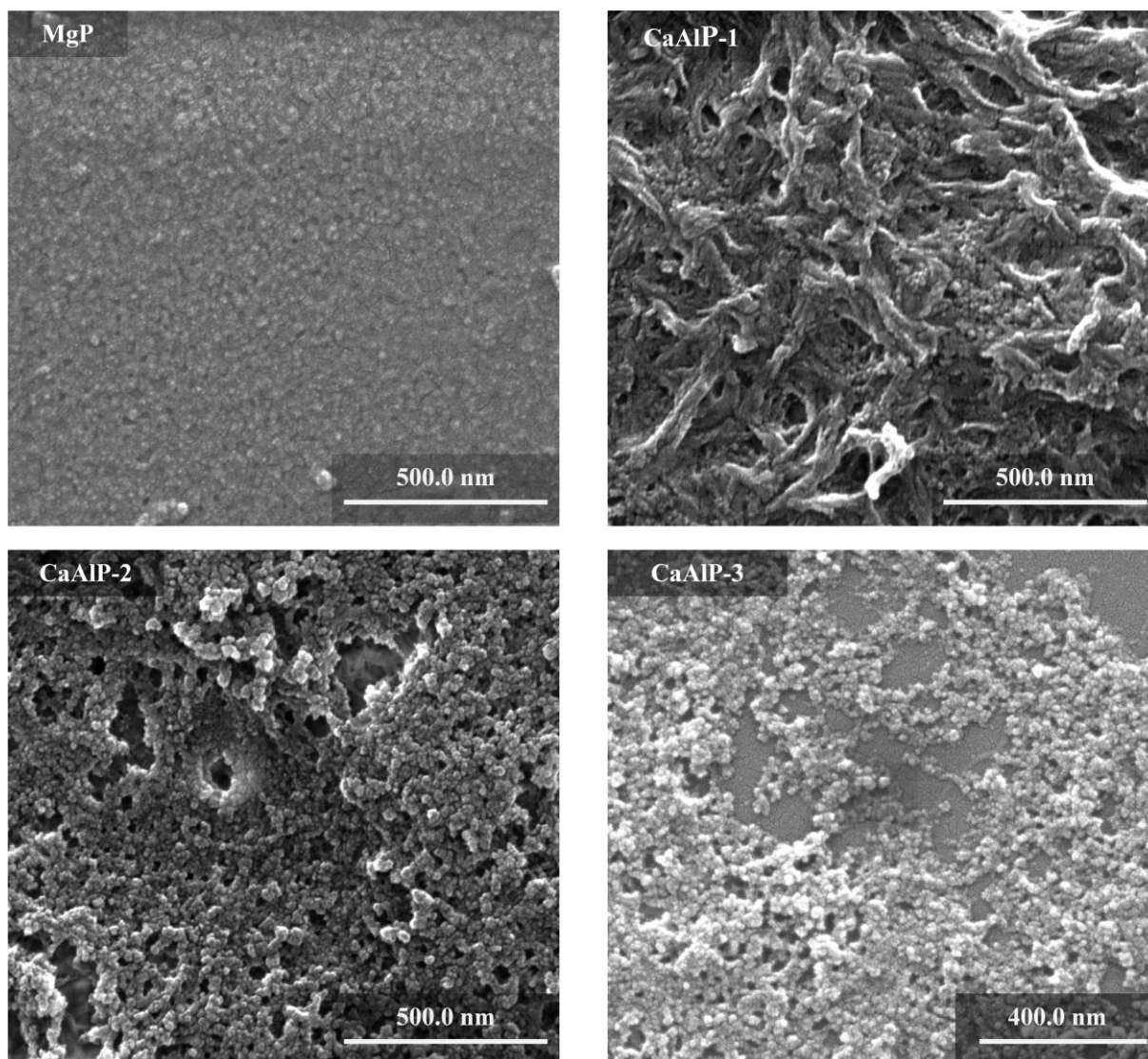


Figure 4.1.1.4: Scanning electron micrographs of magnesium phosphate nanoparticles and aluminum-substituted calcium phosphate nanoparticles precipitated at 4 °C. We performed the nanoparticle synthesis at pH 9 and used 0.2 mg of DNA per mL of the calcium phosphate dispersion.

These data also correlate with those previously obtained and described in Ref.^[121] There we showed that the crystallinity of the samples is reduced with an increase of foreign cation content. In the samples which contained magnesium the completely amorphous structure is reached with a magnesium concentration of 5.21 mM (almost complete substitution of calcium ions with magnesium) and aluminum concentration of 3.13 mM (partial substitution of calcium with aluminum).^[121]

4.1.2 Transfection with calcium phosphate nanoparticles substituted with Al³⁺ and Mg²⁺

The previously described nanoparticles were investigated as carriers of DNA into cells for cell transfection. For these experiments we used NIH3T3 cells (a fibroblast cell culture). The cells were cultured in RPMI 1640 medium supplemented with 10 % fetal calf serum (FCS), 2 mM glutamine, 100 U mL⁻¹ penicillin and 100 µg mL⁻¹ streptomycin at 37 °C under 5% CO₂. 24 h before the transfection the cells were seeded onto 24-well plates with a density 5·10⁴ cells per well.

The cells were transfected with pcDNA3-EGFP to induce the production of enhanced green fluorescent protein (EGFP).^[100,122,123] NIH3T3 cells were incubated in cell culture medium which contained 40 µL of the nanoparticle dispersion per mL of RPMI 1640 for 7 h, then the transfection medium was replaced with fresh cell culture medium and the cells were further incubated for 48 h. The detection of the transfection efficiency was carried out with a fluorescence microscope. The efficiency was calculated as a percentage of fluorescing cells to the total number of cells.

As control we used the classical standard calcium phosphate precipitation method described by Graham and van der Eb.^[83]

The results of the transfection are shown in Table 4.1.2.1 and in Figure 4.1.2.1. Not all the particle types led to a successful cell transfection. Most of the transfection media show very low or no transfection efficiency.

Table 4.1.2.1: Transfection efficiency of magnesium- and aluminum-substituted calcium phosphate nanoparticles synthesized at 4 °C on NIH3T3 cells.

| Sample | Transfection efficiency / % |
|-------------------------------|-----------------------------|
| CaP | 5.7 |
| CaMgP-1 | 5.5 |
| CaMgP-2 | 0 |
| CaMgP-3 | 0 |
| MgP | 0 |
| CaAlP-1 | 1.5 |
| CaAlP-2 | 1.7 |
| CaAlP-3 | 0 |
| Standard precipitation method | 6.5 |

Particles which consisted only of the calcium phosphate core and a DNA shell showed transfection efficiency close to that of the standard precipitation method: 5.7 and 6.5 %, respectively. The nanoparticles where only a small part of calcium was substituted with magnesium (CaMgP-1) showed a similar efficiency: 5.5 %, whereas the nanoparticles with higher content of magnesium or with aluminum substitutions showed very little or no transfection. There are two possible explanations for such low transfection efficiency because the particles showed two morphologies in SEM. This could be a result of the poor crystallinity of smaller particles as described in Ref.^[121] which led to a fast and complete dissolution of the nanoparticles in the acidic medium of the endosomal/lysosomal compartment or in the cytoplasm and, hence, their

inability for successful DNA delivery to the cell nucleus. The larger particles, however, could be aggregated in solution, thus forming too large agglomerates to be taken up by cells.

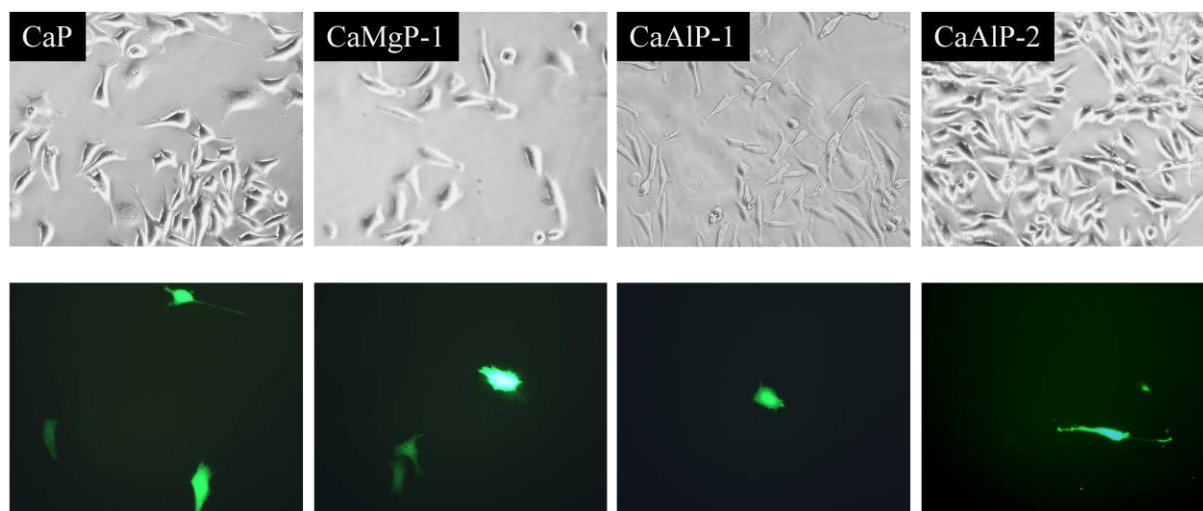


Figure 4.1.2.1: Transmission micrographs (**top row**) and fluorescence micrographs (**bottom row**) of successfully transfected cells. Transfection experiments were performed with magnesium- or aluminum-substituted calcium phosphate nanoparticles on NIH3T3 cells ($N=5$).

4.1.3 Conclusion

We were able to synthesize small calcium phosphate nanoparticles. As optimal conditions we used pH 9 and 0.2 mg of DNA per mL of calcium phosphate dispersion with a partial substitution of calcium with magnesium or aluminum and low temperature. Under these conditions, we synthesized nanoparticles with a negative zeta potential (around -30 mV), spherical morphology and a size around 80-20 nm. However, these nanoparticles were on the one hand aggregated in solution. On the other hand, the smaller particles were poorly crystalline and can therefore hardly act as gene carriers. This all resulted in low transfection efficiency. The transfection efficiency was tested on NIH3T3 cells

using pcDNA3-EGFP. The maximal transfection efficiency of 5.7 and 5.5 % was found for pure calcium phosphate nanoparticles and magnesium-substituted calcium phosphate nanoparticles, respectively. This efficiency was comparable to that of the standard calcium phosphate precipitation method.

4.2 Tracking of the intracellular calcium level during the transfection of cells

4.2.1 Marking of nanoparticles with $^{45}\text{Ca}^{2+}$

The calcium phosphate transfection method is widely used for many years in molecular biology.^[83,89] However, the exact mechanism of the transfection, *i.e.* of the DNA entry and intracellular release, remains still unclear. Moreover, a poor reproducibility of the method and its relatively high toxicity indicates that a more detailed understanding of the process can help enhance the transfection efficiency. Sokolova *et al.* reported a new transfection method based on the precipitation of calcium phosphate nanoparticles and their subsequent functionalization with plasmid DNA.^[91,99,116] The efficiency of this method was additionally increased by using additional shells of calcium phosphate for the DNA encapsulation, thus protecting it from the enzymatic degradation as shown in Figure 4.2.1.1.^[100] This method proved to be more efficient than classical calcium phosphate method and comparable with the commercial polymeric transfection reagent Polyfect[®]. However, the question of the toxicity of the method remained unclear. Usually the intracellular calcium concentration is maintained on a very low level (around 10^{-10} M according to Ref. ^[117]) and its increase could lead to the disturbance of calcium-dependent signaling pathways or even intracellular osmotic balance, which could be both fatal for cell.

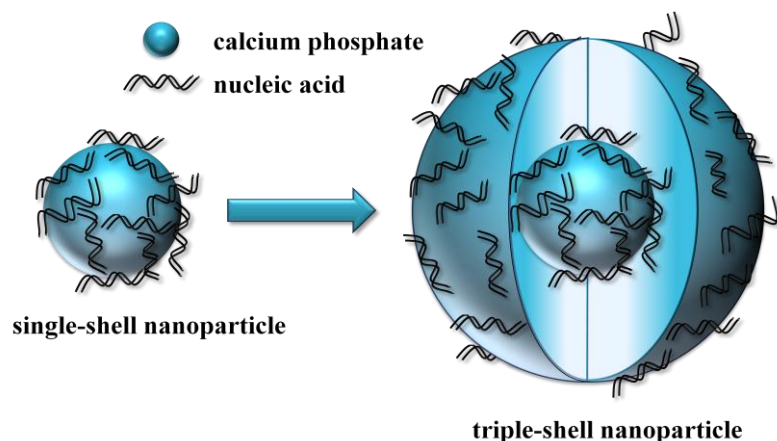


Figure 4.2.1.1: Schematic representation of single- and triple-shell nanoparticles.

Here we analyzed the comparative toxicity of calcium phosphate-based methods and the distribution of calcium phosphate inside the cells to better understand the calcium phosphate-based transfection mechanisms for the further application of nanoparticles *in vivo*.

To reach a successful transfection, DNA should enter the cell by endocytosis and undergo subsequent nuclear targeting (Figure 4.2.1.2).^[38,39,124] Loyter *et al.* reported that calcium phosphate precipitates enter the cell by endocytosis after about 1-2 h.^[125] These data were also confirmed for the TRITC-BSA-marked nanoparticles by Sokolova *et al.*^[126] The CaP-DNA precipitates should escape the endosome before its fusion with lysosome to prevent the lysosomatic degradation of DNA. In the lysosome, the proton pump induces pH decrease followed by the dissolution of calcium phosphate and the release of DNA. There the DNA will be later cleaved by lysosomal nucleases. Thus, DNA needs to leave the lysosome before the protective calcium phosphate will be completely dissolved and it becomes available for nucleases. Nevertheless, Maitra^[92] indicated that partial dissolution of calcium phosphate can destabilize the lysosomal membrane and enhance the release of remaining nanoparticle and DNA into the cytoplasm. There DNA will move in the direction of the

nucleus.^[38,126] However, it is still unclear whether the nanoparticle itself penetrates the nuclear membrane, or whether the DNA enters the nucleus alone. Figure 4.2.1.2 shows a schematic representation of the transfection mechanism.

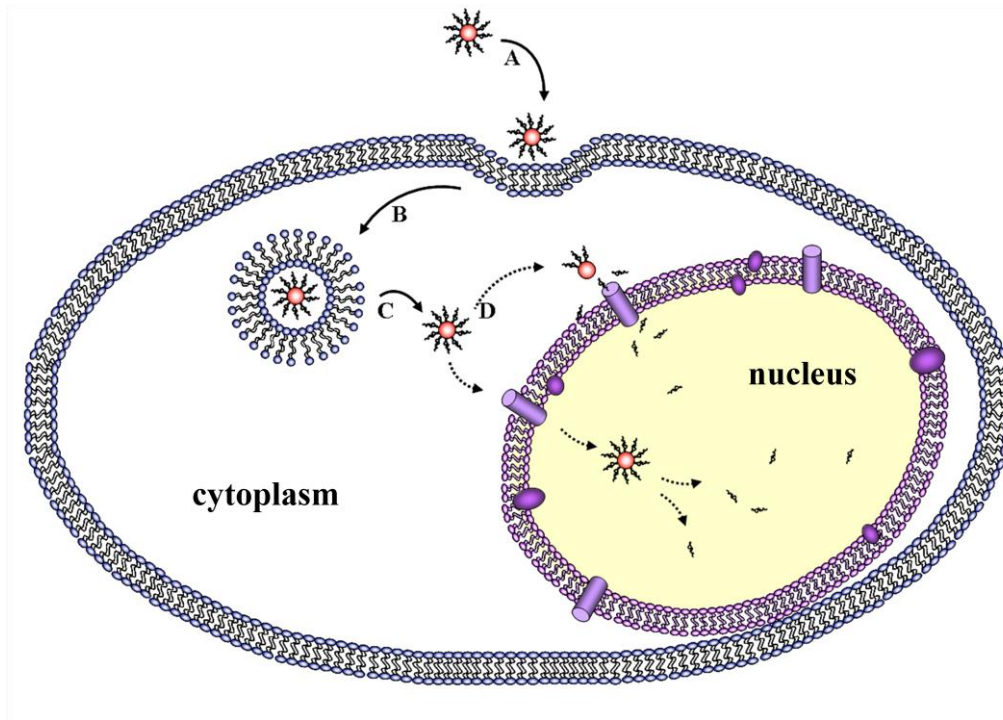


Figure 4.2.1.2: Schematic representation of the transfection mechanism. **A:** Nanoparticle attaches to the cell membrane; **B:** Nanoparticle enters the cell by endocytosis; **C:** Endosomal escape; **D:** Nuclear targeting (nanoparticle or detached DNA enters the nucleus).

Sokolova *et al.* showed that after 6 h of transfection the nanoparticles were concentrated in the nuclear region. Loyter *et al.* and Orrantia and Chang indicated that nanoparticles can also enter the nucleus.^[38,125] Inside the nucleus, DNA can be directly expressed, resulting in a transient transfection (that will disappear after several cell division cycles), or intercalate into the genome resulting in a stable transfection. However, how the calcium phosphate-based transfection influences the intracellular calcium balance was never investigated.

Nevertheless, Ewence *et al.* recently reported that calcium phosphate crystals from the atherosclerotic plaques induced a rapid increase of the intracellular calcium concentration which caused the death of 50 % of the investigated vascular smooth muscle cells.^[106] They also found that this increase occurs due to the dissolution of calcium phosphate crystals in the lysosomes which causes the rupture of the latter, an overall increase of calcium concentration in the cytoplasm, and, finally, cell death. Thus, we were interested to find out, which side effects can occur during the calcium phosphate-based transfection, and whether it also causes cell damage or cell death.

We investigated the maintenance of calcium balance during calcium phosphate-mediated transfection techniques on T24 cells (a human bladder carcinoma cell line). To follow the intracellular calcium we used the radioactive calcium isotope, $^{45}\text{Ca}^{2+}$ as calcium chloride solution, which emits β -radiation and has a half-life period of 162 days. Thus, we could differentiate between calcium taken up by cells and remaining in the medium. We performed the classic calcium phosphate transfection^[39,83,127,128] and transfection with single-shell calcium phosphate nanoparticles as described by Welzel *et al.*^[116,129] and multi-shell nanoparticles as described by Sokolova *et al.*^[91,100] As controls we used untreated cells and cells incubated with the same amount of dissolved calcium ions (as calcium chloride solution) to examine the intracellular calcium level under the conditions of increase of the calcium concentration in cell culture medium. A scheme of the transfection experiments is shown in Figure 4.2.1.3.

After each indicated time point (1 h, 7 h, 48 h and 1 week after the transfection) an aliquot of the cell culture medium was taken to measure the radioactivity of the medium. Simultaneously, the cells were lysed with a 1 % Triton X-100 buffer and one aliquot of the lysate was used to measure the intracellular protein concentration, whereas another aliquot was used for the radioactivity measurement. 7 h after the transfection the cell culture medium contained

^{45}Ca calcium was replaced with a fresh medium without $^{45}\text{Ca}^{2+}$. Thus, 48 h and 1 week after the transfection the detectable amount of calcium was much lower and only calcium which was pumped out of the cells or was adsorbed on the cell membrane was detected.

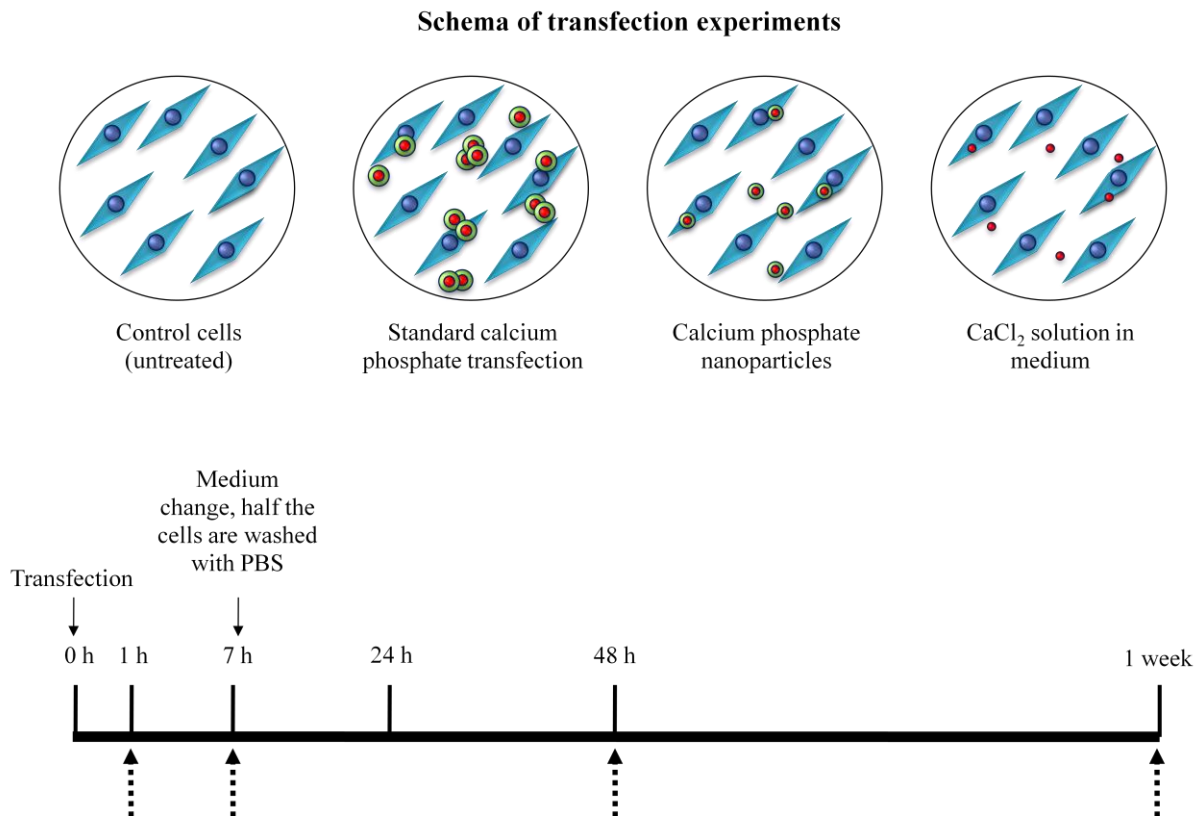


Figure 4.2.1.3: Schema of the transfection experiments. **Top schema:** Types of transfection media used to test the amount of calcium taken up by the cells during transfection. **Bottom schema:** Experimental time points. The time points of radioactivity measurements are indicated by dotted arrows.

The results of radioactive measurements are shown in Figures 4.2.1.4. and 4.2.1.5. The addition of the $^{45}\text{CaCl}_2$ solution alone to the cell culture medium had almost no influence on the intracellular calcium balance. The calcium ions remained in the medium and only a very small amount of calcium penetrated the cell membrane and was detected in the cell lysates. This corresponds to the

generally known data of the stability of the intracellular ionic balance: The intracellular calcium concentration is maintained on a very low level (lower than 10^{-10} M).^[117]

However, after the incubation of the cells with the standard calcium phosphate precipitates for 1 or 7 h, the amount of calcium detected in the cell culture medium did not differ from the theoretical value, *i.e.* from the added to the medium amount of radioactive 45 calcium (Figures 4.2.1.4). This happened presumably due to the very small volume of cells compared to the volume of medium. Therefore, such minor changes were not possible to detect. The application of calcium phosphate/DNA nanoparticles showed also only minor decrease of 45 calcium concentration in the medium.

After 7 h of incubation of cells with transfection media, the media were replaced with fresh medium without 45 calcium and therefore only the calcium which was already taken up by cells and then pumped out could be detected. So, after 48 h and 1 week of the incubation only the intracellular calcium or calcium adsorbed on the cell membrane was detected. These values also did not differ between all three methods, although they were much smaller than the values detected for the first 7 h.

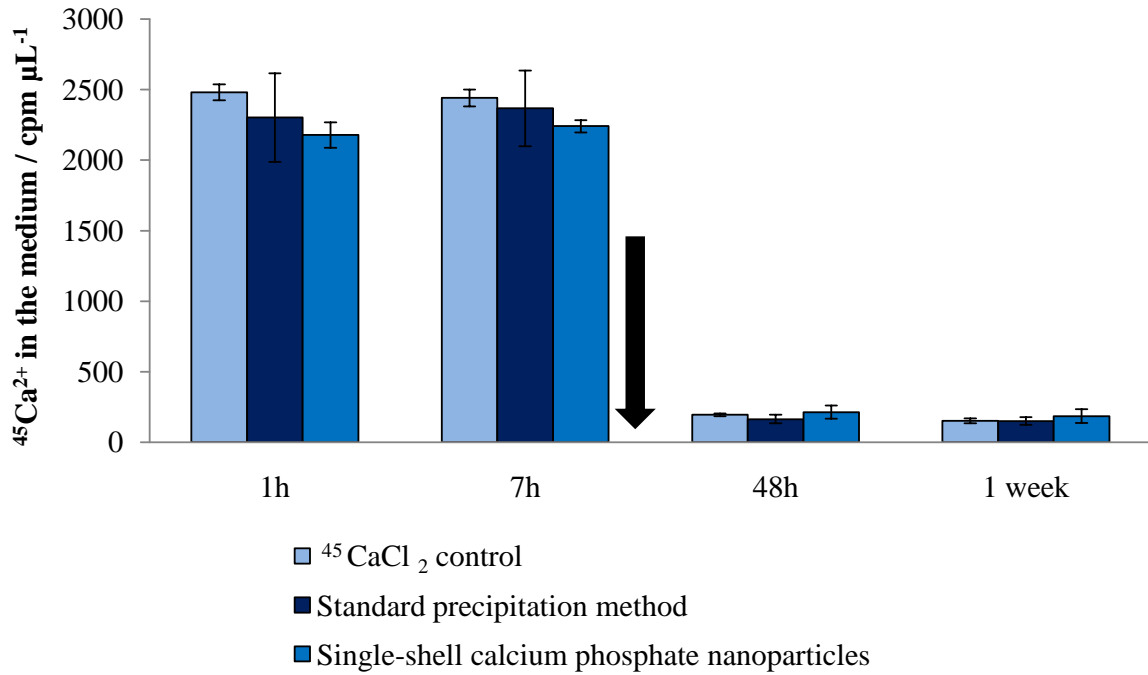


Figure 4.2.1.4: The radioactivity of ^{45}Ca per μL cell culture medium at different time points after the incubation with different transfection media. The arrow indicates the medium exchange after the transfection. The radioactivity of control (untreated) cells was always very close to zero and, therefore, is not shown on the diagram. The error bars represent the standard error of the mean ($N=4$).

The analysis of the cell lysates is shown in Figure 4.2.1.5. We observed that the maximum intracellular ^{45}Ca concentration was achieved after 7 h of incubation of cells with calcium-containing dispersions, independent from the transfection method. Nevertheless, the amount of intracellular calcium was very different for each method. The application of calcium phosphate nanoparticles for the transfection resulted in a much smaller increase of the intracellular calcium concentration than that of standard calcium phosphate precipitates (7 times). Although the transfection efficiency of the calcium phosphate nanoparticles and the standard calcium phosphate precipitates was equal, as

shown in Section 4.1 and in Ref.^[100], the amount of calcium used per well was very different (we used 4.2 μg and 835 μg of Ca per mL of cell culture medium, respectively), as well as the amount of detected intracellular calcium 7 h after the transfection. Nevertheless, the ratio of the intracellular calcium concentration between cells transfected with the standard method and nanoparticles was only 7 times, whereas the difference in the added amounts of calcium for the transfection was almost 200 times. Such differences are due to the optimized transfection protocols described in Ref.^[83,100] Thus, we used stock solutions of CaCl_2 of concentrations 2.5 M and 6.25 mM for synthesis of calcium phosphate precipitates in the case of the standard calcium phosphate transfection method and calcium phosphate nanoparticles, respectively. Therefore, the smaller amount of calcium in the form of DNA-functionalized calcium phosphate nanoparticles was far more effective.

48 h and 1 week after the transfection, the intracellular calcium level was still very high for cells treated with the standard calcium phosphate precipitates. That means that the fast increase of the calcium concentration during the transfection (first 7 h) made it almost impossible for the cell to pump out all the excessive calcium during the further incubation time. In contrast, the transfection of the cells with calcium phosphate/DNA nanoparticles resulted in a reduction of the intracellular calcium concentration to the base level within 48 h.

The addition of CaCl_2 solution alone to cell culture medium had almost no influence on the intracellular calcium balance. The calcium ions remained in medium and only a very small amount of calcium has penetrated the cell membrane and was detected in the cell lysates.

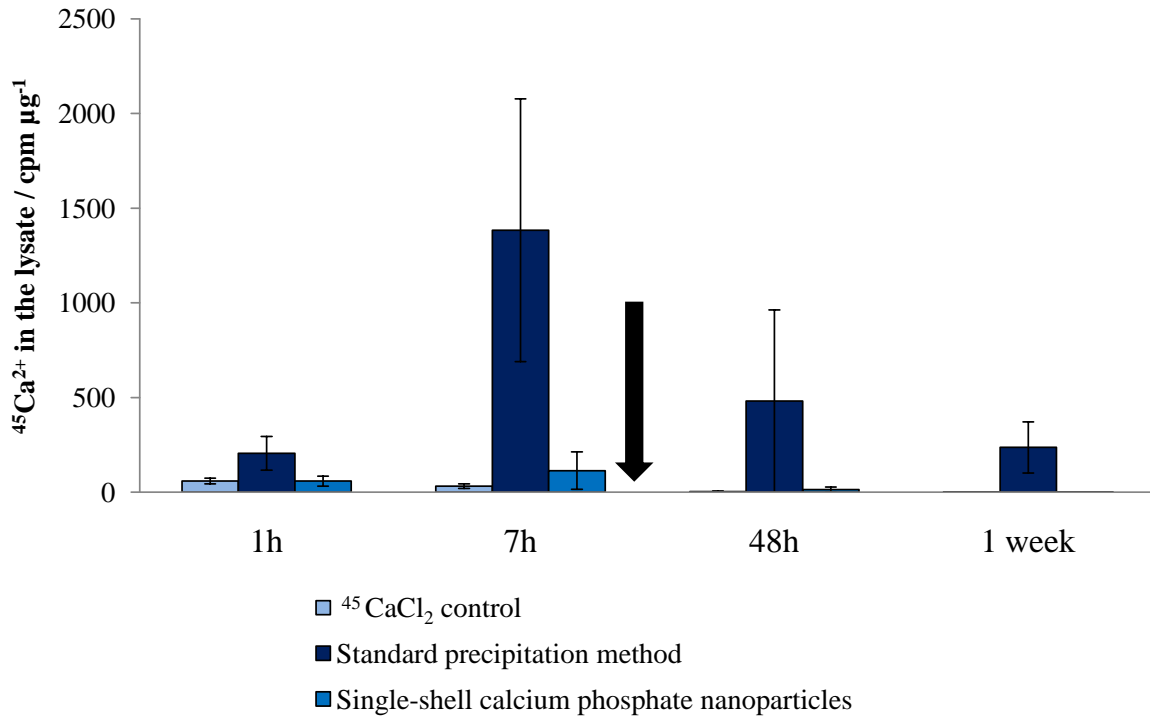


Figure 4.2.1.5: The radioactivity of ^{45}Ca of the cell lysates per μg protein at different time points after the incubation with different transfection media. An arrow indicates the medium exchange after the transfection. The radioactivity of control (untreated) cells was always very close to zero. The error bars represent the standard error of the mean. For standard precipitation method and calcium phosphate nanoparticles the significance is $P < 0.05$ ($N=4$).

To check whether all calcium was taken up during the first 7 h of transfection and not later, we washed all the samples three times with PBS after the first 7 h of transfection to remove all the particles or calcium ions that were attached to the cell membrane. Afterwards the cells were incubated for further 48 h or 1 week in cell culture medium without ^{45}Ca calcium. Surprisingly, the amount of intracellular calcium was much smaller for the samples which were washed with PBS (Figure 4.2.1.6). That means that the calcium phosphate nanoparticles or calcium ions were partially adsorbed on cell surface but not yet inside the cells

so that they could be easily removed by additional washing steps before the medium change. However, when these washing steps were not performed, the particles or ions would be easily taken up by cells during the further incubation time and will also contribute to the successful transfection. Moreover, however minor the real intracellular calcium concentration after the washing steps was, the highest content of 45 calcium was still observed after the standard calcium phosphate transfection. The additional argument is that in a possible application of the gene therapy *in vivo* it will be impossible to wash the cells with PBS. Therefore, we can only conclude that most of the calcium phosphate nanoparticles or calcium ions are adsorbed on the cell membrane during the first 7 h of transfection and will enter the cell only during further incubation time.

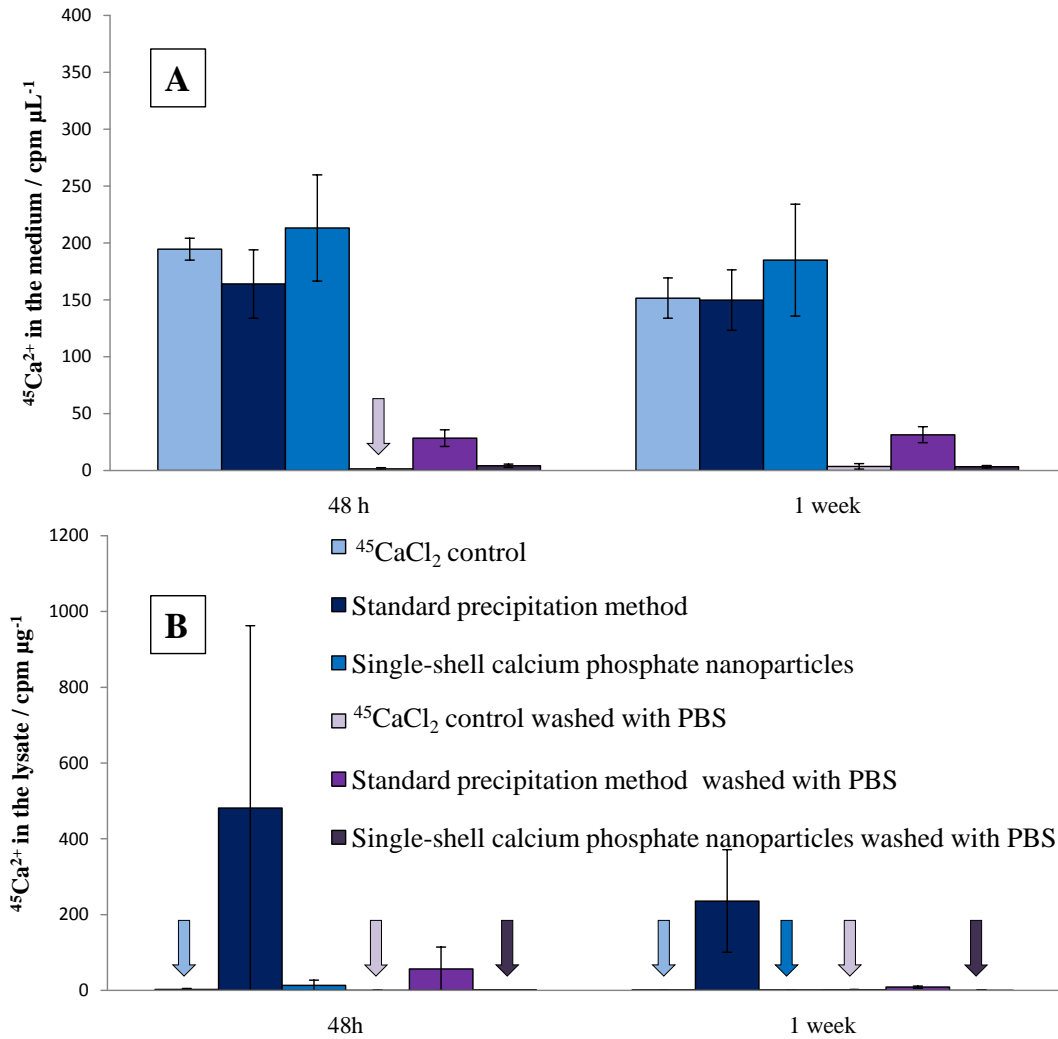


Figure 4.2.1.6: The radioactivity of ^{45}Ca per μL of the cell culture medium (**A**) and per μg of protein in the cells (**B**) after the incubation with different transfection media. After the 7 h of transfection the cells were washed three times with PBS to remove all calcium attached to the cell membrane and to exclude its subsequent penetration into the cells. The arrows indicate very low calcium content in the samples. The error bars represent the standard error of the mean ($N=4$).

4.2.2 Monitoring of the internal calcium level using the calcium-sensitive dye Fura-2

We performed the measurements of intracellular calcium changes in cooperation with the group of Prof. R. Heumann at the Chair of Molecular Biochemistry at the Ruhr-University of Bochum. The time-lapse microscopy of transfected cells was performed mainly by our cooperation partner Sebastian Neumann.

To confirm the results obtained with radioactive $^{45}\text{Ca}^{2+}$ we also performed the measurements of the intracellular calcium concentration using fluorescence time lapse microscopy with the calcium-sensitive dye Fura-2. Fura-2 AM is an esterified cell-permeant form of the Ca^{2+} indicator Fura-2, a polyamino carboxylic acid. In the cytosol Fura-2 AM is completely cleaved by endocellular esterases to Fura-2 which can be excited at two wavelengths: 340 nm and 380 nm, and it fluoresces at 510 nm. These two excitation wavelengths correspond to calcium-bound and calcium-free forms of Fura-2, respectively. Therefore the ratio of the emissions at those wavelengths is directly correlated to the amount of intracellular calcium.^[130-133] Nevertheless, to obtain the quantitative data, each measurement must be previously calibrated, *i.e.* the cell must be loaded with a known amount of calcium and Fura-2 AM and the quantitative changes could be calculated. In this work we only performed qualitative measurements of intracellular calcium concentration to compare different methods.

Fura-2 shows very low cross sensitivity to the other cations (*e.g.* Mg^{2+} , Mn^{2+} or Zn^{2+}) because of its special three-dimensional structure. Four carboxyl groups form a cavity where only one Ca^{2+} ion with a radius $9.9 \cdot 10^{-11}$ m suits. If this position is occupied by smaller ions, *e.g.* Mg^{2+} , only two carboxyl groups would bind it and the complex would not be stable.

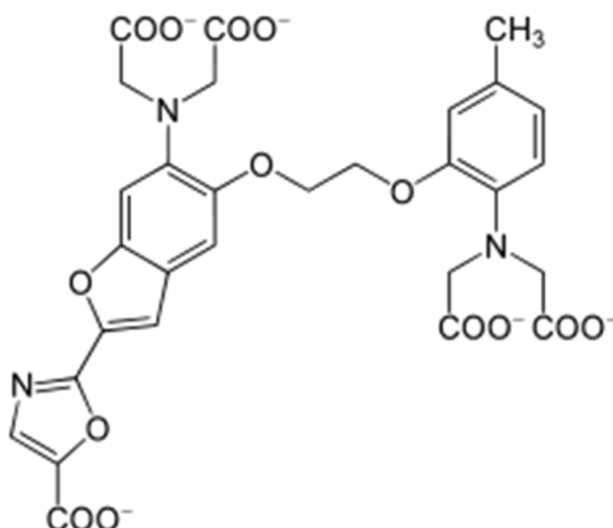


Figure 4.2.2.1: Structures of Fura-2 and Fura-2AM.^[130] Carboxyl groups bind: Fura-2, R=H; Fura-2AM, R=-CH₂-O-CO-CH₃.

Although this dye cannot detect the calcium bound to nanoparticles, it detects dissolved ionic calcium. This calcium can be detected after the dissolution of nanoparticles inside the cells. The nanoparticles penetrate the cell membrane by endocytosis. Afterwards the endocytic vehicle fuses with lysosomes.^[39,92,125]

Usually calcium phosphate undergoes partial or complete dissolution in the acidic medium of lysosomes after the activation of proton pumps in the lysosomal membrane. However, the calcium can on the one hand buffer the low pH of the lysosome, thus protecting DNA from the degradation, and on the other hand destabilize the lysosomal membrane, so that remained particles or free calcium ions can escape the lysosomes. Afterwards the particles and DNA move to the nucleus via passive diffusion or active transport by microtubules.^[134-136]

The intracellular Ca²⁺ changes are shown with the rainbow3 colour scheme in Figure 4.2.2.2 indicating the Ca²⁺-concentration. Whereas the standard calcium phosphate method caused high changes of the cytosolic Ca²⁺-concentration, nanoparticles gave only a moderate change. One can observe that during transfection with standard precipitation method each cell appeared red at a

different time, afterwards returning to its previous state. Nevertheless, some cells remained red for some hours, which corresponds to a very high intracellular calcium concentration. We can predict that this cell will undergo apoptosis within some hours (Figure 4.2.2.2).^[106,137,138]

In contrast, the cells transfected with single- and triple-shell nanoparticles showed no significant changes compared to control cells which were incubated only in cell culture medium without additional calcium. Only local and very moderate changes of the calcium concentration were observed.

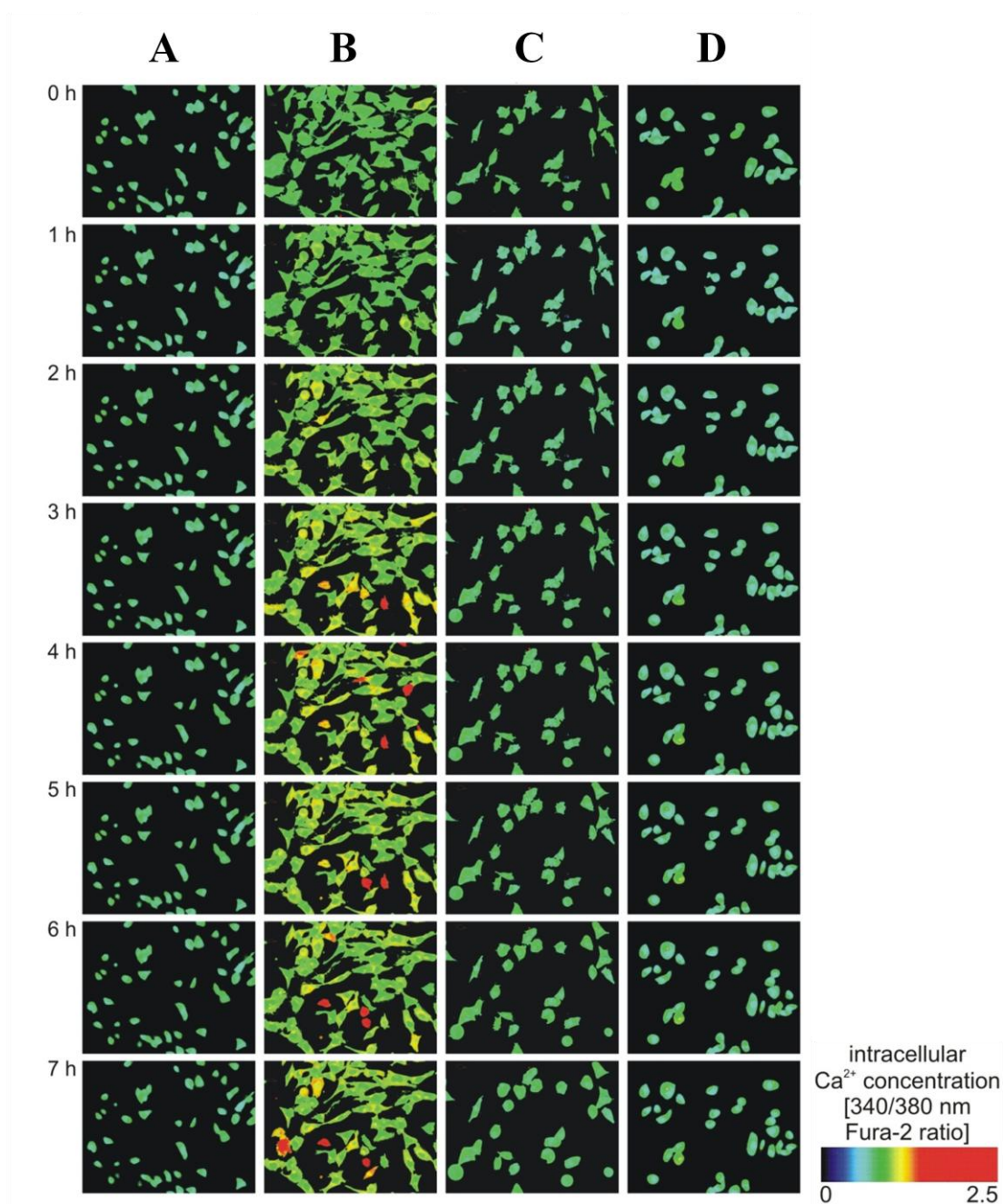


Figure 4.2.2.2: Fluorescence spectroscopic monitoring of the cytosolic Ca^{2+} -level in Fura-2-labelled T24 cells: control cells without additional calcium or transfection (A); cells during the transfection by the standard calcium phosphate method (B); cells transfected by single-shell calcium phosphate/DNA nanoparticles (C) or triple-shell calcium phosphate/DNA nanoparticles (D). Changes of the intracellular calcium level are shown with the rainbow3 scheme on the right. Magnification in all cases: 200x.

We found an interesting tendency: the distribution of the intracellular calcium was different in the case of the standard transfection and nanoparticles (Figure 4.2.2.3). In the case of the cells treated with the standard calcium phosphate precipitates we observed a general increase of the calcium concentration inside the cells. Moreover, the increase of calcium was detected in the whole cytoplasm of the cells, and not in the defined compartment. That means that after the dissolution, calcium destabilized the lysosomal membrane causing big calcium spikes and was released into the cytosol. In contrast, cells transfected with nanoparticles showed a localized increase of the calcium concentration as indicated in Figure 4.2.2.3 with arrows. Presumably, these spikes correspond to the local dissolution of nanoparticles inside the lysosomes.

All these experiments were performed at room temperature, because of the fast metabolization of Fura-2 inside the cells at 37 °C.^[130] If the cells were incubated inside the incubation chamber for 7 h, Fura-2 was metabolized within 2 to 3 h. However, although the calcium balance was impossible to follow for the whole 7 h, the observations during the first 3 h were the same as with the cells incubated at room temperature. Therefore it is likely that the calcium balance behaves in the same way at room temperature and at 37 °C.

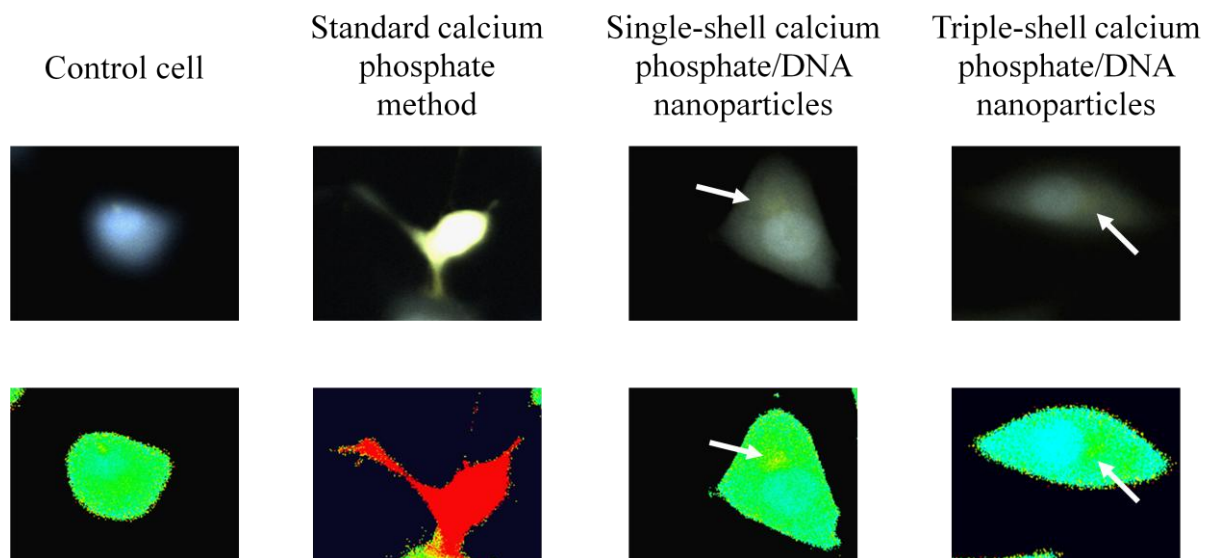


Figure 4.2.2.3: Distribution of the intracellular calcium in fluorescence microscopy (**top row**) and in the rainbow color scheme as in 3.4.2.1 (**bottom row**) in the control cells (**A**), during the transfection with the standard calcium phosphate method (**B**), single-shell (**C**) and triple-shell (**D**) calcium phosphate/DNA nanoparticles. The arrows indicate slightly increased calcium levels which are clearly localized in the cytosol of the cells transfected with nanoparticles.

Figure 4.2.2.4 shows the disturbance of intracellular calcium inside a single cell. The peaks occur at the time when calcium particles are dissolved in the cell because only ionic calcium can be detected using Fura-2. The red curve represents the ground level of the calcium concentration. In the cells treated with a CaCl_2 solution or transfected with single or triple-shell calcium phosphate nanoparticles, we observed only minor changes in the intracellular calcium concentration (green, violet and blue curves). In contrast, in the cells transfected with the standard calcium phosphate method large spikes of calcium concentration were detected (orange curve). These spikes probably correspond to the dissolution of the particles inside the cells. Afterwards the ionic pumps were turned on and the calcium concentration returns to the base level. The

excessive calcium was pumped into intracellular calcium stores (endoplasmatic reticulum and mitochondria) or out of the cell. However, above the critical calcium concentration it can become impossible for cell to pump out excessive calcium and it will die by apoptosis.^[106,137,138]

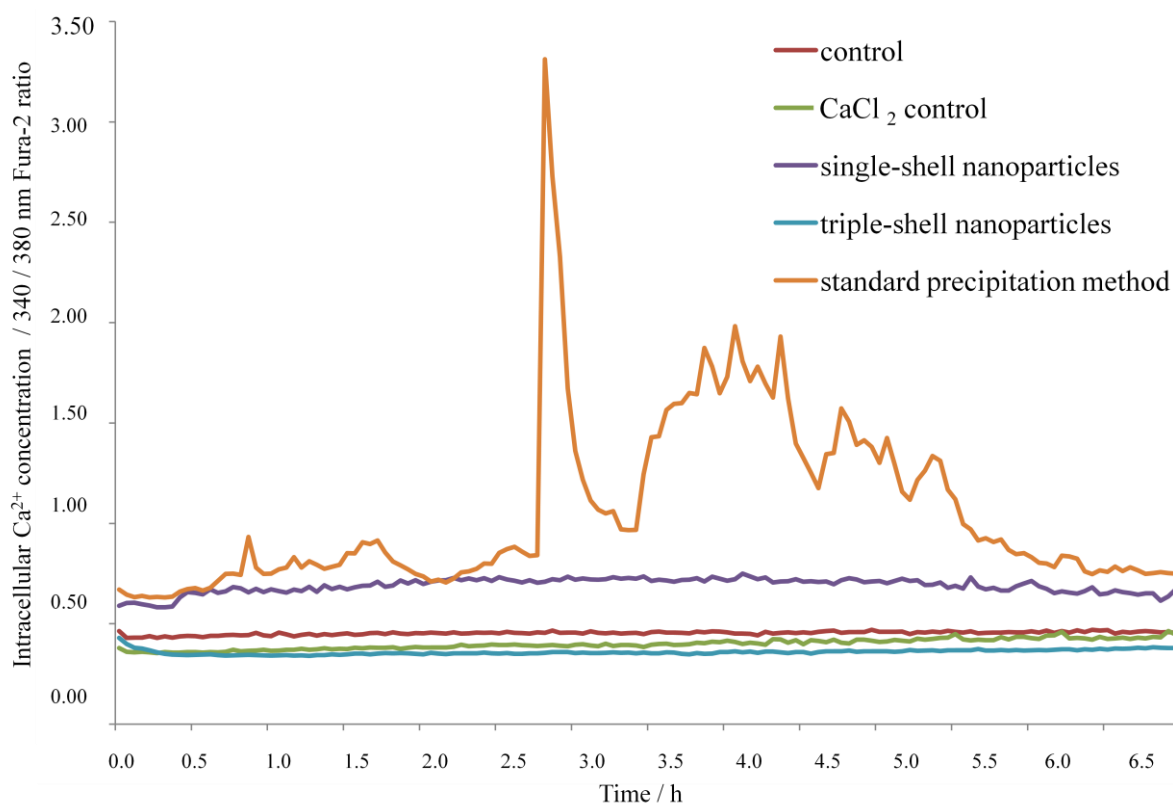


Figure 4.2.2.4: Monitoring of the intracellular calcium concentration of T24 cells (for a selected single cell per experiment) during 7 h of transfection.

However, each cell has its individual occurrence of calcium spikes during the transfection, so the statistic processing of these data gives only integrated and smoothed results as shown in Figure 4.2.2.5.

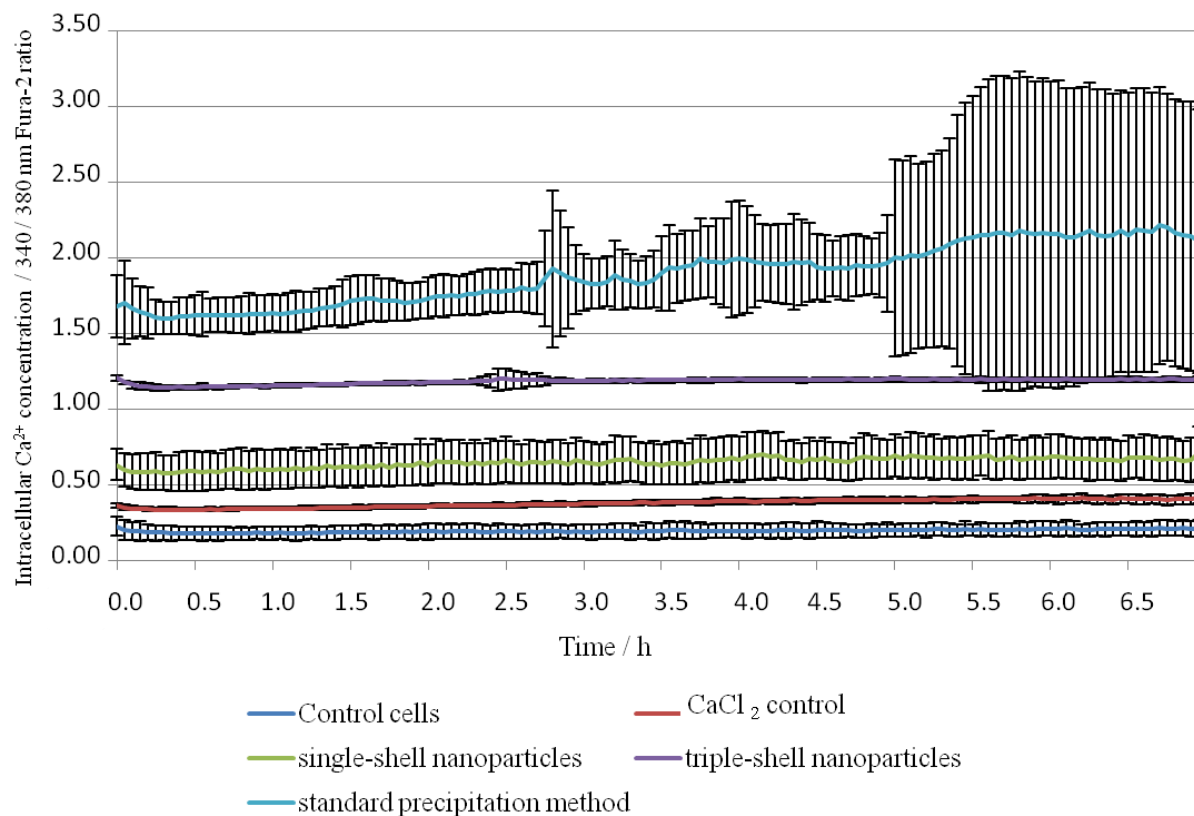


Figure 4.2.2.5: Monitoring of the intracellular calcium concentration of T24 cells ($N=10$ for control cells, $N=7$ for CaCl_2 control experiments, $N=23$ for the standard calcium phosphate method, $N=22$ for single-shell nanoparticles, $N=17$ for triple-shell nanoparticles).

However, even if the analysis of independent peaks in the whole cell culture and not in the single cell was very complicated, the vitality of cells was significantly reduced. Such a large increase of the intracellular calcium concentration disturbs the ionic balance of cells and may cause cell death. This was confirmed by the MTT viability assay. We performed a viability assay on T24 cells transfected with different methods: The calcium phosphate standard precipitation method, the commercial transfection reagent Polyfect[®], single-shell and triple-shell nanoparticles. Polyfect[®] is a dendrimer molecule of spherical architecture, whose branches terminate at amino groups. These amino groups assemble DNA into compact structures and bind to the negatively-charged cell surface. Thus,

Polyfect[®]/DNA complexes enter the cell by nonspecific endocytosis. As negative control we used untreated cells which were incubated in cell culture medium at 37 °C under 5 % CO₂.

The MTT assay showed a decrease of cell viability in the cells treated with standard calcium phosphate precipitates of about 40-50 % (Figure 4.2.2.6). The cells transfected with Polyfect[®] also showed a decrease of cell viability of 20-25 %. However, cells transfected with nanoparticles (single-shell or triple-shell) showed no significant decrease compared to the control.

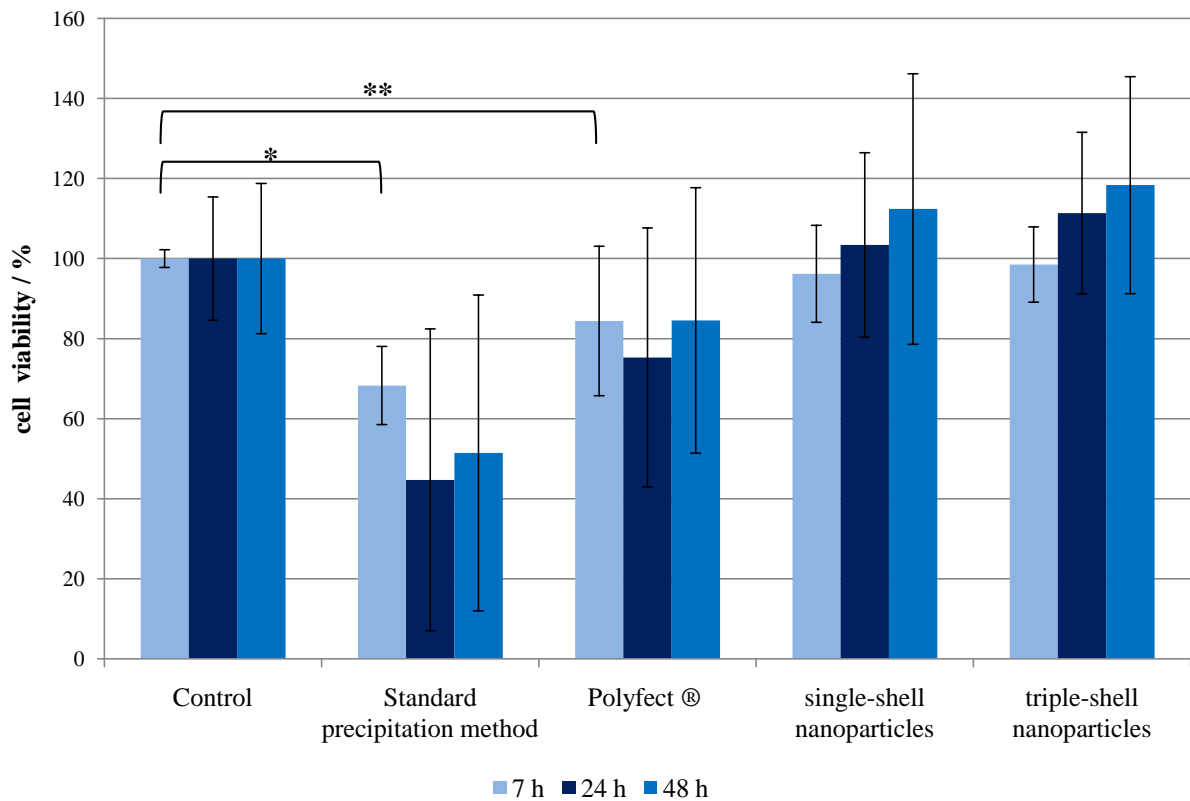


Figure 4.2.2.6: MTT assay after 7, 24 and 48 h of incubation of T24 cells with different transfection media (*: $P < 0.001$; **: $P < 0.05$), $N=4$.

To confirm these results we stained the cells with propidium iodide (PI). This dye binds to nucleic acids and cannot penetrate the cell membrane of a healthy cell. If the integrity of the membrane is damaged, the dye can pass through the

cell membrane, thus staining damaged or dead cells. We stained cell with PI 48 h after the transfection, then cells were washed twice with PBS and analyzed by fluorescence microscopy.

The results of PI staining are shown in Figure 4.2.2.7. Control cells remained healthy and intact, whereas cells with a damaged membrane appeared red. In the case of standard calcium phosphate transfection and Polyfect[®], many cells showed a red staining of cytoplasm and nucleus. However, the cells transfected with nanoparticles showed very few (equal to the control) red cells. The red dots on the images of nanoparticle-transfected cells represent PI bound to the particles on the cell surface, but not the intracellular PI. If PI penetrates the cell membrane it stains the nucleic acids inside the cells, therefore the whole cytoplasm and the nucleus appear red (as in the case of the standard calcium phosphate transfection method). If PI is not inside the cells it stains only DNA on the nanoparticles, thus PI staining appears only as red dots. These results qualitatively confirm quantitative results obtained by using the MTT assay.

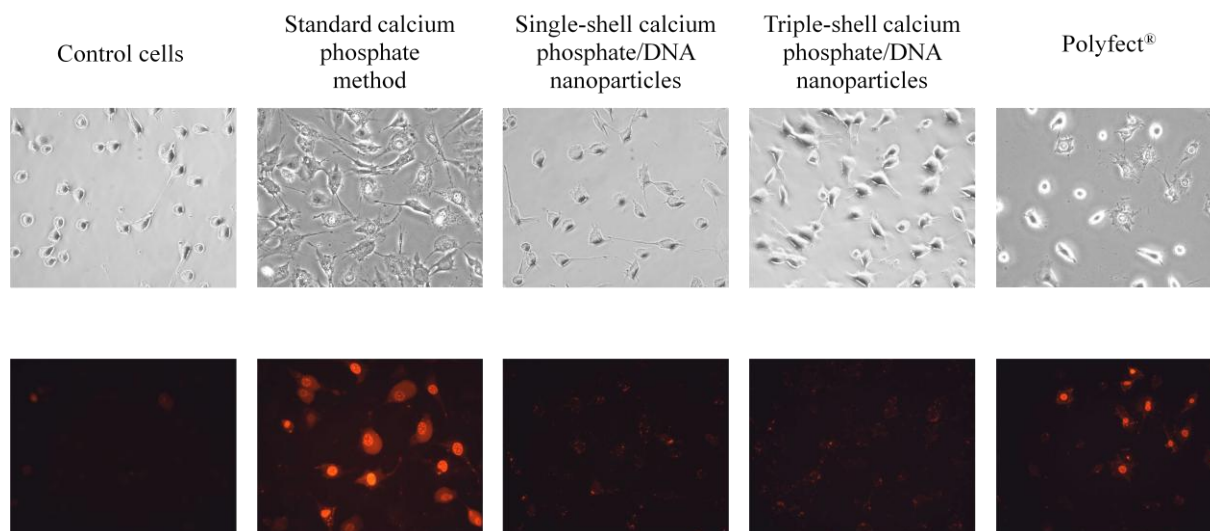


Figure 4.2.2.7: Transmission light microscopy (**upper row**) and fluorescence microscopy (**bottom row**) of T24 cells stained with propidium iodide (magnification: 200x in all cases) 48 h after the transfection. The red cells containing PI are damaged and will die soon.

4.2.3 Conclusion

We were able to follow the intracellular calcium level during different calcium phosphate-mediated transfection methods on T24 cells. We first marked the nanoparticles with $^{45}\text{Ca}^{2+}$. The maximum increase was observed in the cells transfected with the standard calcium phosphate method. In the case of nanoparticle-mediated transfection, it was much smaller.

The results were confirmed by time lapse microscopy using the Ca^{2+} -sensitive dye Fura-2. We observed the general increase of the intracellular Ca^{2+} concentration in the cytoplasm during the transfection with the standard calcium phosphate method, whereas the transfection with nanoparticles showed a smaller and localized increase of calcium concentration. Such a big increase of the intracellular calcium concentration can lead to cell death. The vitality test performed on T24 cells showed that cells transfected with the standard precipitation method suffered a decrease of the cell vitality down to 50 %.

4.3 Calcium phosphate nanoparticles functionalized with siRNA against EGFP

4.3.1 Synthesis and characterization of siRNA-functionalized calcium phosphate nanoparticles

Gene silencing represents a very promising approach for gene therapy. It was shown that oligonucleotides can be introduced into cells for the endogenous regulation of the target gene expression. The mechanism of gene silencing was first described in 1998 by Mello and Fire using the roundworm *Caenorhabditis elegans*.^[17] Since that time many gene silencing experiments were performed with double-stranded small interfering RNAs (siRNA) on different models, e.g. the fruit fly *Drosophila*, trypanosomes and plants.^[12,22,25,26,48,63,139,140] They showed that the reporter gene expression can be effectively inhibited by siRNA-induced pre-mRNA cleavage.

Gene silencing was performed according to Ref.^[139-145] with HeLa-EGFP cells using multi-shell calcium phosphate nanoparticles functionalized by siRNA against the green fluorescing protein EGFP. Double-stranded siRNA containing 22 nucleotides (22-nt) was shown earlier to induce a strong decrease in EGFP expression by post-transcriptional cleavage of the intracellular RNA.^[140] As shown by Sokolova *et al.* it down-regulates the intracellular synthesis of EGFP by interacting with pre-mRNA which is stably expressed in the HeLa-EGFP cell line.^[91] Once the mRNA has been cleaved, the synthesis of EGFP cannot occur anymore, thus no green fluorescence can be detected. Here we performed the experiments using multi-shell calcium phosphate nanoparticles achieving a far more effective gene silencing. We used a final concentration of 45 μ M siRNA as described in Ref.^[95] which was found to be optimal for double-stranded oligonucleotides.

The particles were prepared by the precipitation of calcium phosphate at pH 9 under constant stirring and subsequent functionalization of the particles with siRNA (single-shell nanoparticles). In order to produce triple-shell nanoparticles

we added further shells of calcium phosphate and siRNA for steric and electrostatic stabilization. These shells should protect siRNA in the inner shell from the fast enzymatic degradation in the lysosomal compartment and in the cytosol.

The obtained single- and triple-shell calcium phosphate/siRNA nanoparticles had a particle size up to 200 nm and a spherical morphology as shown by SEM and TEM (Figures 4.3.1.1 and 4.3.1.2). Dynamic light scattering gave an average size of single-shell nanoparticles of 565 nm with a zeta potential of -35 mV for single-shell nanoparticles and 517 nm and -6 mV for triple-shell nanoparticles. However, a small amount of sample and the presence of dissolved siRNA made it very difficult to record the DLS data. Moreover, in both cases the PDI of the dispersion was between 0.5 and 1.0, which means that the data are difficult to interpret, and that some aggregation had occurred.

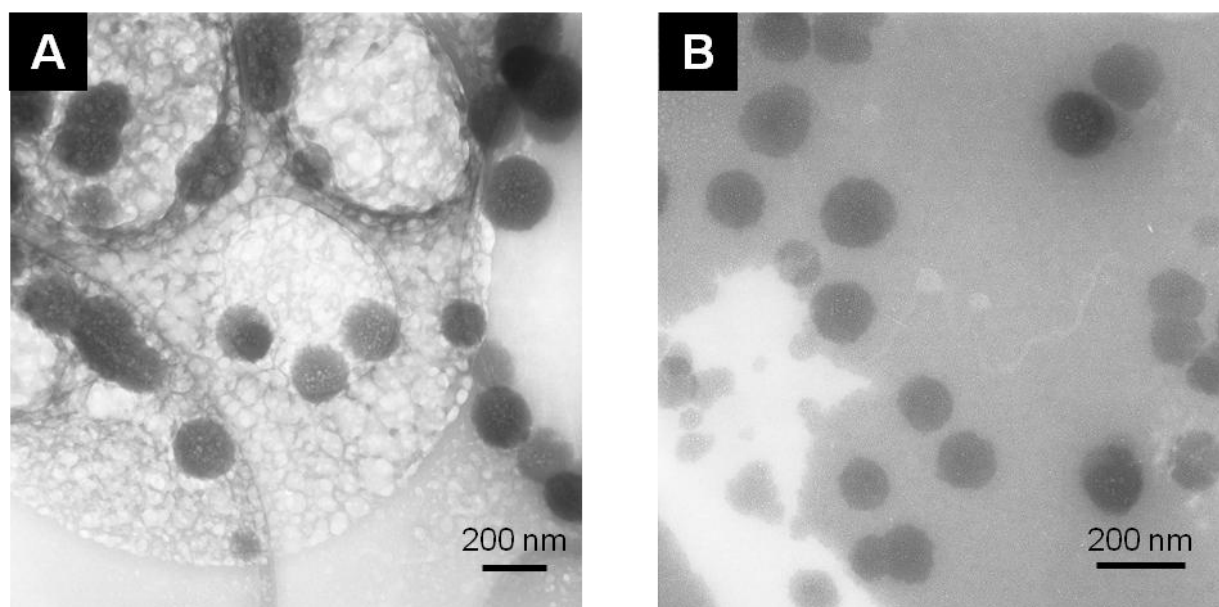


Figure 4.3.1.1: Transmission electron micrographs of calcium phosphate nanoparticles, coated with siRNA. **A:** Single-shell nanoparticles; **B:** Triple-shell nanoparticles.

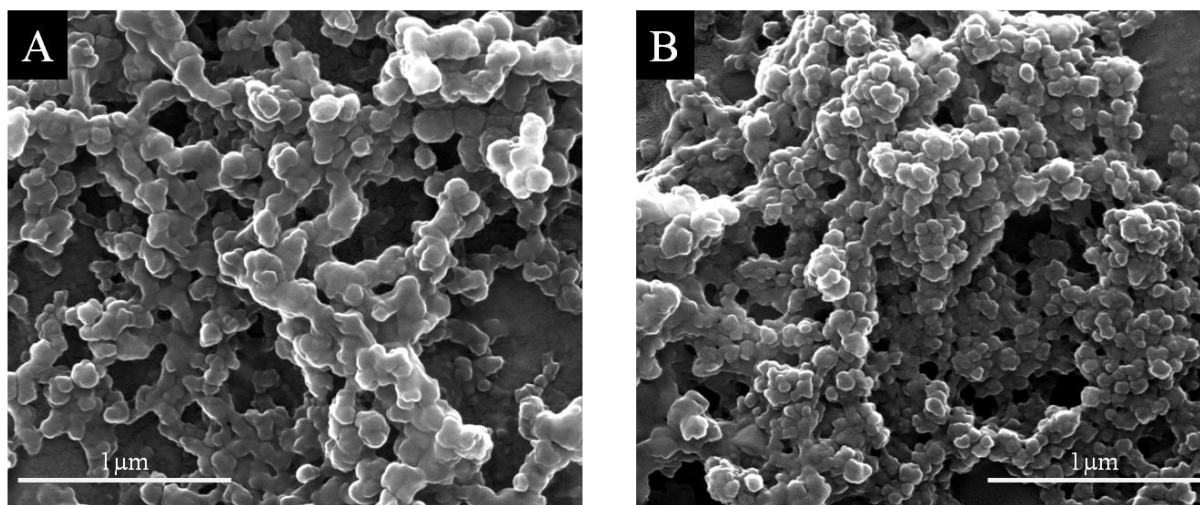


Figure 4.3.1.2: Scanning electron micrographs of siRNA-functionalized calcium phosphate nanoparticles. **A:** Single-shell nanoparticles; **B:** Triple-shell nanoparticles.

4.3.2 Gene silencing on HeLa-EGFP cells by siRNA-functionalized calcium phosphate nanoparticles

For the gene silencing experiment we used two types of calcium phosphate/siRNA nanoparticles: Single-shell particles (core of calcium phosphate, shell of siRNA, described previously in Ref.^[91]) and triple-shell particles (core of calcium phosphate, first shell of siRNA, second shell of calcium phosphate and outer shell of siRNA). In the latter case, siRNA was protected from degradation by intracellular endonucleases, which was previously proved to be efficient by Sokolova *et al.* for transfection with DNA.^[100] Nevertheless, as siRNA does not need to penetrate into the nucleus to exert its gene silencing activity but only needs to enter the cytoplasm, the protecting effect of the calcium phosphate layer in triple-shell particles must be only temporal and adjustable for the cytoplasmatic dissolution and release of siRNA.

As controls, we used cells transfected with siRNA alone (without any transfection reagent or carrier), cells transfected with siRNA by the standard calcium phosphate method,^[83] and the commercial transfection agent Polyfect[®].

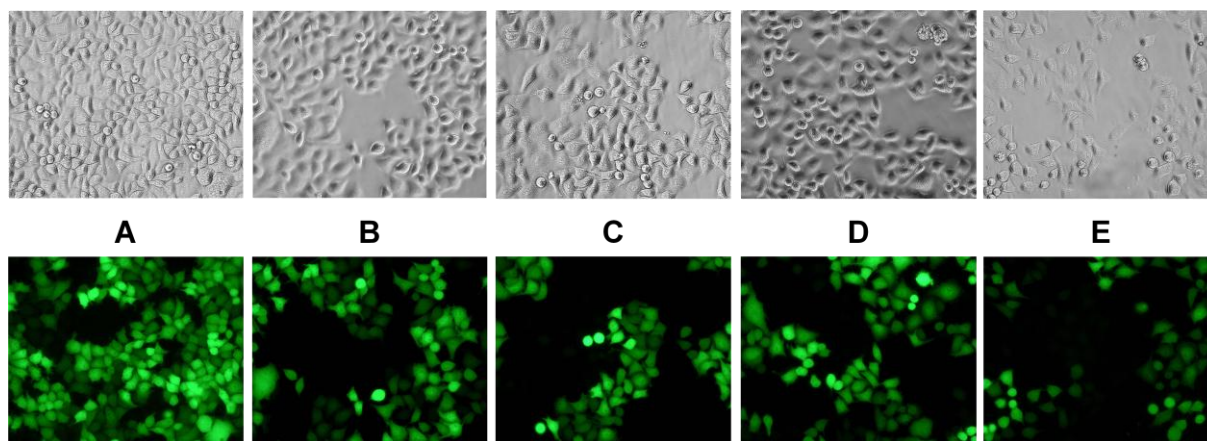


Figure 4.3.2.1: Transmission light microscopy (**top row**) and EGFP fluorescence microscopy (**bottom row**) of HeLa-EGFP after transfection with siRNA for gene silencing. In the top row all cells can be seen. In the bottom row, the cells which still express EGFP appear green. In all cases, the transfection was carried out in DMEM medium with FCS. **A:** Control cells, incubated only with cell culture medium without transfection agent or siRNA; **B:** Cell culture after transfection with single-shell calcium phosphate nanoparticles; **C:** Cell culture after transfection with triple-shell calcium phosphate nanoparticles; **D:** Cells after transfection with the standard calcium phosphate precipitation method; **E:** Cell culture after transfection with the commercial transfection agent Polyfect[®] (magnification 200x in all cases).

Figure 4.3.2.1 shows micrographs of the transfection experiments (light microscopy and fluorescence microscopy). The extent of gene silencing can be easily computed from the ratio of the still fluorescing cells to the total number of cells. This method of course depends on the absolute number of cells within

each image. Nevertheless, these observations allow a preliminary characterization of the toxicity of the method and the cell vitality due to the changes in cell morphology (*e.g.* round and detached cells are damaged or already dead). However, such a calculation of the efficiency gives only relative values which are not comparable for different experiments because the percentage of green fluorescing cells in the control varies between the experiments (not every HeLa-EGFP cell shows the green fluorescence at the start of the experiment). Thus, the relative efficiency must be calculated as the ratio of the fluorescing cells after transfection to the ratio of the fluorescing cells of the control which was run simultaneously with each experiment. The typical percentage of green fluorescing cells in the control was 50 to 80 %, depending on the individual batch of cells. The efficiency of gene silencing is then expressed as

$$\frac{\text{percentage of not fluorescing cells after transfection} - \text{percentage of not fluorescing cells in the control}}{\text{percentage of fluorescing cells in the control}} \times 100 \%$$

(1)

Figure 4.3.2.2 and Table 4.3.2.1 give the numerical results for all methods.

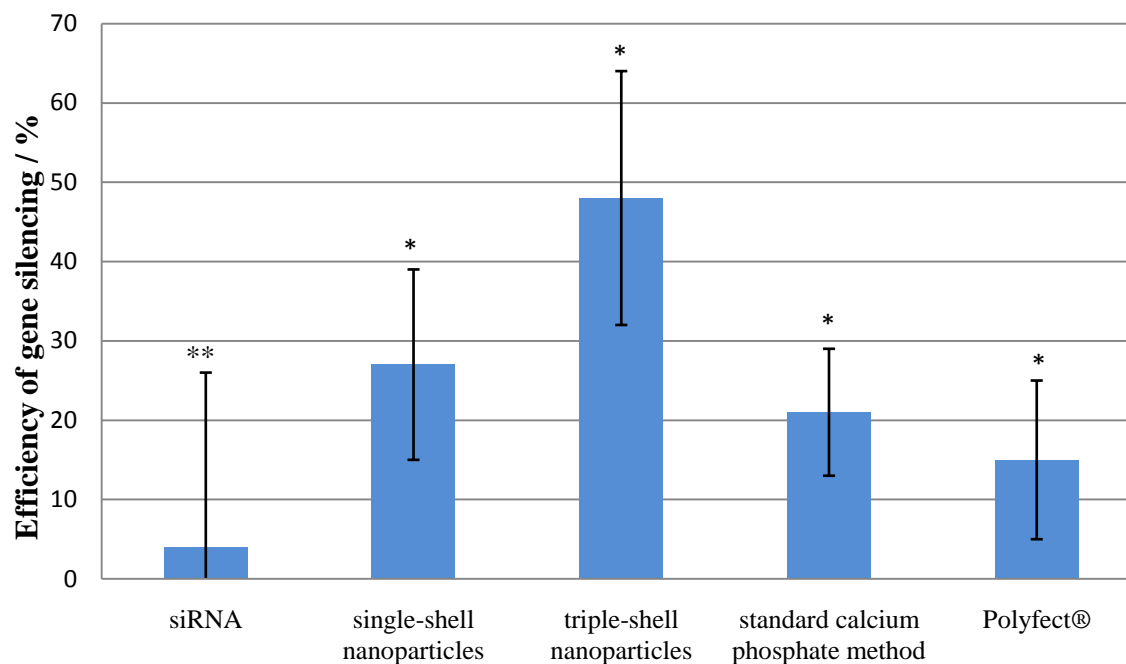


Figure 4.3.2.2: Relative efficiency of EGFP gene silencing on HeLa-EGFP cells. The diagram represents the average means \pm standard deviation (*: $P < 0.001$; **: $P < 0.01$).

Table 4.3.2.1: Results of the transfection experiments with HeLa-EGFP by numerical analysis of the fluorescence micrographs. The transfection efficiency is given as average \pm standard deviation.

| Method | Efficiency of gene silencing / % |
|--|----------------------------------|
| Control | 0 |
| siRNA without calcium phosphate | 4 \pm 22 |
| Single-shell calcium phosphate/siRNA nanoparticles | 27 \pm 12 |
| Triple-shell calcium phosphate/siRNA nanoparticles | 48 \pm 16 |
| Standard calcium phosphate precipitation method | 21 \pm 8 |
| Transfection with Polyfect [®] | 15 \pm 10 |

The efficiency of gene silencing using the single- and triple-shell nanoparticles was 27 and 48 %, respectively. siRNA alone (without calcium phosphate as a carrier) showed almost no gene silencing effect (4 \pm 22 %), nevertheless indicating that siRNA alone can sometimes enter the cytosol. Single-shell nanoparticles, the standard calcium phosphate method and Polyfect[®] did not show statistically significant differences in the efficiency of gene silencing. In contrast, the triple-shell nanoparticles were much more efficient, giving an efficiency of gene silencing of 48 % (and sometimes up to 64 %).

We also investigated the influence of the concentrations of calcium and phosphate on the gene silencing efficiency. Here we used high concentrations of Ca²⁺ and PO₄³⁻ (18 mM and 10.8 mM, respectively) and low concentrations (6.25 mM and 3.74 mM, respectively). In both cases the calcium/phosphate ratio corresponded to that of hydroxyapatite. As shown in Figure 4.3.2.3, triple-shell nanoparticles showed no statistically significant differences in the efficiency if the calcium phosphate concentration was changed. The gene silencing efficiency

only slightly decreased from 61 to 53 %, but these changes are hardly to be considered. On the other hand, the efficiency of single-shell nanoparticles decreased from 50 to 28 % by using lower concentrations of calcium and phosphate ($P < 0.01$).

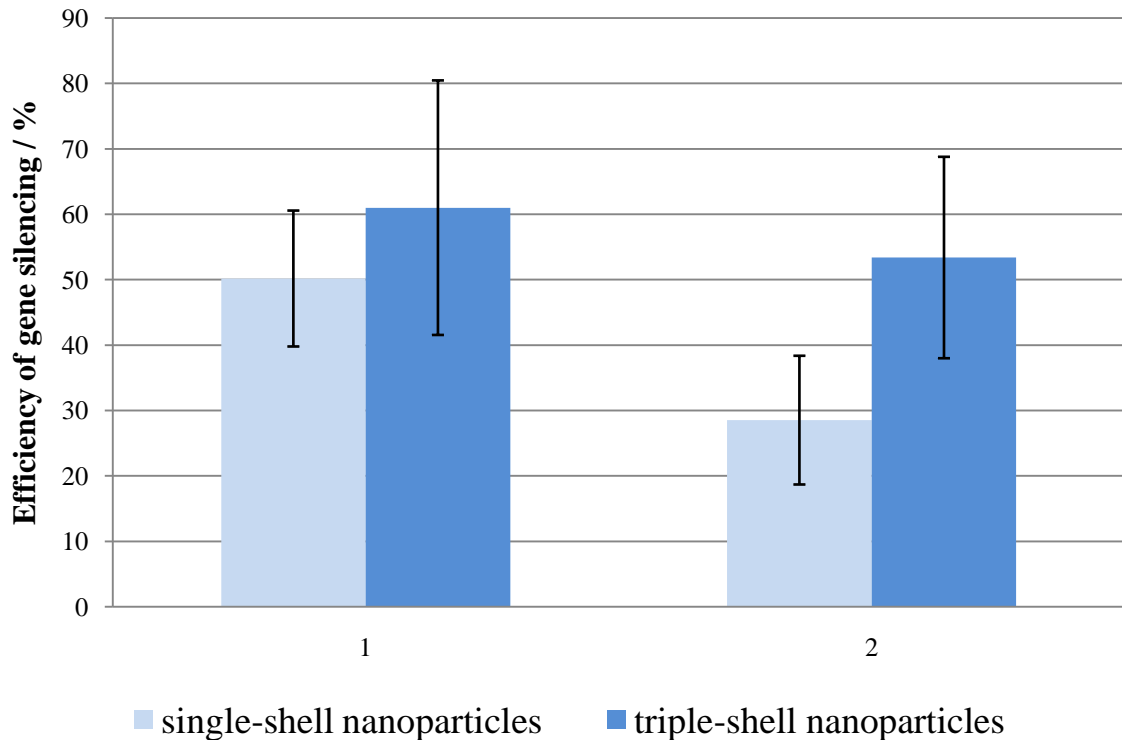


Figure 4.3.2.3: The influence of Ca^{2+} - and PO_4^{3-} concentrations on the gene silencing on HeLa-EGFP cells. **1:** $[\text{Ca}^{2+}] = 18 \text{ mM}$, $[\text{PO}_4^{3-}] = 10.8 \text{ mM}$; **2:** $[\text{Ca}^{2+}] = 6.25 \text{ mM}$, $[\text{PO}_4^{3-}] = 3.74 \text{ mM}$.

In both cases we used an equal amount of siRNA for the functionalization of the nanoparticles and for the transfection. Presumably, the nucleic acid on nanoparticles maintains equilibrium between the dissolved nucleic acid and the acid adsorbed on the particle surface. Thus, the increase of calcium phosphate concentration leads only to the increase of the number of particles resulting in

more efficient gene silencing with single-shell nanoparticles. The increase of the nanoparticle number increases the possibility for particles to reach the cytoplasm successfully and escape the degradation in the lysosomes. However, in triple-shell particles the siRNA is already protected from the degradation by an additional shell of calcium phosphate, thus the number of particles is not so critical for the successful gene silencing and leads only to a minor and insignificant increase of the gene silencing efficiency.

4.3.3 Conclusion

In the present study we showed how to prepare calcium phosphate nanoparticles functionalized with siRNA as delivery system for efficient gene silencing. We prepared single- and triple-shell nanoparticles and tested them *in vitro* on HeLa-EGFP cells for the down-regulation of the EGFP expression. The particles had a size around 200 nm with spherical morphology and negative zeta potential. These particles were easily taken up by cells by endocytosis. Moreover, in the case of triple shell nanoparticles the inner layer of siRNA is protected from the endosomal nucleases, thus resulting in far more effective silencing in cytosol. Single-shell nanoparticles showed an efficiency of gene silencing of around 27 %, whereas triple shell nanoparticles had an efficiency of around 50 %.

Thus, siRNA-functionalized calcium phosphate multi-shell nanoparticles represent a very effective delivery system showing many advantages over other non-viral and viral systems. They are not toxic for cells and highly biocompatible. Moreover, they can be easily and cost-effectively prepared, comparing with many other polymeric agents. The triple-shell particles even exceeded the efficiency of the classical transfection agent Polyfect[®].

4.4 Calcium phosphate nanoparticles functionalized with shRNAs

4.4.1 Synthesis and characterization of the nanoparticles functionalized with shRNAs

We were already able to synthesize nanoparticles stabilized with DNA^[91] and siRNA.^[95] All these particles carry a negative charge due to the presence of negatively charged nucleic acids on their surface.

In this study we prepared nanoparticles functionalized with small hairpin RNA (short hairpin RNA or shRNA). This name comes from its structure which makes a hairpin-like turn, thus providing a double-stranded structure, as shown in Figure 4.4.1.1.

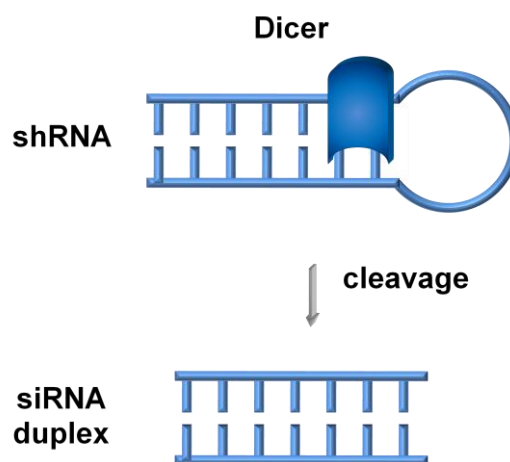


Figure 4.4.1.1: Schematic representation of shRNA structure.

In shRNAs an oligonucleotide sequence containing the siRNA sequence is followed by a ~ 9-nucleotide (9-nt) loop and a reverse complement of the siRNA sequence. It is usually introduced into cells in a viral vector or plasmid ensuring endogenous long-time expression of shRNA, which is subsequently processed in the cytoplasm by Dicer to siRNA and leads to gene silencing, either by inducing the sequence-specific degradation of complementary mRNA or by inhibiting translation.^[12,13,19] While the synthetic siRNA effects are short-lived probably because of siRNA dilution with cell division and also degradation, the shRNA

effects are lasting longer because siRNA is continually produced within the cells.

The ultimate aim of this project was to produce shRNA-functionalized calcium phosphate nanoparticles and then embed them into polyelectrolyte multilayers using the layer-by-layer technique,^[146] thus localizing the application of the nanoparticles.^[147-149] The layer-by-layer buildup of polyelectrolyte multilayered films from oppositely charged polyelectrolytes offers new opportunities for the preparation of functionalized biomaterial coatings. This technique allows the preparation of supramolecular nanoarchitectures with the specific ability to control cell activation^[147] and may also play a role in the development of local drug delivery systems.^[150]

Rives *et al.* already used DNA encapsulating in PLGA (poly(lactide-co-glycolide)) scaffolds for efficient *in vivo* gene delivery. They were able to transfect adipose tissue and macrophages.^[151] Lu *et al.* used the layer-by-layer technique to integrate DNA into layers of poly(2-aminoethyl propylene phosphate) on quartz substrate pre-coated with poly(ethylene imine) to achieve prolonged gene expression.^[152]

As model system, we synthesized multi-shell calcium phosphate/shRNA nanoparticles to observe their abilities to inhibit the osteopontin and osteocalcin expressions in human osteoblasts.^[153] These proteins play a central role in the mineralization and the remodeling of bone, thus maintaining the calcium ion homeostasis.^[154,155]

shRNA-functionalized calcium phosphate nanoparticles were prepared by rapid mixing of aqueous solutions of calcium and phosphate salts and subsequent functionalization of the precipitate with shRNA to prevent the aggregation of nanoparticles. We used two types of shRNA: Spp1 (81 bp) for silencing the osteopontin expression and Bglap-rs1 (70 bp) for silencing the osteocalcin expression. These nanoparticles consisted of a calcium phosphate core and an

outer layer of shRNA for electrostatic and steric functionalization (single-shell nanoparticles).

In order to produce a multilayer structure we subsequently added to the mixture of the single-shell nanoparticles $\text{Ca}(\text{NO}_3)_2$ solution (6.25 mM) and $(\text{NH}_4)_2\text{HPO}_4$ solution (3.74 mM), and then 0.1 mg of shRNA for further functionalization of the particles. These particles consisted of the layers CaP – shRNA – CaP – shRNA and were named “triple-shell”.

The characterization of the nanoparticles by scanning electron microscopy showed spherical particles with a particle size from 100 nm up to 250 nm, both for single- and triple-shell nanoparticles functionalized with Spp1 and 80-200 nm for the nanoparticles functionalized with Bglap-rs1 (Figures 4.4.1.2 and 4.4.1.3).

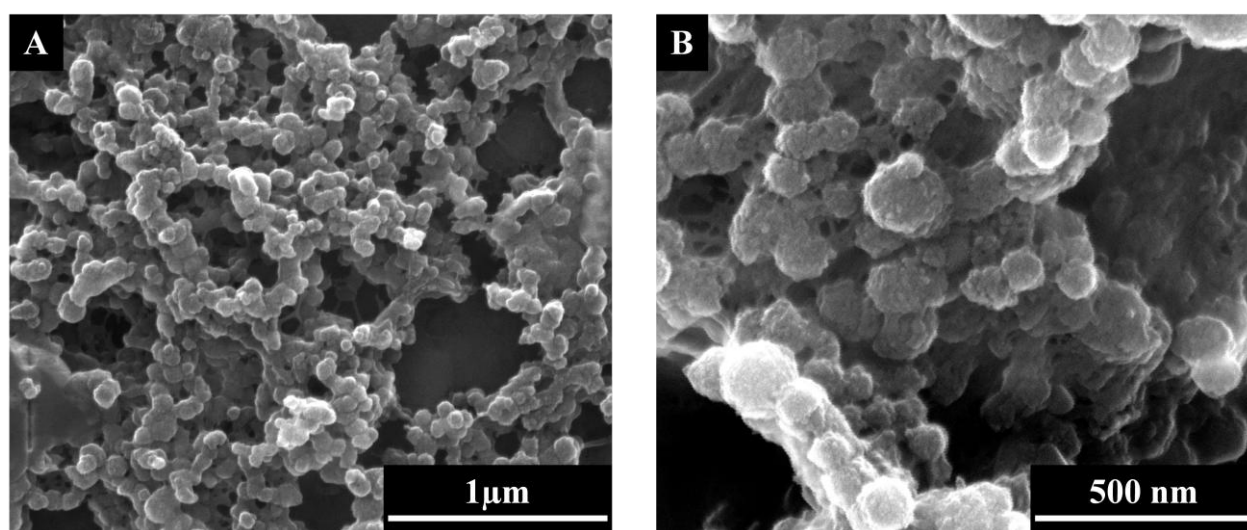


Figure 4.4.1.2: Scanning electron micrographs of calcium phosphate nanoparticles functionalized with shRNA against osteopontin (Spp1). **A:** single-shell nanoparticles; **B:** triple-shell nanoparticles.

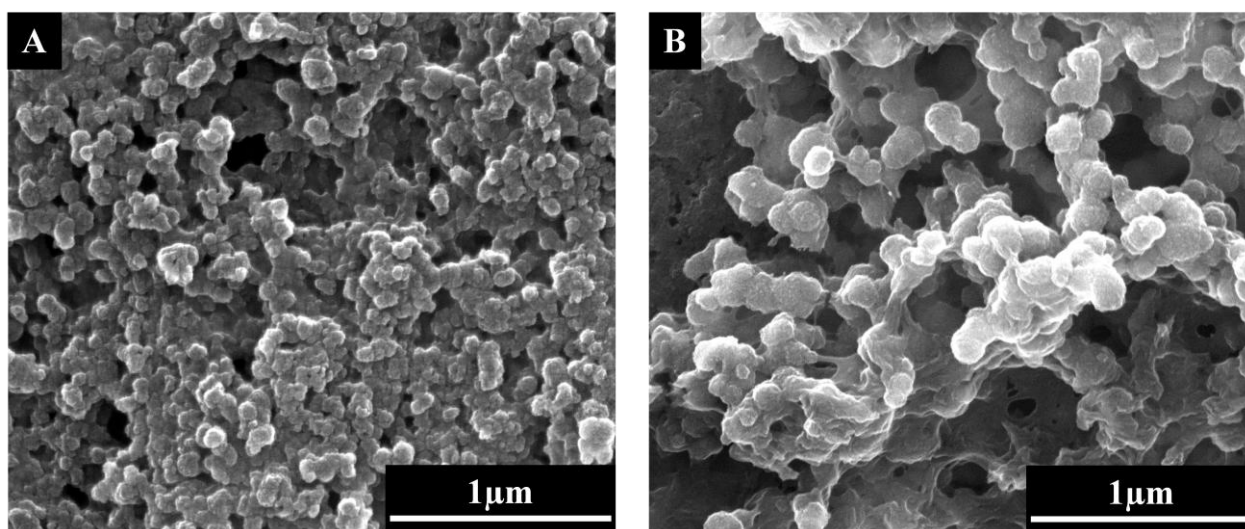


Figure 4.4.1.3: Scanning electron micrographs of calcium phosphate nanoparticles functionalized with shRNA against osteocalcin (Bglap-rs1). **A:** single-shell nanoparticles; **B:** triple-shell nanoparticles.

The dynamic light scattering of the nanoparticles was complicated due to very small amounts of the samples and, therefore, their strong dilution. However, peaks in the range of 110-220 nm were always present. In addition, the particles showed a negative zeta potential.

4.4.2 Gene silencing using calcium phosphate nanoparticles functionalized with shRNAs

The tests of the nanoparticles in cell culture were performed at the group of Dr. Nadia Benkirane-Jessel at the *Institut National de la Santé et de la Recherche Médicale* in Strasbourg, France.

First, the biological activities of nanoparticles were tested by the production of osteopontin and osteocalcin in the human osteoblasts (HOb) which were brought into contact with dispersions of nanoparticles. The cells grew in Osteoblast Growth Medium at 37 °C in humidified atmosphere with 5 % CO₂.

Different controls were performed: Untreated cells which were incubated only in cell culture medium; cells incubated with calcium phosphate/pcDNA3-EGFP nanoparticles (single- and triple-shell, 8 μ g calcium phosphate were used per well); HOb cells incubated in medium containing free Spp1 or Bglap-rs1 and cells transfected with Spp1 and Bgrap-rs1 using commercial multicomponent reagent FuGENE[®].

We incubated the cells with the transfection medium for 21 days replacing the medium every 3 days with the fresh transfection medium. Then the cells were fixed with 2 % paraformaldehyde in phosphate buffered saline solution (PBS). The protein expression in HOb cells was detected by immunofluorescence. The cells were incubated overnight at room temperature with goat anti-osteopontin or osteocalcin antibody as primary antibody and then washed with PBS containing 0.1 % Triton X-100 and incubated with a donkey anti-goat antibody as secondary antibody for 1 h at room temperature. The nuclei were visualized by Hoechst 33258 staining. Here the cell nuclei are visualized in blue to detect the general number of cells per image, and red color represents osteopontin or osteocalcin, respectively. The results of the experiments are shown in the Figure 4.4.2.1.

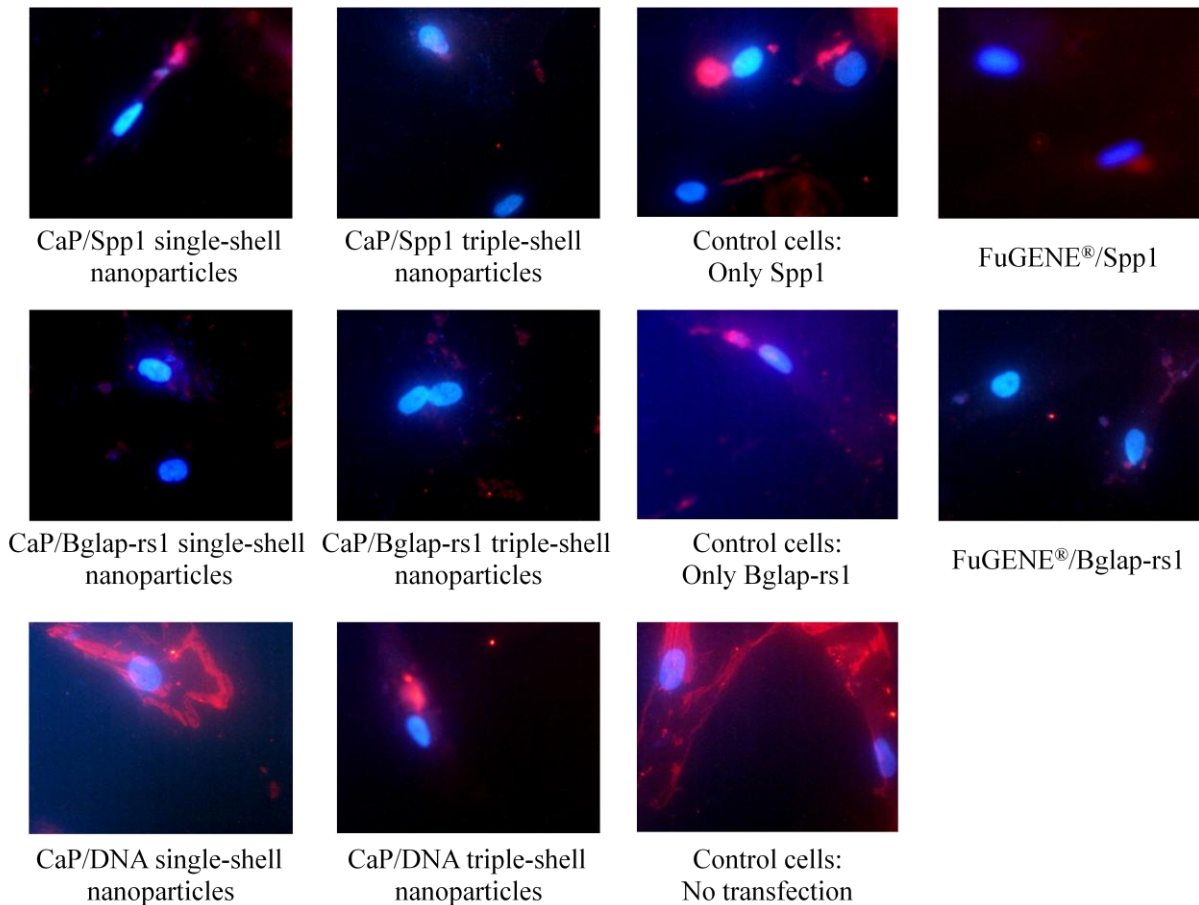


Figure 4.4.2.1: Gene silencing on human osteoblasts using calcium phosphate nanoparticles functionalized with shRNA against osteopontin (Spp1) and osteocalcin (Bglap-rs1) after 21 days of transfection from the suspension. **Top row:** Cells transfected with Spp1 shRNA by different ways; **middle row:** Cells transfected with Bglap-rs1 shRNA by different ways; **bottom row:** Control cells.

A high level of expression of osteopontin and osteocalcin was detected in the control osteoblasts incubated only in the cell culture medium and in the cells transfected with calcium phosphate/pcDNA3-nanoparticles (Figure 4.4.2.1, bottom row). We detected the red fluorescence of almost the whole cell cytoplasm. The protein expression was only slightly inhibited in the cells incubated in the presence of free Spp1 and Bglap-rs1 and partially inhibited in

the cells transfected with FuGENE[®]. In this case we observed some expression but not very high and only as local islands and not in the whole cytoplasm. However, the expression of desired proteins was almost fully inhibited using single- and triple-shell calcium phosphate/shRNA nanoparticles. We observed no red fluorescence of desired proteins after gene silencing with both types of particles.

The next step was to introduce the nanoparticles into the layers using the layer-by-layer technique to achieve a local particle application and the gradual release of the particles from the layers and, thus, the gradual transfection of the cells to balance the loss of nucleic acid by metabolic degradation.^[156]

Jewell *et al.* already showed that multilayered films consisted of pDNA and a polyamine are able to release pDNA from the surfaces under physiological conditions for transfection of adherent cells.^[157,158] They suggested that the films present DNA in a condensed form which improved the internalization of DNA by cells. Rives and co-workers also encapsulated DNA in PLGA scaffolds for efficient *in vivo* gene delivery.^[151]

For the formation of multilayer films we used triple-shell nanoparticles, which showed the best results in the previous experiment. We produced multilayer films consisting of nanoparticles and cationic polymer poly-(L-lysine) (PLL) for locally defined and temporarily variable gene silencing. The chemical structure of PLL is shown in Figure 4.4.2.2.

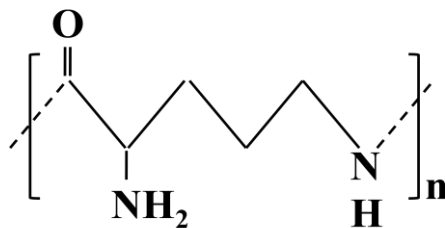


Figure 4.4.2.2: Chemical structure of poly-(L-lysine).

The layers were prepared according to standard procedure, as described in Ref.^[147]

To test the gene silencing abilities of the nanoparticles embedded in the multilayer system, the HOb cells were seeded on (PLL-nanoparticles)₁ (one bilayer) and (PLL-nanoparticles)₆ multilayer films (six bilayers; PLL as bottom layer, nanoparticles as upper layer) and incubated for 21 days. The results are shown in Figure 4.4.2.3.

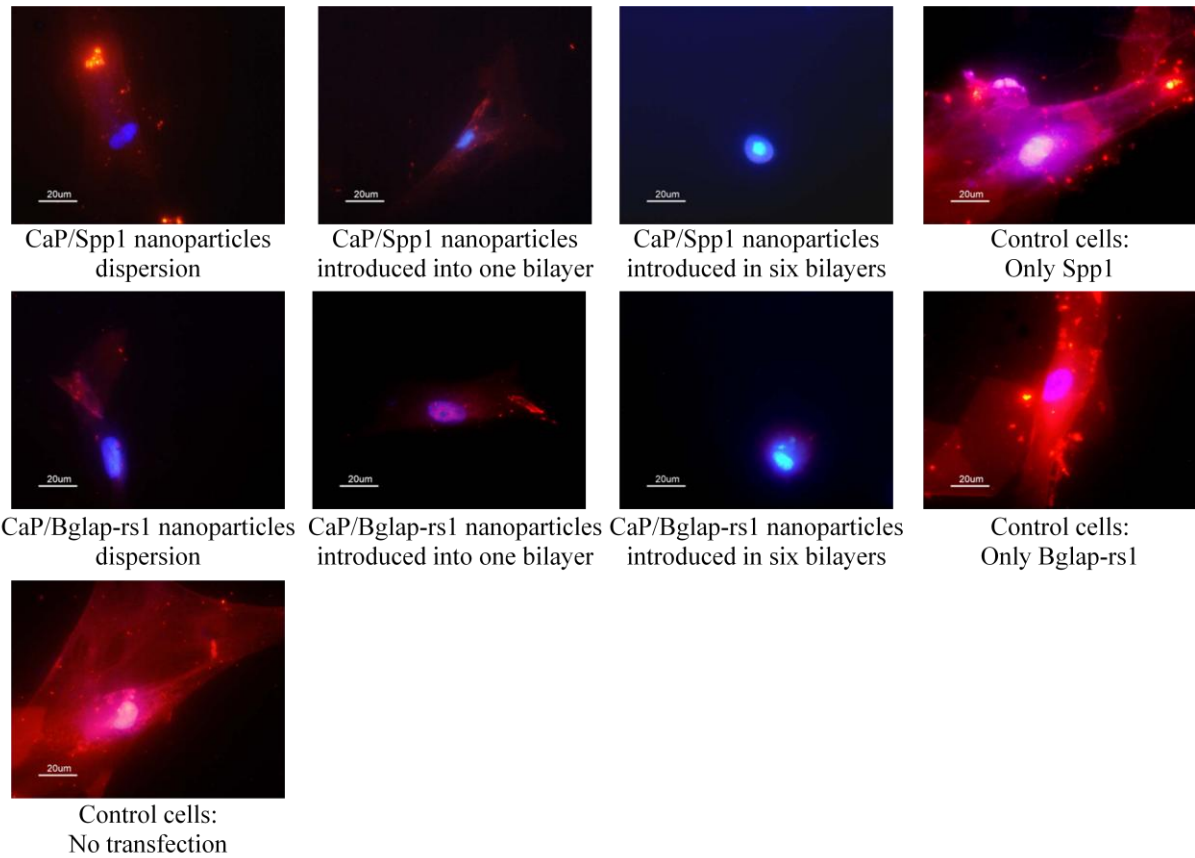


Figure 4.4.2.3: Gene silencing on human osteoblasts after 21 days of transfection with different transfection methods: with triple-shell calcium phosphate nanoparticles from dispersion and from multilayer films prepared by layer-by-layer technique with shRNA-functionalized calcium phosphate nanoparticles. **Top row:** Cells transfected with Spp1 shRNA by different ways; **middle row:** Cells transfected with Bglap-rs1 shRNA by different ways; **bottom row:** Control cells.

Our results clearly indicated that when incorporated into the multilayered film, the shRNA nanoparticles induced a much stronger specific inhibition of the expressions of target proteins than the same nanoparticles used as dispersions or naked Spp1 and Bglap-rs1 in the solution (Figure 4.4.2.3). In the latter case the expression of osteopontin and osteocalcin was still present and almost as strong as in the control cells.

The “normal” osteopontin or osteocalcin expression was detected in untreated cells HOB cells and in cells treated with the solutions of free shRNAs (Spp1 and Bglap-rs1, respectively). Nevertheless, the cells transfected with the nanoparticles from the dispersion show a significant decrease of the osteopontin and osteocalcin expression. Moreover, when the particles were embedded in the multilayered film consisted of one bilayer (PLL-nanoparticles)₁, the gene expressions of osteopontin and osteocalcin were inhibited slightly more than those in dispersion. Furthermore, in the case of film consisted of six bilayers (PLL-nanoparticles)₆, the gene expressions of both osteopontin and osteocalcin were both drastically inhibited. There no red fluorescence of desired proteins was detected. Thus, the best gene silencing was obtained with triple-shell shRNA-functionalized nanoparticles embedded in six bilayers.

4.4.3 Conclusion

We reported here the first application of a multilayered films-based delivery system containing shRNA-functionalized nanoparticles for gene silencing of osteopontin and osteocalcin which are specific for bone cells. The nanoparticles had a size up to 250 nm and a negative zeta potential. shRNA-functionalized nanoparticles were effectively embedded into the PLL multilayers and used for local gene silencing of osteopontin and osteocalcin in human osteoblasts. The expressions of proteins were effectively inhibited both in the case of transfection from a dispersion or from the (PLL-nanoparticles)_n multilayer films. However, gene silencing from the films consisted of six bilayers was most efficient.

4.5 Functionalization of nanoparticles with oligonucleotides for the activation of dendritic cells

4.5.1 Synthesis and characterization of the nanoparticles functionalized with Poly(I:C) and CpG

In our previous work (Sections 4.3 and 4.4) we were able to show that it is possible to stabilize calcium phosphate nanoparticles with oligonucleotides. Sokolova *et al.* prepared nanoparticles functionalized with single- and double-stranded oligonucleotides of different length.^[95] Although the optimal concentration was different, the binding occurs presumably by interaction of the negatively-charged phosphate groups of nucleic acids and positively-charged calcium ions. Thus, the interaction is not specific and depends only on the conformation of phosphate backbone. Therefore, the concentration of oligonucleotides needed for the stabilization of nanoparticles does not depend on the length of the oligonucleotides, but highly depends on the conformation of nucleic acid, *i.e.* whether it is single- or double-stranded.

The aim of the present research was to functionalize the calcium phosphate nanoparticles with oligonucleotides able to activate the immune system. We chose two different oligonucleotides: CpG and Poly(I:C).

CpG (cytosin-phosphatidyl-guanosin) islands are genomic regions with an increased density of C and G nucleotides. They are able to mimic the ability of microbial DNA to activate the innate immune system.^[27,28,30-33]

Poly(I:C) (polyinosinic-polycytidylic acid, double-stranded homopolymer) sequences are synthetic analogues of double-stranded RNAs associated with viral infection. They can also induce an immune response and are used for the generation of mature dendritic cells.^[34,35]

Our aim was to use both CpG (sequence: 5'-TCC ATG ACG TTC CTG ACG TT-3', 6364 g mol⁻¹) and Poly(I:C) for the maturation of dendritic cells (DC), thus breaking the tolerance and activating the immune system against previously undetectable antigens.^[36]

The synthesis of nanoparticles was performed as follows: The solutions of calcium nitrate and diammonium hydrogen phosphate were adjusted to pH 9 with 0.1 M NaOH and then mixed with a peristaltic pump. Immediately afterwards the dispersion was functionalized with 167 μL CpG (63 μM) or a mixture of 2.5 μL CpG (63 μM) and 198 μL Poly(I:C) (1 mg mL^{-1}). The obtained nanoparticles were characterized using scanning electron microscopy (Figure 4.5.1.1) and dynamic light scattering.

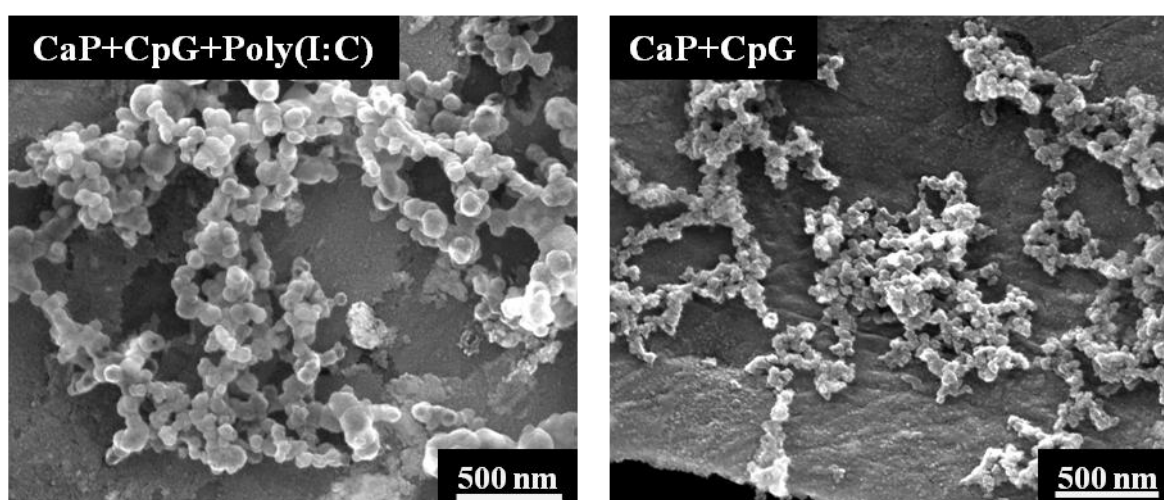


Figure 4.5.1.1: Scanning electron micrographs of calcium phosphate nanoparticles functionalized with CpG and Poly(I:C) oligonucleotides.

The nanoparticles with CpG had a size around 70 nm and spherical morphology. The nanoparticles functionalized with CpG and Poly(I:C) were also spherical, but had a size around 120 nm.

DLS measurements showed that calcium phosphate/CpG nanoparticles had a size around 282 nm and a zeta potential of -19 mV (PDI=0.5), whereas calcium phosphate/CpG/Poly(I:C) nanoparticles had a diameter of 350 nm with a zeta potential of -17 mV (PDI=0.3). However, due to the small amount of material and therefore their strong dilution it was difficult to obtain better results.

Moreover, the DLS measurements showed only the hydrodynamic radius of the particles.

4.5.2 Activation of dendritic cells using nanoparticles functionalized with Poly(I:C) and CpG

The cell experiments were performed by Dr. Mathias Krummen from the University of Münster.

In these experiments we used pure solutions of calcium nitrate (6.25 mM) diammonium hydrogen phosphate (3.74 mM) and their mixture, and CpG solution (63 μM) as controls. We also centrifuged the dispersion of the nanoparticles for 2 h at 40,000x g to find out whether the supernatant still contained free CpG molecules.

The efficiency of the delivery of CpG and Poly(I:C) was detected by the release of interleukin 12 (IL-12), a cytokine with many functions in the immune system. As shown in Figure 4.5.2.1, almost no effect was observed after the addition of pure Ca^{2+} or PO_4^{3-} solutions to the dendritic cells (DC) or their mixture. This effect was comparative to the activity of control (untreated) cells and was between 0 and 20 pg mL^{-1} . A moderate effect (about 76 pg mL^{-1}) was observed after the incubation of cells with free CpG or the supernatant of the nanoparticles, thus confirming that the dispersion of the nanoparticles still contained free CpG molecules which were not adsorbed on the particle surface. However, it was not possible to obtain stable particles by functionalizing them with smaller amounts of CpG. This indicates that the equilibrium between free and adsorbed CpG is essential for the functionalization of the particles. However, the effect detected after the incubation of the nanoparticles with DC was almost two times higher, *i.e.* around 170 pg mL^{-1} .

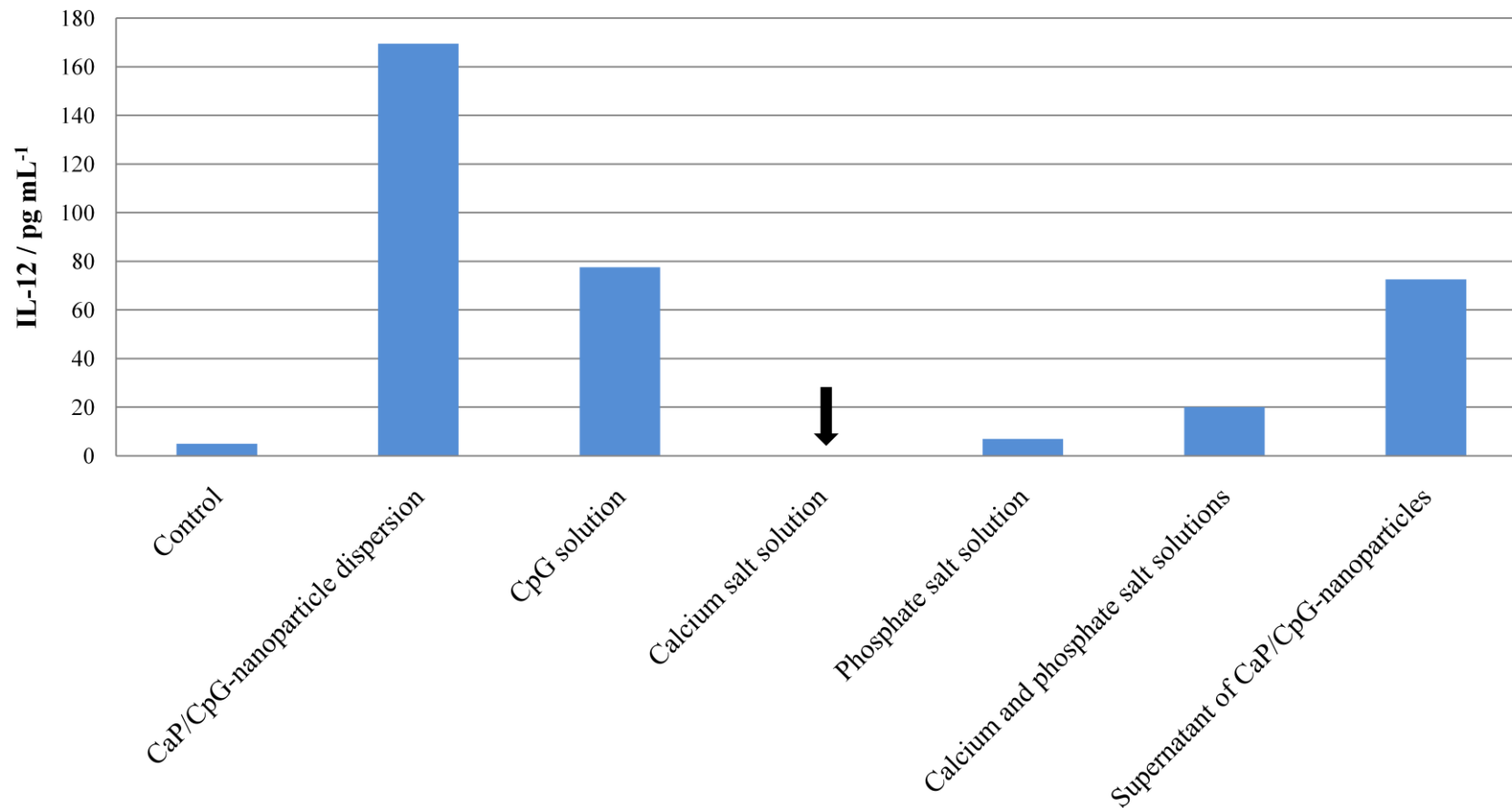


Figure 4.5.2.1: The release of IL-12 by dendritic cells after the activation with calcium phosphate nanoparticles functionalized with CpG. $[\text{Ca}^{2+}] = 6.25 \text{ mM}$, $[\text{PO}_4^{3-}] = 3.74 \text{ mM}$, $[\text{CpG}] = 0.063 \text{ mM}$. An arrow indicates release of IL-12 from the DC after the stimulation with calcium salt solution (0 pg mL^{-1}).

To check whether the stimulation of DC was so efficient due to the nanoparticles, we performed experiment with a further control. We compared the nanoparticle activity compared to the precipitate of particles obtained *in situ* using mixture of inorganic salts ($[\text{Ca}^{2+}] = 6.25 \text{ mM}$ and $[\text{PO}_4^{3-}] = 3.74 \text{ mM}$) and CpG, which approximately corresponds to the standard precipitation method of Graham and van der Eb.^[83] In the latter case calcium phosphate/CpG particles are built up spontaneously and are polydisperse, *i.e.* we have microparticles as well as nanoparticles. The observed results are shown in Figure 4.5.2.2. Moreover, it was already described that calcium phosphate precipitates can increase gene expression in DC.^[36]

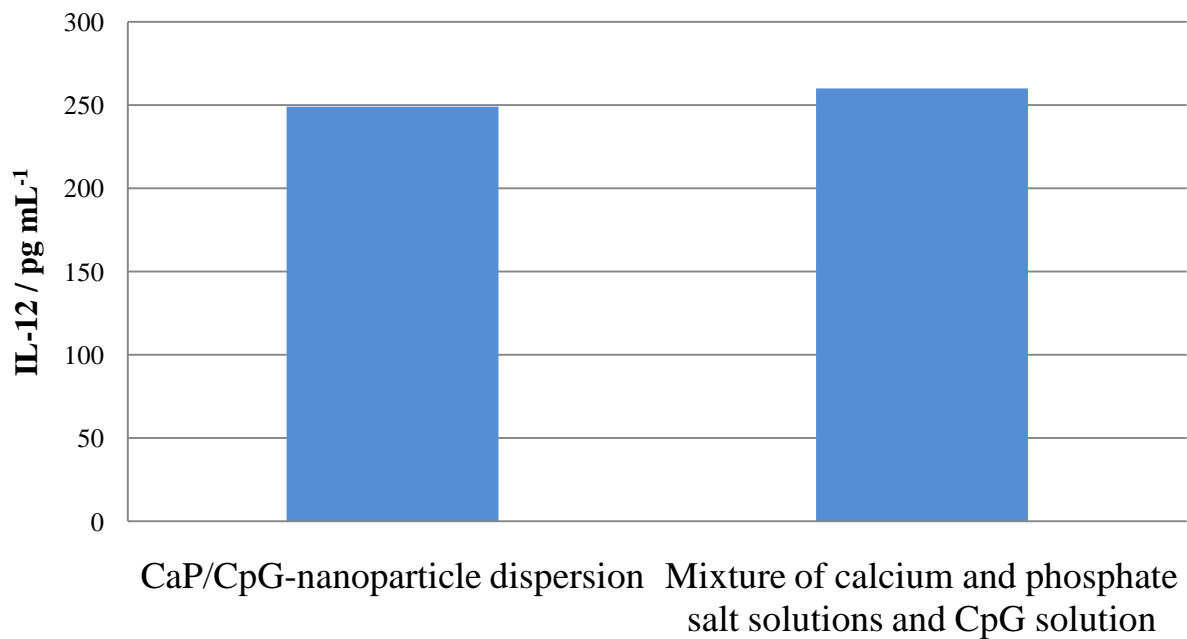


Figure 4.5.2.2: The release of IL-12 by dendritic cells after the activation using calcium phosphate nanoparticles functionalized with CpG and after precipitation of particles *in situ*.

The cells treated with calcium phosphate/CpG nanoparticles or *in situ* synthesized particles from the mixture of calcium and phosphate salt solutions and CpG solution showed an equally high release of the IL-12 – around 250 pg mL⁻¹.

We can conclude that the activation of DC (and therefore the release of IL-12) occurred due to the uptake of the calcium phosphate/CpG particles, but not due to the presence of free CpG or inorganic ions in cell culture medium. Moreover, this stimulation effect did not depend on the synthesis method; the results obtained after controlled precipitation of the particles and after synthesis *in situ* were equal and led to the 2 times higher release of IL-12. However, the method of particles synthesis can be very important for further experiments, *e.g.* for further functionalization of particles by antibodies or markers. Therefore, the controlled synthesis of particles is preferred.

4.5.3 Conclusion

Calcium phosphate nanoparticles were functionalized with nucleic acids not only for transfection, but also for the activation of dendritic cells. Such particles appear to be an effective matrix for the delivery of maturation signals into the dendritic cells. The maturation of the cells was detected by the release of IL-12. The efficiency of the nanoparticles was 2.5 times higher than the effect of free CpG solution.

These results provide us with a diversity of applications of the nanoparticles functionalized with different nucleic acids both *in vitro* and *in vivo*. We were able to deliver not only specific genes or gene's inhibitors into the cells, but differentiation signals while still maintaining low toxicity.

4.6 Surface-mediated transfection with DNA-functionalized calcium phosphate nanoparticles

4.6.1 Preparation of electrophoretically coated titanium substrates

The coatings were partially prepared by Dr. Henning Urch and Dipl.-Chem. Manuel Neumeier in our group.

All previously discussed delivery systems come as dispersions and have to be administered into the desired tissue or given systemically. Even if a delivery system has high transfection efficiency, there still remains the question of the local application of therapeutic agent. Thus, materials that provide spatial and temporal control over the DNA delivery play an important role in localized nucleic acid-based therapies.

Usually such delivery systems consist of DNA embedded into polyelectrolyte layers. One can use poly(ethylene imine) and poly(allylamine hydrochloride),^[159] poly-L-lysine,^[160] poly(2-aminoethyl propylene phosphate)^[152] and poly(L-tartaramido pentaethylene tetramine).^[161] DNA can also be encapsulated into porous PLGA scaffolds. Such scaffolds were already shown to be effective *in vivo* by Rives *et al.*^[151]

However, the main disadvantage of all these techniques is an application of synthetic polymers which, after the degradation in the organism, may be toxic.

We were able to produce bioactive metal surfaces coated with calcium phosphate nanoparticles via electrophoretic deposition.

A conducting surface of any shape can be electrophoretically coated with DNA-loaded calcium phosphate nanoparticles if these particles are transferred into 2-propanol or ethanol to avoid the electrolytic decomposition of water. Multilayers of nanoparticles with a thickness of a few μm were prepared.^[162] As substrate we used titanium plates with a size of 10·10 mm. Unfortunately, it was impossible to produce thin and smooth coatings with calcium phosphate/DNA nanoparticles alone. Therefore, we prepared calcium phosphate nanoparticles

functionalized with poly(ethylene imine) (PEI) which were coated in a second step with DNA. This system gave an excellent smooth coating of the titanium surfaces. Electrophoretic coating was carried out at a voltage of 50 V for 30 s, giving a layer thickness of about 1 μm . A schematic setup of the electrophoresis apparatus is shown in Figure 4.6.1.1.

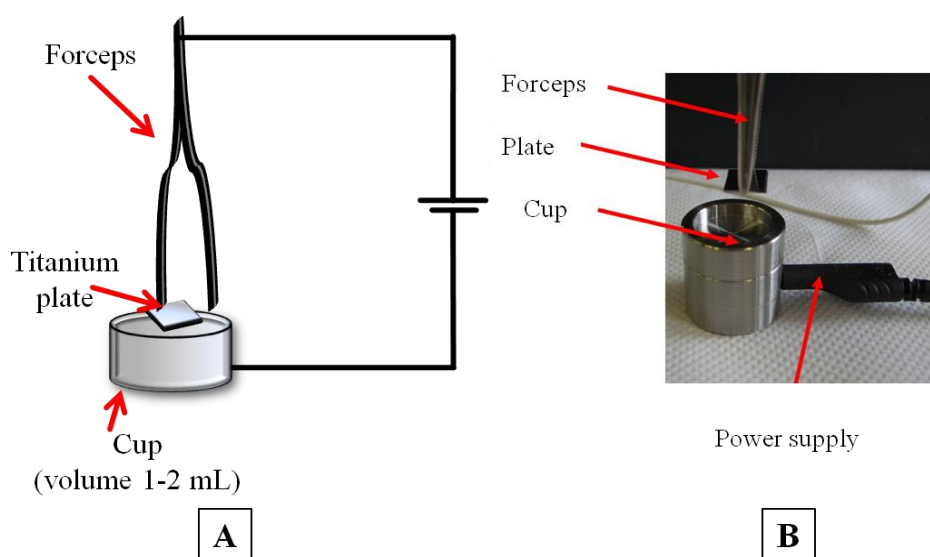


Figure 4.6.1.1: Scheme (A) and photograph (B) of the electrophoresis setup.

The nanoparticles were prepared by precipitation of calcium phosphate/PEI nanoparticles, their redispersion in 2-propanol^[162,163] and the addition of another layer of the plasmid DNA (pcDNA3-EGFP). Dynamic light scattering of the particles gave a size of the calcium phosphate/PEI nanoparticles of 149 nm and a zeta potential of +38 mV.^[164] Scanning electron micrographs (SEM) showed a thin and smooth layer of nanoparticles on the metal surface with a thickness of about 1 μm as shown in Figure 4.6.1.2.

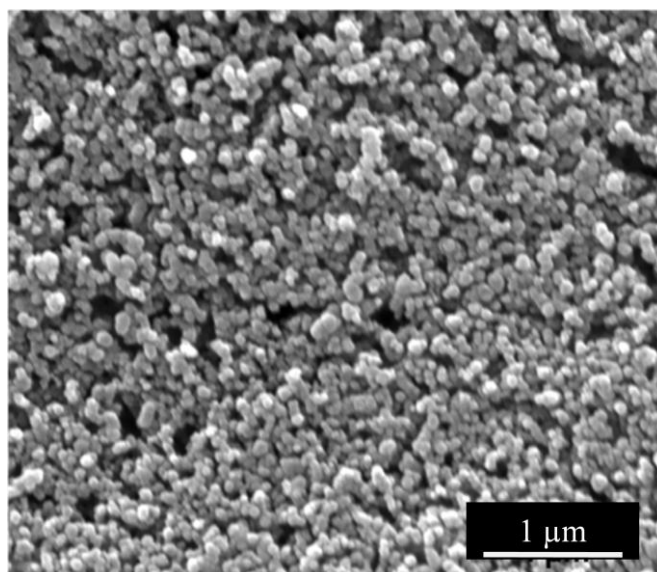


Figure 4.6.1.2: Scanning electron micrograph of the titanium substrate coated with calcium phosphate/PEI/DNA nanoparticles.^[164]

4.6.2 Surface-mediated transfection of cells

After the successful deposition of nanoparticles on metal surface we tested this delivery system in the cell culture. Fibroblasts (NIH3T3) were cultivated on titanium plates coated with pcDNA3-EGFP/PEI-functionalized nanoparticles. Titanium was used as typical implant material. The efficiency of transfection was monitored by the expression of the characteristic green fluorescence of EGFP. In a 24-well plate, $5 \cdot 10^4$ cells per well were seeded on coated titanium plates in growth medium (RPMI 1640 supplemented with 10 % FCS, 2 mM glutamine, 100 U mL^{-1} penicillin, $100 \mu\text{g mL}^{-1}$ streptomycin) and incubated at $37 \text{ }^\circ\text{C}$ in humidified atmosphere with 5 % CO_2 . After 7 h the incubation medium was replaced with the fresh medium to remove the nanoparticles which had been detached from the metallic substrate and dispersed in the medium.

As control we used the following systems:

1. Cells cultivated on pure titanium plates;

2. Cells cultivated on pure titanium plates and transfected with the commercial agent Polyfect[®] from the dispersion;
3. Cells cultivated on calcium phosphate/PEI nanoparticle-coated plates;
4. Cells cultivated on calcium phosphate/PEI nanoparticle-coated surface with DNA which was dripped onto the coating and dried at 37 °C before seeding of the cells.

The schematic representation of the experiment and one of the controls is shown in Figure 4.6.2.1.

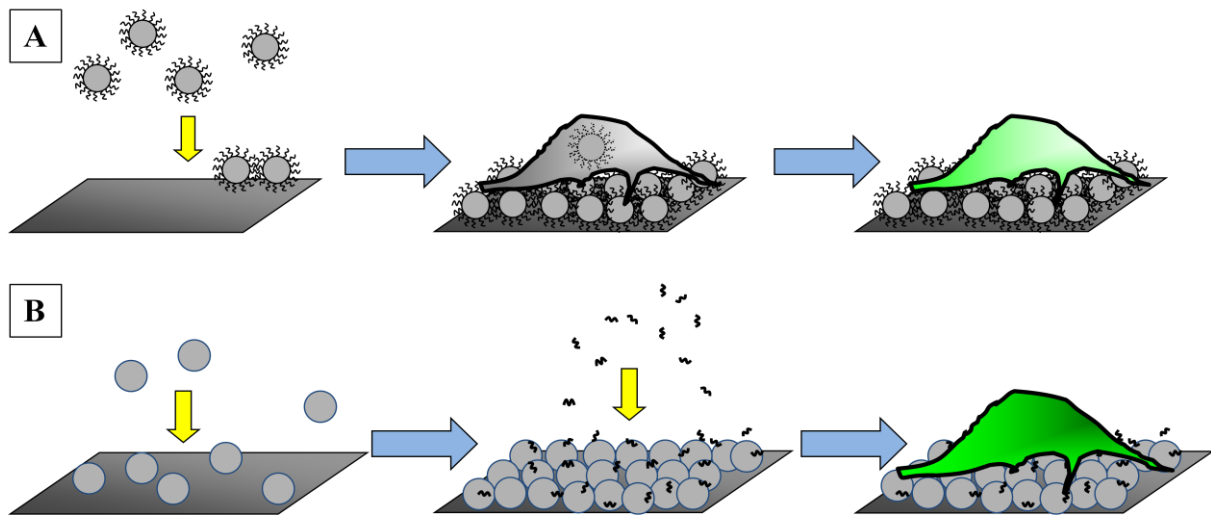


Figure 4.6.2.1: Schematic representation of the coating of the titanium surface with (A) calcium phosphate/PEI/DNA and (B) calcium phosphate/PEI nanoparticles with subsequent addition of DNA solution and the subsequent transfection.

First we analyzed the cytocompatibility of the coatings and the attachment of cells to the surface by scanning electron microscopy. The cells were cultivated on coated titanium plates for 48 h, then fixed with 3% paraformaldehyde, dehydrated in an ascending ethanol row (20, 40, 60, 80 and 96 %) and then subjected to critical point drying. A morphological analysis of the cell culture by

SEM showed an excellent adhesion of the cells to the substrate and also a large number of nanoparticles on the cell surface (Figure 4.6.2.2). The nanoparticles were found also on the upper side of cells presumably due to the special method of cell locomotion on the coating. Such a tight contact of the cell membrane with a large number of particles enhances the chance of the nanoparticles to be taken up via endocytosis, in contrast to the usual methods where dispersed nanoparticles are used which only rarely meet the cell surface. Also, the spreading of the cells on the coating and their good adhesion indicated that cells remained healthy.

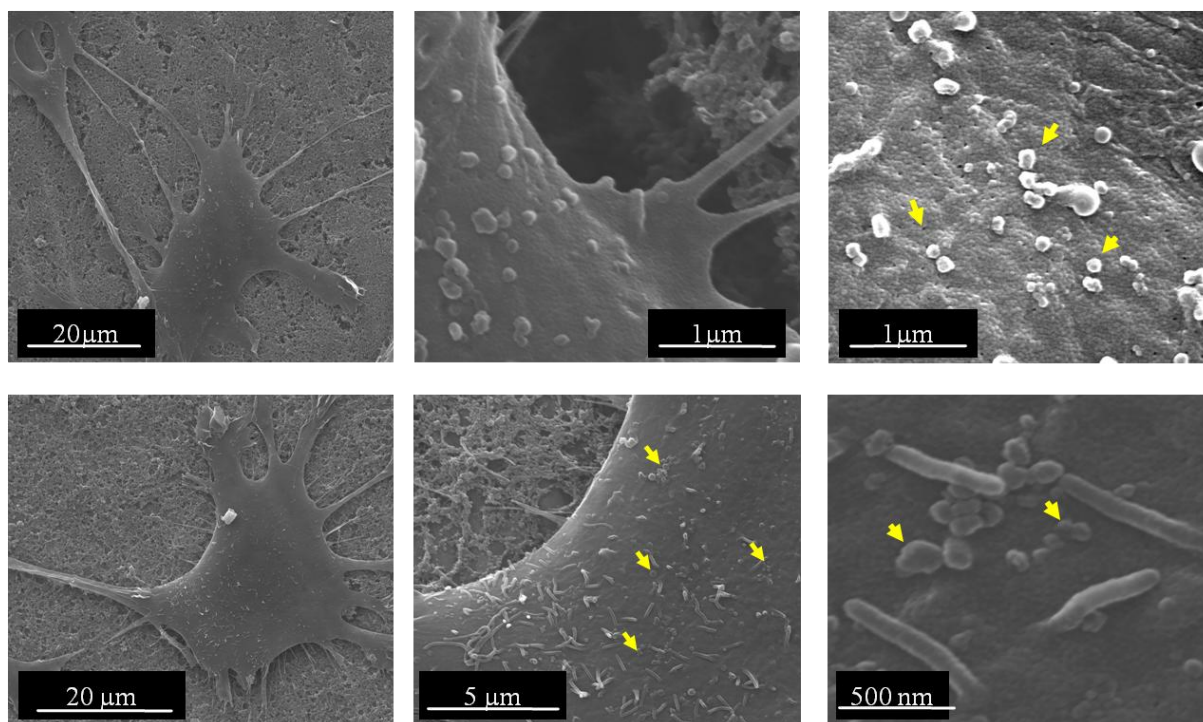


Figure 4.62.2.2: Scanning electron micrograph of NIH3T3 fibroblasts grown on calcium phosphate/PEI/DNA nanoparticle-loaded titanium surfaces. **Top row:** Cells seeded on the calcium phosphate/PEI/DNA nanoparticle coating; **bottom row:** Cells seeded on the calcium phosphate/PEI nanoparticle coating with dripped DNA. Yellow arrows indicate nanoparticles on the cell surface.

Therefore, we subjected the cells to the further incubation and measured the transfection efficiency. After 48 h of incubation, we observed a successful transfection by fluorescence microscopy, flow cytometry (fluorescence-activated cell sorting, FACS) and Western Blot. The cell nuclei were additionally stained with DAPI (4',6-diamidino-2-phenylindole, a fluorescent dye, which strongly binds to DNA) to detect the general number of cells on the substrate in comparison to the green fluorescing cells. The results of reflected-light fluorescence microscopy are shown in Figure 4.6.2.3.

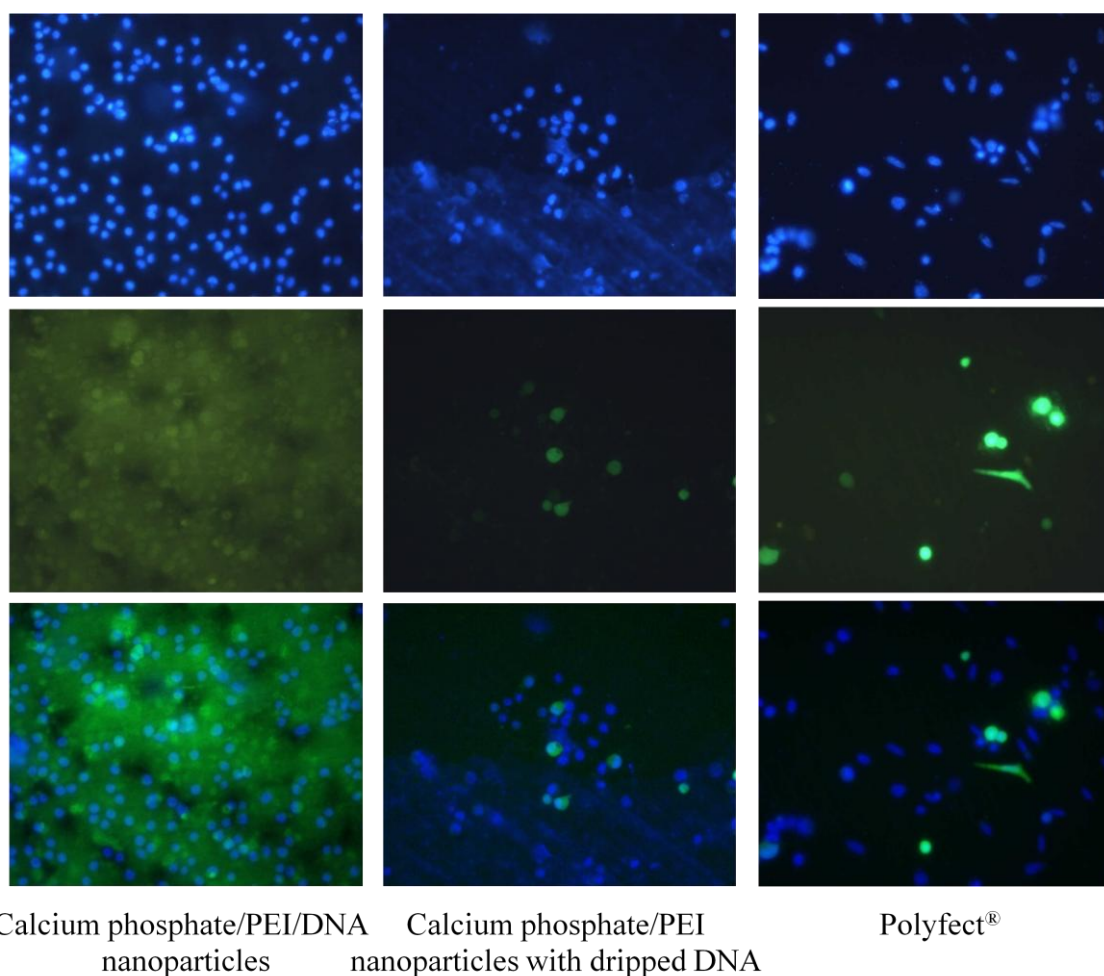


Figure 4.6.2.3: Fluorescence microscopy of NIH3T3 cells seeded on coated titanium surfaces, cells seeded on titanium and transfected from dispersion and of cells transfected with Polyfect[®]. Transfected cells are green due to the expression of EGFP. **Upper row:** Cell nuclei stained with DAPI; **middle row:** Cells expressing EGFP; **bottom row:** Overlay of both images (magnification: 200x in all cases).

Figure 4.6.2.3 shows the general number of cells on the plate (all living cell nuclei were stained blue with DAPI) and successfully transfected cells (green due to the expression of EGFP). However, due to the strong autofluorescence of the cells and the fluorescence of the coating (particularly in Figure 4.6.2.3, first

column), the numerical analysis of the micrographs was not possible. Therefore, we performed flow cytometry of the samples. The graphical results of the FACS analysis are shown in Figures 4.6.2.4-4.6.2.5 and the numerical results are presented in Table 4.6.2.1.

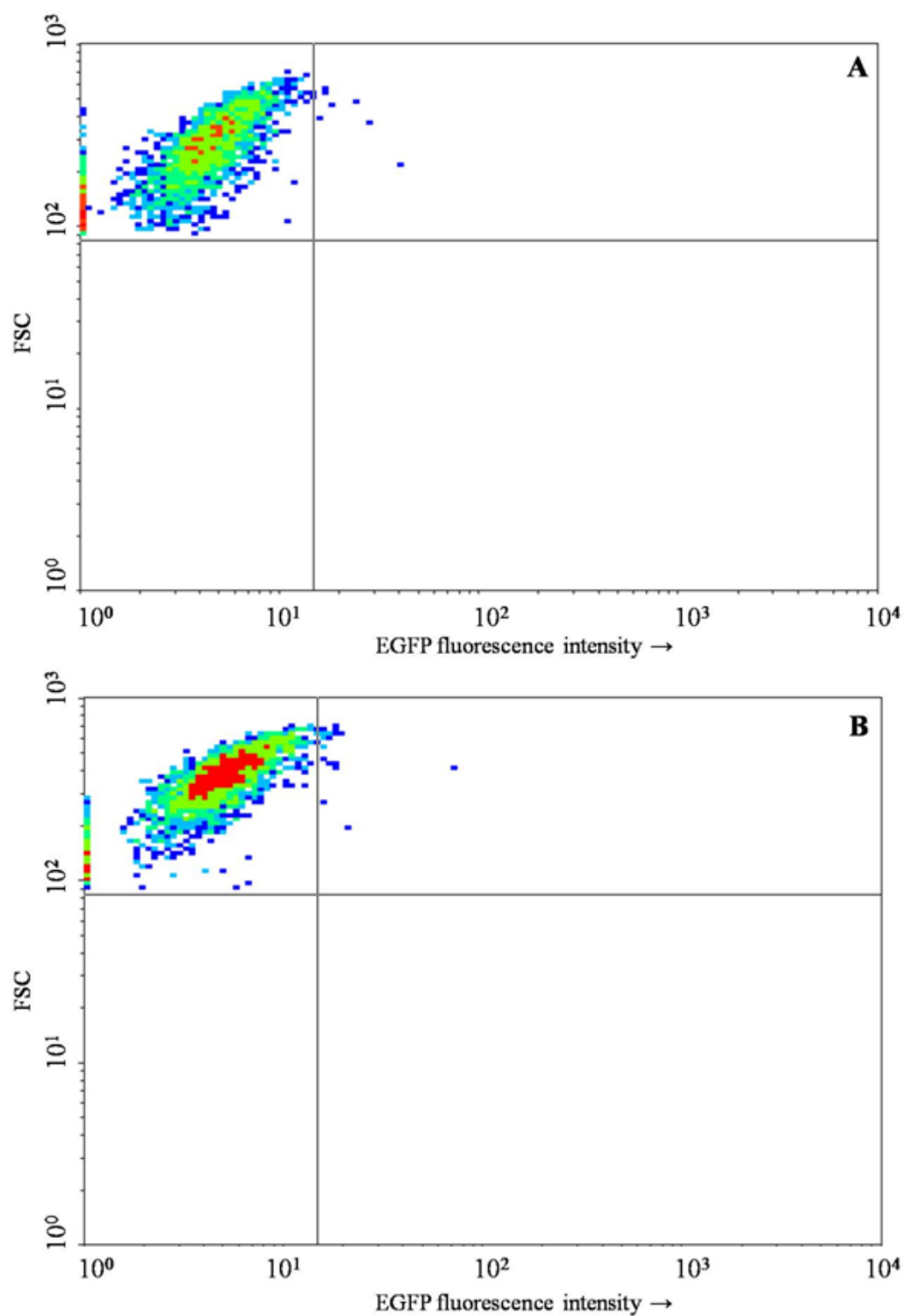


Figure 4.6.2.4: Flow cytometry of control NIH3T3 cells seeded on titanium surface (A) and cells seeded on the titanium plates and transfected with Polyfect[®] from dispersion (B).

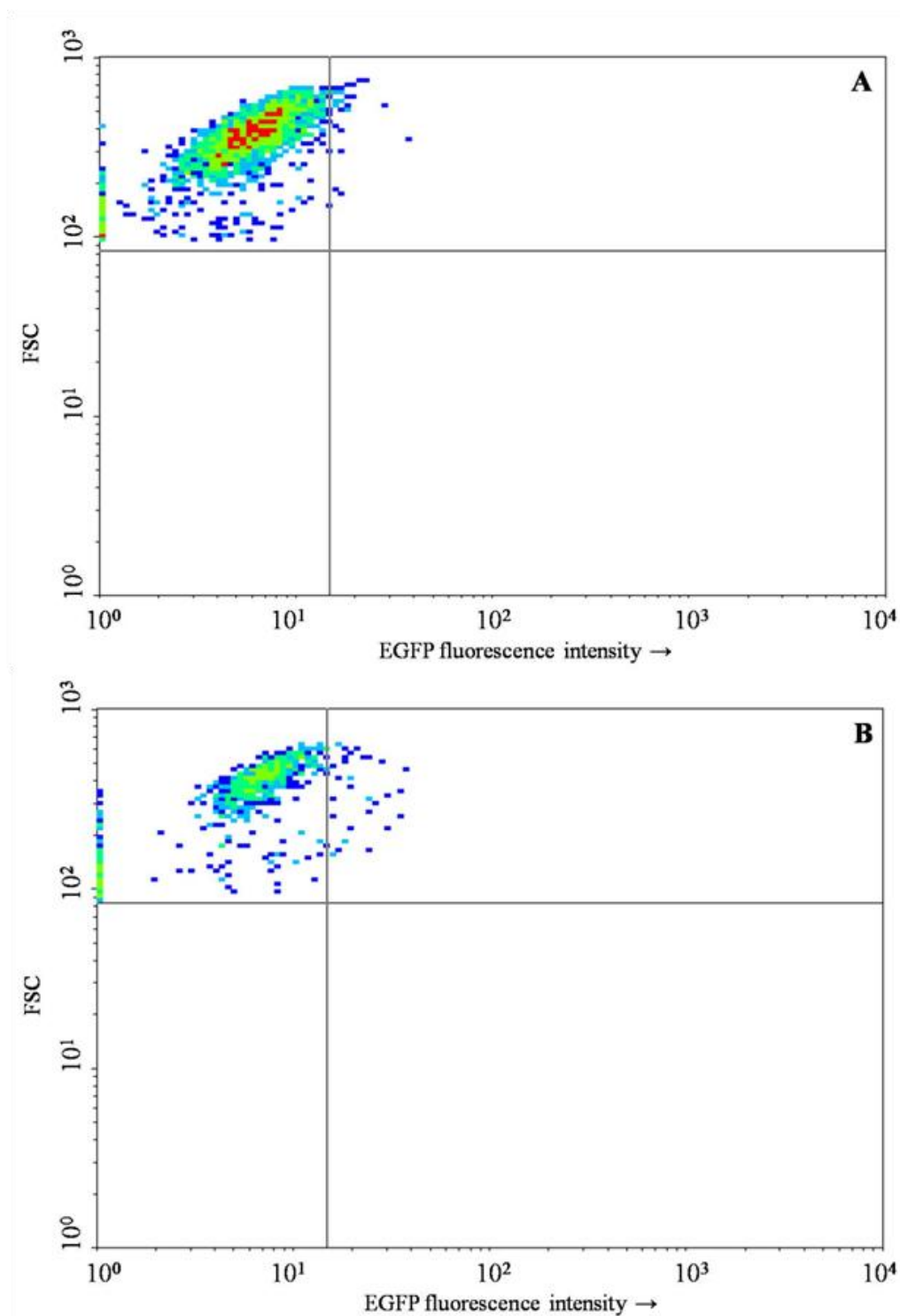


Figure 4.6.2.5: Flow cytometry of NIH3T3 cells transfected with calcium phosphate/PEI nanoparticles with later dripped DNA from the coating (**A**) and cells transfected with calcium phosphate/PEI/DNA nanoparticles from the coating (**B**).

NIH3T3 cells seeded on titanium substrate were used as a standard for the living population and as a negative control for the EGFP transfection efficiency (Figure 4.6.2.4, A). The living population was defined and gated according to the FSC/SSC parameters (Forward Scatter or FSC, a detector in line with the light beam and Side Scatter or SSC, a detector perpendicular to the light beam) individually for each set of experiments. The region with living cells was analyzed by dot plot analysis using two parameters: FSC and EGFP fluorescence intensity. The square statistics were used to analyse single positive (only on one axis) and double positive (on both axes) cells. Alive cells were selected according to their granularity, gated in the left upper square and were assumed to be EGFP negative. The gate for EGFP was set up according to this population and all samples were analyzed accordingly to this square statistics. The background in the negative control (NIH3T3 cells seeded on titanium substrate) was around 2 %. Presumably these were dust particles or impurities in dispersion. The cells transfected with Polyfect[®] showed a moderate transfection efficiency of about 16.8 %. Cells seeded on titanium substrate coated with calcium phosphate/PEI/DNA and calcium phosphate/PEI nanoparticles with dripped DNA showed a similar transfection efficiency of 14.5 and 16.3 %, respectively.

Table 4.6.2.1: Efficiency of gene transfer as determined by FACS ($N=3$).

| Sample | Efficiency \pm SD / % |
|--|-------------------------|
| Control cells on titanium plates | 2.4 \pm 0.3 |
| CaP/PEI/DNA-nanoparticle coating | 14.5 \pm 5.1 |
| CaP/PEI-nanoparticles coating with dripped DNA | 16.3 \pm 8.8 |
| CaP/PEI nanoparticle coating | 5.8 \pm 2.9 |
| Polyfect [®] as dispersion | 16.8 \pm 11.8 |

To be entirely sure that observed fluorescence belonged to EGFP we performed Western Blot analysis of all samples. The results are shown in Figure 4.6.2.6. $5 \cdot 10^4$ cells were initially seeded per well, therefore Western Blotting was complicated due to the small amount of protein. Anti-GFP, N-terminal primary antibody produced in rabbit^[165,166] was used to compare the levels of EGFP expression. Tubulin was used as loading control and detected using monoclonal mouse anti-tubulin antibody.^[167]

According to the loading of the equal amount of the total protein per well during the SDS-gel running procedure, we found the same amounts of tubulin by Western Blotting in all samples including the untransfected negative control. Thus, we observed bands of tubulin as loading control in the sample. The bands of EGFP were clearly seen in all cases.

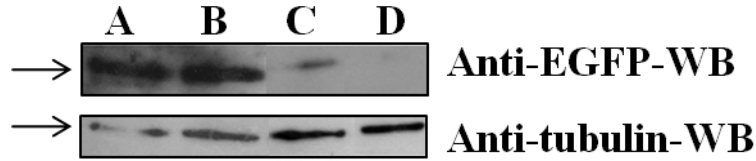


Figure 4.6.2.6: Western Blot of NIH3T3 cells after transfection with different techniques. **A:** Cells onto calcium phosphate/PEI nanoparticle-coating with later dripped DNA; **B:** cells onto calcium phosphate/PEI/DNA nanoparticle-coating; **C:** Polyfect[®] in dispersion; **D:** control untransfected cells.

However, the amount of EGFP was different in each case. We could clearly observe the strongest band in the case of cells transfected with calcium phosphate/PEI nanoparticles with later dripped DNA and in the case of calcium phosphate/PEI/DNA nanoparticles. Using Polyfect[®] we also detected EGFP expression; however, in this case the level of expression was slightly lower. These data correspond to the results previously obtained by FACS analysis and reflected-light fluorescence microscopy.

Thus, such a localized application of calcium phosphate nanoparticles leads to a successful transfection of cells and can be further applied *in vivo*. The coating of implants with transfection agents helps to avoid the systemic application of gene carriers and therefore to minimize the side effects of such application. For example, calcium as one of the important intracellular ions is involved in muscle contraction or intracellular signaling pathways. Thus, the increase of calcium concentration in bloodstream can lead to, *e.g.*, formation of atherosclerotic plaques, or cell death due to the disturbance of intracellular ionic balance, as shown in Section 4.2. Therefore, the localized therapy of local tissue is very promising.

4.6.3 Conclusion

We developed an easy method of electrophoretic deposition of DNA-loaded calcium phosphate nanoparticles on conducting implants which could be used for an efficient gene therapy. The addition of PEI as a first step of particle functionalization considerably improved the structure of nanoparticle layer.

The transfection efficiency of such coatings on NIH3T3 cells was comparable to that of commercial reagent Polyfect[®] and probably achieved due to the locomotion of the cells on the substrate which leads to a greater and tighter surface contact of cells with many nanoparticles, thereby enhancing the chance of particles to penetrate the cell membrane. Fluorescent reflected-light microscopy, flow cytometry and Western Blotting showed that cells expressed EGFP after 48 h cultivation on the nanoparticle-coated titanium substrate. The electrophoretic deposition of functionalized nanoparticles on any conducting material offers a way for the localized gene therapy avoiding long circulation of therapeutic agent in blood and, therefore, possibly minimizing the side effects on the organism due to the presence foreign agents (*i.e.* calcium phosphate nanoparticles).

5 Summary

In this study chemical, biological and biochemical investigations were carried out in collaboration with our partners: The Chair of Molecular Neurobiochemistry at the Ruhr-University of Bochum, the Department of Dermatology at the University of Münster and the *Institut National de la Santé et de la Recherche Médicale* at the *Université Louis Pasteur*, Strasbourg, France. The main purpose of these collaborations was to apply calcium phosphate nanoparticles as carriers for nucleic acids into different cell systems to test its properties.

First, we performed an easy and straightforward synthesis of calcium phosphate nanoparticles partially or completely substituted by magnesium or aluminum. However, although these nanoparticles were much smaller than the pure calcium phosphate nanoparticles, they did not prove to be very efficient for the delivery of nucleic acids.

In order to test the toxicity of the system we monitored the intracellular calcium level by using of ^{45}Ca -marked nanoparticles and the calcium dye Fura-2. Our nanoparticulate delivery system proved to be nontoxic to the cells compared to other delivery systems (the commercial agent Polyfect[®] and the standard calcium-based method). Nanoparticles also did not lead to the disturbances of the intracellular calcium level which, otherwise, could be lethal for cells.

In the next steps we functionalized the calcium phosphate nanoparticles with different oligonucleotides and tested them on cell culture. The nanoparticles functionalized with siRNA were far more effective than Polyfect[®] and still nontoxic. The nanoparticles functionalized with shRNA effectively inhibited the synthesis of osteopontin and osteocalcin when also embedded into polyelectrolyte multilayers. This also allows the localized application of gene silencing.

We functionalized the nanoparticles with the oligonucleotides which are able to mimic the microbial antigens, thus activating the immune system and breaking the innate tolerance of the organism. We used CpG oligonucleotides for the activation of the dendritic cells which leads to the synthesis of IL-12 and presumably other signaling molecules.

We performed localized transfection experiments via deposition of the nanoparticles on metal substrates. In this case we could achieve high transfection efficiency and a local direct application.

Thus, we showed that the synthesis of calcium phosphate nanoprecipitates and their subsequent functionalization is possible. Such system was effectively used as a carrier for DNA and RNAs into the different cell cultures and proved to be effective and nontoxic for cells.

6 Literature

- [1] J. D. Watson, F. H. C. Crick, *Nature*, **171**, (1953), 737.
- [2] M. Feughelman, R. Langridge, W. E. Seeds, A. R. Stokes, H. R. Wilson, C. W. Hooper, M. H. F. Wilkins, R. K. Barclay, L. D. Hamilton, *Nature*, **175**, (1955), 834
- [3] D. M. Crothers, V. A. Bloomfield, I. Tinoco, *Nucleic acids: Structures, properties, and functions*, University Science Books, (2000).
- [4] J. D. Watson, F. H. C. Crick, *Am. J. Psychiatr.*, **160**, (2003), 623.
- [5] J. Iball, H. R. Wilson, *Nature*, **198**, (1963), 1193.
- [6] G. M. Blackburn, M. J. Gait, D. Loakes, *Nucleic acids in chemistry and biology*, 3 ed., RSC Publishing, (2005).
- [7] J. D. Brown, M. Lyall, *Aust. J. Chem.*, **15**, (1962), 851.
- [8] P. E. Squires, R. F. L. James, N. J. M. London, M. J. Dunne, *Pflügers Archiv Eur. J. Physiol.*, **427**, (1994), 181.
- [9] G. E. Billman, *Cardiovasc. Res.*, **28**, (1994), 762.
- [10] R. F. Gesteland, J. F. Atkins, T. R. Cech, *The RNA world: The nature of modern RNA suggests a prebiotic RNA*, 2 ed., CSHL Press, (1999).
- [11] R. W. Holley, J. Apgar, G. A. Everett, J. T. Madison, M. Marquisee, S. H. Merrill, J. R. Penswick, A. Zamir, *Science*, **147**, (1965), 1462.
- [12] A. Z. Fire, *Angew. Chem. Int. Ed.*, **46**, (2007), 6966.
- [13] C. C. Mello, *Angew. Chem. Int. Ed.*, **46**, (2007), 6985.
- [14] J. Kurreck, *Angew. Chem.*, **121**, (2009), 1404.
- [15] E. J. Sontheimer, R. W. Carthew, *Cell*, **122**, (2005), 9.
- [16] F. Crick, *Nature*, **227**, (1970), 561.
- [17] A. Fire, S. Xu, M. K. Montgomery, S. A. Kostas, S. E. Driver, C. C. Mello, *Nature*, **391**, (1998), 806.
- [18] L. Gitlin, R. Andino, *J. Virol.*, **77**, (2003), 7159.
- [19] C. C. Mello, D. Conte Jr., *Nature*, **431**, (2004), 338.

- [20] G. Meister, T. Tuschl, *Nature*, **431**, (2004), 343.
- [21] J. Martinez, A. Patkaniowska, H. Urlaub, R. Lührmann, T. Tuschl, *Cell*, **110**, (2002), 563.
- [22] S. K. Radhakrishnan, T. J. Layden, A. L. Gartel, *Virology*, **323**, (2004), 173.
- [23] R. Lu, M. Maduro, F. Li, H. Li, G. Broitman-Maduro, W. Li, S. Ding, *Nature*, **436**, (2005).
- [24] S. M. Elbashir, J. Harborth, K. Weber, T. Tuschl, *Methods*, **26**, (2002), 199.
- [25] R. Wadhwa, S. C. Kaul, M. Miyagishi, K. Taira, *Mutat. Res. Fund. Mol. Mech. Mutagen.*, **567**, (2004), 71.
- [26] D. Ovcharenko, R. Jarvis, S. Hunicke-Smith, K. Kelnar, D. Brown, *RNA*, **11**, (2005), 985.
- [27] M. Kerkmann, D. Lochmann, J. Weyermann, A. Marschner, H. Poeck, M. Wagner, J. Battiany, A. Zimmer, S. Endres, G. Hartmann, *Oligonucleotides*, **16**, (2006), 313.
- [28] Y. Krishnamachari, A. K. Salem, *Adv. Drug Deliv. Rev.*, **61**, (2009), 205.
- [29] M. J. Heffernan, S. P. Kasturi, S. C. Yang, B. Pulendran, N. Murthy, *Biomaterials*, **30**, (2009), 910.
- [30] G. Mutwiri, S. van Drunen Littel-van den Hurk, L. A. Babiuk, *Adv. Drug Deliv. Rev.*, **61**, (2009), 226.
- [31] N. Bessis, F. J. Garcia Cozar, M. C. Boissier, *Gene Ther.*, **11**, (2004), S10.
- [32] D. Verthelyi, D. M. Klinman, *Clin. Immunol.*, **109**, (2003), 64.
- [33] J. A. Aebig, G. E. D. Mullen, G. Dobrescu, K. Rausch, L. Lambert, O. Ajose-Popoola, C. A. Long, A. Saul, A. P. Miles, *J. Immunol. Meth.*, **323**, (2007), 139.

- [34] R. Spisek, J. Brazova, D. Rozkova, K. Zapletalova, A. Sediva, J. Bartunkova, *Vaccine*, **22**, (2004), 2761.
- [35] C. Wischke, J. Zimmermann, B. Wessinger, A. Schendler, H. H. Borchert, J. H. Peters, T. Nesselhut, D. R. Lorenzen, *Int. J. Pharm.*, **365**, (2009), 61.
- [36] M. P. Seiler, S. Gottschalk, V. Cerullo, M. Ratnayake, V. P. Mane, C. Clarke, D. J. Palmer, P. Ng, C. M. Rooney, B. Lee, *Mol. Ther.*, **15**, (2007), 386.
- [37] J. R. Kovacs, Y. Zheng, H. Shen, W. S. Meng, *Biomaterials*, **26**, (2005), 6754.
- [38] E. Orrantia, P. L. Chang, *Exp. Cell. Res.*, **190**, (1990), 170.
- [39] P. Batard, M. Jordan, F. Wurm, *Gene*, **270**, (2001), 61.
- [40] V. Sokolova, M. Epple, *Angew. Chem. Int. Ed.*, **47**, (2008), 1382.
- [41] D. T. Curiel, S. Agarwal, E. Wagner, M. Cotton, *Proc. Natl. Acad. Sci. USA*, **88**, (1991), 8850.
- [42] J. H. Lee, M. J. Welsh, *Gene Ther.*, **6**, (1999), 676.
- [43] S. K. Tripathy, H. B. Black, E. Goldwasser, J. M. Leiden, *Nat. Med.*, **2**, (1996), 545.
- [44] N. Ishii, J. Fukushima, T. Kaneko, E. Okada, K. Tani, S. I. Takana, *AIDS Res. Hum. Retroviruses*, **13**, (1997), 1421.
- [45] S. Yang, R. Delgado, S. R. King, C. Woffendin, C. S. Barker, Z. Y. Yang, L. Xu, G. P. Nolan, G. J. Nabel, *Hum. Gene Ther.*, **10**, (1999), 123.
- [46] A. A. Bukovsky, J. P. Song, L. Naldini, *J. Virol.*, **73**, (1999), 7087.
- [47] J. P. Burand, M. D. Summers, G. E. Smith, *Virology*, **101**, (1980), 286.
- [48] J. Weyermann, D. Lochmann, A. Zimmer, *J. Contr. Release*, **100**, (2004), 411.
- [49] M. R. Capecchi, *Cell*, **22**, (1980), 479.
- [50] T. Masuda, H. Akita, H. Harashima, *FEBS Lett.*, **579**, (2005), 2143.
- [51] G. L. Andreason, G. A. Evans, *Anal. Biochem.*, **180**, (1989), 269.

- [52] H. Aihara, J. Miyazaki, *Nat. Biotechnol.*, **16**, (1998), 867.
- [53] E. Neumann, M. Schaefer-Ridder, Y. Wang, P. H. Hofschneider, *EMBO J.*, **1**, (1982), 841.
- [54] A. Fasbender, J. Zabner, B. G. Zeiher, M. J. Welsh, *Gene Ther.*, **4**, (1997), 1173.
- [55] M. Junghans, S. M. Loitsch, S. C. Steiniger, J. Kreuter, A. Zimmer, *Eur. J. Pharm. Biopharm.*, **60**, (2005), 287.
- [56] H. T. Lv, S. B. Zhang, B. Wang, S. H. Cui, J. Yan, *J. Contr. Release*, **114**, (2006), 100.
- [57] S. E. McNeil, Y. Perrie, *Expert Opin. Ther. Pat.*, **16**, (2006), 1371.
- [58] J. Zabner, A. J. Fasbender, T. Moninger, *J. Biol. Chem.*, **270**, (1995), 18997.
- [59] J. Kunisawa, T. Masuda, K. Katayama, T. Yoshikawa, Y. Tsutsumi, M. Akashi, T. Mayumi, S. Nakagawa, *J. Contr. Release*, **105**, (2005), 344.
- [60] D. D. Lasic, N. S. Templeton, *Adv. Drug Deliv. Rev.*, **20**, (1996), 221.
- [61] X. Zhou, L. Huang, *Biochim. Biophys. Acta*, **1189**, (1994), 195.
- [62] R. I. Mahato, K. Kawabata, Y. Takakura, M. Hashida, *J. Drug Target.*, **3**, (1995), 149.
- [63] A. Swami, R. K. Kurupati, A. Pathak, J. Singh, P. Kumar, K. C. Gupta, *Biochem. Biophys. Res. Comm.*, **362**, (2007), 835.
- [64] A. N. Zelikin, Q. Li, F. Caruso, *Angew. Chem.*, **118**, (2006), 7907.
- [65] X. Zhu, L. Lu, B. L. Currier, A. J. Windebank, M. J. Yaszemski, *Biomaterials*, **23**, (2002), 2683.
- [66] D. Lochmann, Dissertation, Goethe-Universität Frankfurt am Main, Frankfurt am Main, (2004).
- [67] D. Lochmann, J. Weyermann, C. Georgens, R. Prassl, A. Zimmer, *Eur. J. Pharm. Biopharm.*, **59**, (2005), 419.

- [68] J. Weyermann, D. Lochmann, C. Georgens, A. Zimmer, *Eur. J. Pharm. Biopharm.*, **59**, (2005), 431.
- [69] V. Vogel, D. Lochmann, J. Weyermann, G. Mayer, C. Tziatzios, J. A. van der Broek, W. Haase, D. Wouters, U. S. Schubert, J. Kreuter, A. Zimmer, D. Schubert, *J. Contr. Release*, **103**, (2005), 99.
- [70] I. Puebla, S. Esseghir, A. Mortlock, A. Brown, A. Crisanti, W. Low, *J. Biotechnol.*, **105**, (2003), 215.
- [71] M. Tsoli, H. Kuhn, W. Brandau, H. Esche, G. Schmid, *Small*, **1**, (2005), 841.
- [72] R. Jin, G. Wu, Z. Li, C. A. Mirkin, G. C. Schatz, *J. Am. Chem. Soc.*, **125**, (2003), 1643.
- [73] N. L. Rosi, D. A. Giljohann, C. S. Thaxton, A. K. R. Lytton-Jean, M. S. Han, C. A. Mirkin, *Science*, **312**, (2006), 1027.
- [74] M. Thomas, A. M. Klibanov, *Proc. Natl. Acad. Sci. USA*, **100**, (2003), 9138.
- [75] J. Zhang, J. Malicka, I. Gryczynski, J. R. Lakowicz, *Anal. Biochem.*, **330**, (2004), 81.
- [76] A. A. Zinchenko, K. Yoshikawa, D. Baigl, *Adv. Mater.*, **17**, (2005), 2820.
- [77] A. Campo, T. Sen, J.-P. Lellouche, I. J. Bruce, *J. Magn. Magn. Mater.*, **293**, (2005), 33.
- [78] A. Jordan, R. Scholz, P. Wust, H. Schirra, T. Schiestel, H. Schmidt, R. Felix, *J. Magn. Magn. Mater.*, **194**, (1999), 185.
- [79] X. M. Lin, A. C. S. Samia, *J. Magn. Magn. Mater.*, **305**, (2006), 100.
- [80] M. Boissière, J. Allouche, C. Chanéca, R. Braynerb, J. M. Devoissellec, J. Livagea, T. Coradin, *Int. J. Pharm.*, **344**, (2007), 128.
- [81] Z. Liu, M. Winters, M. Holodniy, H. Dai, *Angew. Chem. Int. Ed.*, **46**, (2007), 2023
- [82] G. Bhakta, S. Mitra, A. Maitra, *Biomaterials*, **26**, (2005), 2157.

- [83] F. L. Graham, A. J. van der Eb, *Virology*, **52**, (1973), 456.
- [84] S. V. Dorozhkin, M. Epple, *Angew. Chem. Int. Ed.*, **41**, (2002), 3130.
- [85] F. Neues, W. H. Arnold, J. Fischer, F. Beckmann, P. Gängler, M. Epple, *Mat.-wiss. u. Werkstofftech.*, **37**, (2006), 426.
- [86] P. Girard, L. Porte, T. Berta, M. Jordan, F. Wurm, *Cytotechnology*, **35**, (2001), 175.
- [87] S. Chenuet, D. Martinet, N. Besuchet-Schmutz, M. Wicht, N. Jaccard, A. C. Bon, M. Derouazi, D. L. Hacker, J. S. Beckmann, F. Wurm, *Biotechnol. Bioeng.*, **101**, (2008), 937
- [88] S. Y. Watanabe, A. M. Albsoul-Younes, T. Kawano, H. Itoh, Y. Kaziro, S. Nakajima, Y. Nakajima, *Neurosci. Res.*, **33**, (1999), 71.
- [89] I. Segura, M. A. Gonzalez, A. Serrano, J. L. Abad, A. Bernad, H. H. Riese, *Anal. Biochem.*, **296**, (2001), 143.
- [90] A. Watson, D. Latchman, *Methods*, **10**, (1996), 289.
- [91] V. Sokolova, Dissertation, Universität Duisburg-Essen, Essen, (2006).
- [92] A. Maitra, *Expert. Rev. Mol. Diagn.*, **5**, (2005), 893.
- [93] M. Jordan, A. Schallhorn, F. M. Wurm, *Nucl. Acids Res.*, **24**, (1996), 596.
- [94] M. Jordan, F. Wurm, *Methods*, **33**, (2004), 136.
- [95] V. Sokolova, A. Kovtun, O. Prymak, W. Meyer-Zaika, E. A. Kubareva, E. A. Romanova, T. S. Oretskaya, R. Heumann, M. Epple, *J. Mater. Chem.*, **17**, (2007), 721.
- [96] S. Bisht, G. Bhakta, S. Mitra, A. Maitra, *Int. J. Pharm.*, **288**, (2005), 157.
- [97] H. Fu, Y. Hu, T. McNelis, J. O. Hollinger, *J. Biomed. Mater. Res.*, **74**, (2005), 40.
- [98] D. Olton, J. Li, M. E. Wilson, T. Rogers, J. Close, L. Huang, N. P. Kumta, C. Sfeir, *Biomaterials*, **28**, (2007), 1267.
- [99] V. Sokolova, O. Prymak, W. Meyer-Zaika, H. Cölfen, H. Rehage, A. Shukla, M. Epple, *Mat.-wiss. u. Werkstofftech.*, **37**, (2006), 441.

- [100] V. V. Sokolova, I. Radtke, R. Heumann, M. Epple, *Biomaterials*, **27**, (2006), 3147.
- [101] F. Caruso, *Colloids and Colloid Assemblies*, Wiley-VCH, Weinheim, (2004).
- [102] Z. Adamczyk, P. Weronki, *Adv. Colloid Interface Sci.*, **83**, (1999), 137.
- [103] R. J. Hunter, *Foundations of colloid science*, Clarendon Press, Oxford, (1986).
- [104] D. H. Everett, *Basic Principles of Colloid Science*, Royal Society of Chemistry, London, (1988).
- [105] R. J. Hunter, *Zeta potential in colloid science*, Academic Press, (1988).
- [106] A. E. Ewence, M. Bootman, H. L. Roderick, J. N. Skepper, G. McCarthy, M. Epple, M. Neumann, C. M. Shanahan, D. Proudfoot, *Circ. Res.*, **103**, (2008), e28.
- [107] A. Doat, P. F., N. Gardant, A. Lebugle, *J. Solid State Chem.*, **177**, (2004), 1179.
- [108] A. Doat, M. Fanjul, F. Pelle, E. Hollande, A. Lebugle, *Biomaterials*, **24**, (2003), 3365.
- [109] S. Padilla Mondejar, A. Kovtun, M. Epple, *J. Mater. Chem.*, **17**, (2007), 4153.
- [110] Y. Guo, D. Shi, J. Lian, Z. Dong, W. Wang, H. Cho, G. Liu, L. Wang, R. C. Ewing, *Nanotechnology*, **19**, (2008), 175102.
- [111] R. Ramachandran, W. Paul, C. P. Sharma, *J. Biomed. Mater. Res. B Appl. Biomater.*, **88**, (2009), 41.
- [112] X. Cheng, L. Kuhn, *Int. J. Nanomed.*, **2**, (2007), 667.
- [113] B. Palazzo, M. Iafisco, M. Laforgia, N. Margiotta, G. Natile, C. L. Bianchi, D. Walsh, S. Mann, N. Roveri, *Adv. Funct. Mater.*, **17**, (2007), 2180.

- [114] M. Kester, Y. Heakal, T. Fox, A. Sharma, G. P. Robertson, T. T. Morgan, E. I. Altinoğlu, A. Tabaković, M. R. Parette, S. M. Rouse, V. Ruiz-Velasco, J. H. Adair, *Nano Lett.*, **8**, (2008), 4116.
- [115] T. T. Morgan, H. S. Muddana, E. I. Altinoglu, S. M. Rouse, A. Tabaković, T. Tabouillot, T. J. Russin, S. S. Shanmugavelandy, P. J. Butler, P. C. Eklund, J. K. Yun, M. Kester, J. H. Adair, *Nano Lett.*, **8**, (2008), 4108.
- [116] T. Welzel, W. Meyer-Zaika, M. Epple, *Chem. Commun.*, (2004), 1204.
- [117] M. C. F. Magalhaes, P. A. A. P. Marques, R. N. Correia, in *Biomineralization: Medical aspects of solubility, Calcium and magnesium phosphates: Normal and pathological mineralization*, Wiley & Sons, (2006), 71.
- [118] C. Exley, J. D. Birchall, *J. Theor. Biol.*, **159**, (1992), 83.
- [119] E. H. Chowdhury, M. Kunou, M. Nagaoka, A. K. Kundu, T. Hoshiba, T. Akaike, *Gene*, **341**, (2004), 77.
- [120] E. H. Chowdhury, F. T. Zohra, S. Tada, C. Kitamura, T. Akaike, *Anal. Biochem.*, **335**, (2004), 162.
- [121] A. Kovtun, Diploma thesis, University of Duisburg-Essen, Essen, (2006).
- [122] A. Kovtun, R. Heumann, M. Epple, *Biomed. Mater. Eng.*, **19**, (2009), 241.
- [123] T. Welzel, I. Radtke, W. Meyer-Zaika, R. Heumann, M. Epple, *J. Mater. Chem.*, **14**, (2004), 2213.
- [124] M. Nakanishi, T. Akuta, E. Nagoshi, A. Eguchi, H. Mizuguchi, T. Senda, *Eur. J. Pharm. Sci.*, **13**, (2001), 17.
- [125] A. Loyter, G. Scangos, D. Juricek, D. Keene, F. H. Ruddle, *Exp. Cell Res.*, **139**, (1982), 223.
- [126] V. Sokolova, A. Kovtun, R. Heumann, M. Epple, *J. Biol. Inorg. Chem.*, **12**, (2007), 174.

- [127] Z. P. Xu, Q. H. Zeng, G. Q. Lu, A. B. Yu, *Chem. Eng. Sci.*, **61**, (2006), 1027.
- [128] C. E. Pedraza, D. C. Basset, M. D. McKee, V. Nelea, U. Gbureck, J. E. Barralet, *Biomaterials*, **29**, (2008), 3384.
- [129] T. Welzel, Diplomarbeit, Universität Duisburg-Essen, Essen, (2004).
- [130] S. G. Oakes, W. J. Martin, C. A. Lisek, G. Powis, *Anal. Biochem.*, **169**, (1988), 159.
- [131] K. Billing-Marczak, M. Przybyszewska, J. Kuznicki, *Biochim. Biophys. Acta*, **1449**, (1999), 169.
- [132] W. Almers, E. Neher, *FEBS Lett.*, **192**, (1985), 13.
- [133] G. Gryniewicz, M. Poenie, R. Y. Tsien, *J. Biol. Chem.*, **260**, (1985), 3440.
- [134] J. Suh, D. Wirtz, J. Hanes, *Proc. Natl. Acad. Sci. USA*, **100**, (2003), 3878.
- [135] J. Suh, D. Wirtz, J. Hanes, *Biotechnol. Prog.*, **20**, (2004), 598.
- [136] R. P. Kulkarni, D. D. Wu, M. E. Davis, S. E. Fraser, *Proc. Natl. Acad. Sci. USA*, **102**, (2005), 7523.
- [137] M. P. Mattson, S. L. Chan, *Nat. Cell Biol.*, **5**, (2003), 1041.
- [138] D. J. McConkey, S. Orrenius, *Biochem. Biophys. Res. Comm.*, **239**, (1997), 357.
- [139] N. J. Caplen, S. Parrish, F. Imani, A. Fire, R. A. Morgan, *Proc. Natl. Acad. Sci. USA*, **98**, (2001), 9742.
- [140] P. Sazani, A. Astriab-Fischer, R. Kole, *Antisense Nucleic Acid Drug Dev.*, **13**, (2003), 119.
- [141] S. M. Elbashir, J. Harborth, W. Lendeckel, A. Yalcin, K. Weber, T. Tuschl, *Nature*, **411**, (2001), 494.
- [142] S. M. Elbashir, W. Lendeckel, T. Tuschl, *Genes Dev.*, **15**, (2001).
- [143] T. J. Davidson, S. Harel, V. A. Arboleda, G. F. Prunell, M. L. Shelanski, L. A. Green, C. M. Troy, *J. Neurosci.*, **24**, (2004), 10040.

- [144] O. Donzé, D. Picard, *Nucleic Acids Res.*, **30**, (2002), e46.
- [145] C. D. Kaufman, Z. Izsvak, A. Katzer, Z. Ivics, *J. RNAi Gene Silencing*, **1**, (2005), 97.
- [146] J. Schwiertz, W. Meyer-Zaika, L. Ruiz-Gonzalez, J. M. Gonzales-Calbet, M. Vallet-Regi, M. Epple, *J. Mater. Chem.*, **18**, (2008), 3831.
- [147] N. Jessel, M. Oulad-Abdelghani, F. Meyer, P. Lavalley, Y. Haikel, P. Schaaf, J.-C. Voegel, *Proc. Natl. Acad. Sci. USA*, **103**, (2006), 8618.
- [148] J. Méndez Garza, N. Jessel, G. Ladam, V. Dupray, S. Muller, J.-F. Stoltz, P. Schaaf, J.-C. Voegel, P. Lavalley, *Langmuir*, **21**, (2005), 12372.
- [149] X. Zhang, K. Sharma, M. Boeglin, J. Ogier, D. Mainard, J.-C. Voegel, Y. Mély, N. Benkirane-Jessel, *Nano Lett.*, **8**, (2008), 2432.
- [150] J. Hiller, J. D. Mendelsohn, M. F. Rubner, *Nat. Mater.*, **1**, (2002), 59.
- [151] C. B. Rives, A. des Rieux, M. Zelivyanskaya, S. R. Stock, W. L. Lowe, L. D. Shea, *Biomaterials*, **30**, (2009), 394.
- [152] Z. Z. Lu, J. Wu, T. M. Sun, J. Ji, L. F. Yan, J. Wang, *Biomaterials*, **29**, (2008), 733.
- [153] Y. L. Li, L. D. Quarles, H. H. Zhou, Z. S. Xiao, *Biochem. Biophys. Res. Comm.*, **361**, (2007), 817.
- [154] J. J. Li, M. Han, J. K. Wen, A. Y. Li, *Biochem. Biophys. Res. Comm.*, **356**, (2007), 13.
- [155] J. Zhao, L. Dong, B. Lu, G. Wu, D. Xu, J. Chen, K. Li, X. Tong, J. Dai, S. Yao, M. Wu, Y. Guo, *Gastroenterology*, **135**, (2008), 956.
- [156] L. D. Shea, E. Smiley, J. Bonadio, D. J. Mooney, *Nat. Biotechnol.*, **17**, (1999), 551.
- [157] C. M. Jewell, D. M. Lynn, *Adv. Drug Deliv. Rev.*, **60**, (2008), 979.
- [158] C. M. Jewell, D. M. Lynn, *Curr. Opin. Colloid Interface Sci.*, **13**, (2008), 395.

- [159] F. Meyer, M. Dimitrova, J. Jedrzejenska, Y. Arntz, P. Schaaf, B. Frisch, J.-C. Voegel, J. Ogier, *Biomaterials*, **29**, (2008), 618.
- [160] K. Ren, J. Ji, J. Shen, *Bioconjug. Chem.*, **17**, (2006), 77.
- [161] V. P. Taori, Y. Liu, T. M. Reineke, *Acta Biomater.*, **5**, (2009), 925.
- [162] H. Urch, C. Geismann, M. Ulbricht, M. Epple, *Mat.-wiss. u. Werkstofftech.*, **37**, (2006), 422.
- [163] H. Urch, S. Franzka, D. Dahlhaus, N. Hartmann, E. Hasselbrink, M. Epple, *J. Mater. Chem.*, **16**, (2006), 1798.
- [164] H. Urch, Dissertation, Universität Duisburg-Essen, Essen, (2008).
- [165] M. Ormö, A. B. Cubitt, K. Kallio, L. A. Gross, R. Y. Tsien, S. J. Remington, *Science*, **273**, (1996), 1392.
- [166] T. Tsukamoto, N. Hashiguchi, S. M. Janicki, T. Tumber, A. S. Belmont, D. L. Spector, *Nat. Cell Biol.*, **2**, (2000), 871.
- [167] S. Bär, L. Daeffler, J. Rommelaere, J. P. F. Nüesch, *PLoS Pathog.*, **4**, (2008), e1000126.

7 Appendix

7.1 List of abbreviations

| | |
|-------------------|--|
| A | adenine |
| bp | base pair |
| BSA | bovine serum albumin |
| C | cytosine |
| CaP | calcium phosphate |
| <i>C. elegans</i> | <i>Caenorhabditis elegans</i> |
| CpG | cytosin-phosphatidyl-guanosin |
| DAPI | 4',6-diamidino-2-phenylindole |
| DC | dendritic cells |
| DLS | dynamic light scattering |
| DLVO | Derjaguin, Landau, Verwey, Overbeek |
| DMEM | Dulbecco's modified Eagle medium |
| DMSO | dimethyl sulfoxide |
| DNA | deoxyribonucleic acid |
| ds | double stranded |
| <i>E. coli</i> | <i>Escherichia coli</i> |
| EDTA | ethylenediaminetetraacetate |
| EGFP | enhanced green fluorescent protein |
| FACS | fluorescence-activated cell sorting |
| FCS | fetal calf serum |
| FSC | forward scatter |
| G | guanine |
| G418 | Geneticin |
| HA | hydroxyapatite |
| HBS | HEPES buffered solution |
| HeLa | Henrietta Lacks |
| HEPES | 4-(2-hydroxyethyl)-1-piperazineethanesulfonic acid |
| HOb | human osteoblasts |
| IL | interleukin |
| kDa | kilodalton |
| LB | Luria Bertani |
| mRNA | messenger RNA |
| MTT | 3-(4,5-dimethylthiazol-2-yl)-2,5-diphenyltetrazolium bromide |
| miRNA | microRNA |
| nm | nanometer |
| NIH3T3 | mouse embryonic fibroblast cell line |
| NP | nanoparticle |

| | |
|-----------|--|
| nt | nucleotide |
| PBS | phosphate buffered saline |
| PDI | polydispersity index |
| PEG | poly(ethylene glycol) |
| PGLA | poly(lactide- <i>co</i> -glycolic acid) |
| PI | propidium iodide |
| PLL | poly-L-lysine |
| PMSF | phenylmethylsulphonyl fluoride |
| Poly(I:C) | poly(inosinic acid)-poly(cytidilic acid) |
| RISC | RNA induced silencing complex |
| RNA | ribonucleic acid |
| RNAi | RNA interference |
| rRNA | ribosomal RNA |
| SD | standard deviation |
| SDS | sodium dodecyl sulfate |
| SEM | scanning electron microscopy |
| siRNA | small interfering RNA |
| shRNA | short hairpin RNA |
| SSC | side scatter |
| T | thymine |
| T24 | human bladder carcinoma cells |
| TRITC | tetramethylrhodamine isothiocyanate |
| TEM | transmission electron microscopy |
| tRNA | transfer RNA |
| U | uracil |
| UV | ultraviolet |
| WB | Western Blotting |

7.2 Publications

7.2.1 Regular papers in refereed journals

1. V. Sokolova, A. Kovtun, O. Prymak, W. Meyer-Zaika, E. A. Kubareva, E. A. Romanova, T. S. Oretskaya, R. Heumann, M. Epple "Functionalisation of calcium phosphate nanoparticles by oligonucleotides and their application for gene silencing", *J. Mater. Chem.* 17 (2007) 721-727.
2. V. Sokolova, A. Kovtun, R. Heumann, M. Epple "Tracking the pathway of calcium phosphate/DNA nanoparticles during cell transfection by incorporation of red-fluorescing TRITC-BSA into the nanoparticles", *J. Biol. Inorg. Chem.* 12 (2007) 174-179.
3. S. Padilla Mondéjar, A. Kovtun, M. Epple "Lanthanide-doped calcium phosphate nanoparticles with high internal crystallinity and with a shell of DNA as fluorescent probes in cell experiments", *J. Mater. Chem.* 17 (2007) 4153-4159.
4. K. Ganesan, A. Kovtun, S. Neumann, R. Heumann, M. Epple "Calcium phosphate nanoparticles: Colloidally stabilized and made fluorescing by a phosphate-functionalized porphyrin" *J. Mater. Chem.* 18 (2008) 3655-3661.
5. Kovtun, R. Heumann, M. Epple "Calcium phosphate nanoparticles for the transfection of cells", *Biomed. Mater. Eng.* 19 (2009) 241-247.
6. S. Neumann, A. Kovtun, I. Dietzel-Meyer, M. Epple, R. Heumann "The use of size-defined DNA-functionalized calcium phosphate nanoparticles to minimise intracellular calcium disturbance during transfection", *Biomaterials*, 30 (2009) 6794-6802.
7. M. Epple, K. Ganesan, R. Heumann, J. Klesing, A. Kovtun, S. Neumann, V. Sokolova "Application of calcium phosphate nanoparticles in biomedicine", *J. Mater. Chem.*, 20 (2010) 18 - 23.

8. V. Sokolova, S. Neumann, A. Kovtun, S. Chernousova, R. Heumann, M. Epple "An outer shell of positively charged poly(ethyleneimine) strongly increases the transfection efficiency of calcium phosphate/DNA nanoparticles", *J. Mater. Sci.* (in press).
9. X. Zhang, A. Kovtun, C. Mendoza-Palomares, M. Oulad-Abdelghani, S. Facca, F. Fioretti, J.-C. Voegel, D. Mainard, M. Epple, N. Benkirane-Jessel "SiRNA-loaded multi-shell nanoparticles incorporated into a multilayered film as a reservoir for gene silencing", *Biomaterials* (accepted).
10. V. Sokolova, T. Knuschke, A. Kovtun, J. Buer, M. Epple, A. M. Westendorf "The use of calcium phosphate nanoparticles encapsulating Toll-like receptor ligands and the antigen hemagglutinin to induce dendritic cell maturation and T cell activation", *Biomaterials*, 31 (2010) 5627-5633.
11. J. Klesing, S. Chernousova, A. Kovtun, S. Neumann, L. Ruiz, J. M. Gonzalez-Calbet, M. Vallet-Regi, R. Heumann, M. Epple "An injectable paste of calcium phosphate nanorods, functionalized with nucleic acids, for cell transfection and gene silencing", *J. Mater. Chem.* (in press).

7.2.2 Other publications

1. V. Sokolova, G. Kovtun, R. Heumann, M. Epple, "Tracking the pathway of calcium phosphate/DNA nanoparticles during cell transfection by marking with red-fluorescing TRITC-BSA", *Biomaterialien* 7 (2006) 225.
2. V. Sokolova, G. Kovtun, O. Prymak, W. Meyer-Zaika, E. A. Kubareva, E. A. Romanova, T. S. Oretskaya, R. Heumann, M. Epple, "Functionalisation of calcium phosphate nanoparticles by oligonucleotides and their application for gene silencing", *Biomaterialien* 7 (2006) 226.

3. A. Kovtun, V. Sokolova, R. Heumann, M. Epple "Mehrschalige Calciumphosphat-Nanopartikel als biokompatible Träger für Nukleinsäuren", *Laborwelt* 8 (2007) 17-21.
4. S. Padilla Mondejar, A. Kovtun, M. Neumeier, S. Neumann, R. Heumann, M. Epple, "Biokompatible fluoreszierende Calciumphosphat-Nanopartikel zur Transfektion von Zellen", *Biomaterialien* 8 (2007) 154.
5. Kovtun, H. Urch, M. Neumeier, S. Neumann, R. Heumann, M. Köller, M. Epple "Transfizierende Metalloberflächen", *Biomaterialien* 9 (2008) 128.

7.3 Presentations and posters

1. 9th Essen Symposium Biomaterials and Biomechanics: Fundamentals and Clinical Applications, Essen, 05.-08.09.2006, V. Sokolova, A. Kovtun, O. Prymak, W. Meyer-Zaika, E.A. Kubareva, E.A. Romanova, T.S. Oretskaya, R. Heumann, M. Epple, "Functionalization of calcium phosphate nanoparticles by oligonucleotides and their application for gene silencing" (oral presentation).
2. 9th Essen Symposium Biomaterials and Biomechanics: Fundamentals and Clinical Applications, Essen, 05.-08.09.2006, V. Sokolova, A. Kovtun, R. Heumann, M. Epple, "Tracking the pathway of calcium phosphate/DNA nanoparticles during cell transfection by marking with red-fluorescing TRITC-BSA" (poster).
3. 13. Heiligenstädter Kolloquium: Technische Systeme fuer Biotechnologie und Umwelt, Heilbad Heiligenstadt, 25.-27.2006, V. Sokolova, A. Kovtun, W. Meyer-Zaika, I. Radtke, R. Heumann, M. Epple, "Oligonucleotide-functionalized calcium phosphate nanoparticles for antisense strategy" (oral presentation).
4. Joint Summer School: Materials – Synthesis, Characterisation and Properties, Bochum, 08.-14.10.2006, V. Sokolova, G. Kovtun, R. Heumann, M. Epple, "Tracking the pathway of calcium phosphate/DNA nanoparticles during cell transfection by marking with red-fluorescing TRITC-BSA" (poster).
5. Joint Summer School: Materials – Synthesis, Characterisation and Properties, Bochum, 08.-14.10.2006, V. Sokolova, G. Kovtun, O. Prymak, W. Meyer-Zaika, E.A. Kubareva, E.A. Romanova, T.S. Oretskaya, R. Heumann, M. Epple, "Functionalization of calcium phosphate nanoparticles by oligonucleotides and their application for gene silencing" (poster).

6. 2006 MRS Fall Meeting, Boston, USA, 27.11.-01.12.2006, V. Sokolova, A. Kovtun, R. Heumann, M. Epple, "Tracking the pathway of inorganic particles in living cells" (oral presentation).
7. 2006 MRS Fall Meeting, Boston, USA, 27.11.-01.12.2006, V. Sokolova, A. Kovtun, O. Prymak, W. Meyer-Zaika, E.A. Kubareva, T.S. Oretskaya, R. Heumann, M. Epple, "Functionalisation of calcium phosphate nanoparticles by oligonucleotides and their application to gene silencing" (oral presentation).
8. 12th Symposium "Nanostructured Biomaterials: Characterization and Properties", Lutherstadt Wittenberg, 10.-11.05.2007, S. Padilla-Mondejar, A. Kovtun, M. Epple, "Synthesis and application of fluorescent calcium phosphate nanoparticles" (poster).
9. NanoBio-Europe 2007, Münster, 13.-15.06.2007, M. Epple, A. Kovtun, R. Heumann, V. Sokolova, "Calcium phosphate nanoparticles as versatile carriers for DNA and siRNA into living cells" (oral presentation).
10. NanoBio-Europe 2007, Münster, 13.-15.06.2007, A. Kovtun, M. Epple, "Chromatography with substituted calcium phosphates for the separation of nucleic acids" (poster).
11. The Royal Society of Chemistry's 8th International Conference on Materials Chemistry, London, Great Britain, 02.-05.07.2007, V. Sokolova, A. Kovtun, O. Prymak, W. Meyer-Zaika, E. A. Kubareva, E. A. Romanova, T. S. Oretskaya, R. Heumann, and M. Epple, "Surface modification of calcium phosphate nanoparticles and their application for gene transfer" (oral presentation).
12. 10th International Conference of Advanced Materials, Bangalore, India, 8.-13.10.2007, M. Epple, R. Heumann, H. Urch, A. Kovtun, "Bioactive coatings for the in-situ transfection of cells after implantation" (oral presentation).

13. Bioceramics 20: 20th International Symposium of Ceramics in Medicine, Nantes, France, 24-26.10.2007, A. Kovtun, V. Sokolova, O. Prymak, W. Meyer-Zaika, R. Heumann, M. Epple, "Calcium phosphate nanoparticles for cell transfection" (oral presentation).
14. Bioceramics 20: 20th International Symposium of Ceramics in Medicine, Nantes, France, 24-26.10.2007, A. Kovtun, V. Sokolova, W. Meyer-Zaika, R. Heumann, M. Epple, "Calcium phosphate nanoparticles as carriers of oligonucleotides for gene silencing in cells" (poster).
15. Jahrestagung der Deutschen Gesellschaft für Biomaterialien e.V. DGBM, Hannover, 22.-24.11.2007, S. Padilla Mondejar, A. Kovtun, M. Neumeier, S. Neumann, R. Heumann, M. Epple, "Biokompatible fluoreszierende Calciumphosphat-Nanopartikel zur Transfektion von Zellen" (oral presentation).
16. 8th World Biomaterials Congress, Amsterdam, Netherlands, 28.05.-1.06.2008, H. Urch, A. Kovtun, R. Heumann, M. Epple, "Calcium phosphate/DNA nanoparticles can be immobilized on metal surfaces and used for the transfection of cells" (poster).
17. 8th World Biomaterials Congress, Amsterdam, Netherlands, 28.05.-1.06.2008, A. Kovtun, M. Neumeier, S. Padilla Mondejar, R. Heumann, M. Epple, "Synthesis of fluorescent calcium phosphate nanoparticles and their tracking in cell culture" (poster).
18. International Symposium on "Nanotoxicology Assessment and Biomedical, Environmental Application of Fine Particles and Nanotubes (ISNT 2008) Sapporo, Japan 16.-17.06.2008, A. Kovtun, R. Heumann, M. Epple, "Calcium phosphate nanoparticles for cell transfection" (oral presentation).
19. German-Ukrainian Symposium of Nanoscience and Nanotechnology 2008 (GUS), Essen, Germany, 22.-25.09. 2008, A. Kovtun, S. Neumann, R.

- Heumann, M. Epple, "Calcium phosphate nanoparticles as carriers of nucleic acids" (oral presentation).
20. Jahrestagung der Deutschen Gesellschaft für Biomaterialien e.V. DGBM, Hamburg, 20.-22.11.2008, A. Kovtun, H. Urch, M. Neumeier, S. Neumann, R. Heumann, M. Köller, M. Epple, "Transfizierende Metalloberflächen" (oral presentation).
- 21.11th International and Interdisciplinary Symposium "Biomaterials and Biomechanics: Fundamentals and Clinical Applications 2009", 5.-7.03.2009, Essen, S. Neumann, A. Kovtun, I. D. Dietzel-Meyer, M. Epple, R. Heumann, "Size-defined calcium phosphate nanoparticles serve as a superior tool for cellular DNA transfection: Absence of intracellular Ca²⁺ disturbance" (oral presentation).
- 22.60. Mosbacher Kolloquium "Molecular and Cellular Mechanisms of Memory", Mosbach/Baden, Germany, 19.-21.03.2009, S. Neumann, A. Kovtun, I. Dietzel-Meyer, M. Epple, R. Heumann, "Cellular transfection with DNA-functionalised calcium phosphate nanoparticles circumvents disturbance of intracellular calcium levels" (poster).
- 23.2009 MRS Spring Meeting, San Francisco, USA, 13.-17.04.2009, A. Kovtun, S. Neumann, M. Neumeier, H. Urch, R. Heumann, M. Köller, M. Epple, "Nanoparticle-mediated gene transfer from metal surfaces" (poster).
24. BioAmorPhys, Max-Planck Summer School on Amorphous Solids in Physics and Biology, Neuhardenberg, 01.-03.06.2009, K. Ganesan, A. Kovtun, S. Neumann, R. Heumann, M. Epple, "Amorphous calcium phosphate nanoparticles: Colloidally stabilized and made fluorescent by a phosphate-functionalized porphyrin" (oral presentation).
- 25.3rd European Conference on Chemistry for Life Sciences (ECCLS), Frankfurt am Main, 02.-05.09.2009, S. Neumann, A. Kovtun, I. D. Dietzel, M. Epple,

- R. Heumann, "Low intracellular calcium disturbance by transfection with calcium phosphate/DNA nanoparticles" (poster).
- 26.22nd European Conference on Biomaterials, Lausanne, Switzerland, 08.-12.09.2009, A. Kovtun, S. Neumann, M. Neumeier, H. Urch, R. Heumann, M. Köller, M. Epple, "Local gene transfer from nanoparticle-loaded titanium surfaces" (oral presentation).
- 27.11th International Conference on Advanced Materials (ICAM 2009), Rio de Janeiro, Brazil, 20.-25.09.2009, A. Kovtun, S. Neumann, R. Heumann, M. Epple, "Functionalized calcium phosphate nanoparticles: Application for gene transfer" (oral presentation).
- 28.44. Jahrestagung der Deutschen Kolloidgesellschaft, 28.-30.09.2009, Hamburg, M. Epple, A. Kovtun, V. Sokolova, J. Klesing, M. Neumeier, S. Neumann, R. Heumann, "Colloidal stability of calcium phosphate nanoparticles functionalized with nucleic acids for gene transfer into living cells" (oral presentation).
29. IRUN Symposium on Nanotechnology, Krakow, Polen, 08.-09.10.2009, V. Sokolova, A. Kovtun, S. Chernousova, S. Neumann, R. Heumann, M. Epple, "Transfection of cells with multi-shell calcium phosphate-DNA-PEI nanoparticles" (oral presentation).
30. World Conference on Regenerative Medicine, Leipzig, 29.-31.10.2009, V. Sokolova, A. Kovtun, A. Westendorf, J. Buer, M. Epple, "Application of calcium phosphate-oligonucleotide nanoparticles for the activation of dendritic cells" (oral presentation).
31. 2009 MRS Fall Meeting, Boston, USA, 30.11.-04.12.2009, A. Kovtun, S. Neumann, M. Neumeier, H. Urch, R. Heumann, M. Köller, M. Epple, "Transfection of cells from nanoparticle-functionalized metal surfaces" (poster).

32. International Conference on Nanomaterials: Synthesis, Characterization and Applications, Kerala, Indien, 27.-29.04.2010, S. Neumann, Y. Algür, K. Kuteykin-Teplyakov, A. Kovtun, I. D. Dietzel, M. Epple, R. Heumann, "The use of size-defined DNA-functionalized calcium phosphate nanoparticles for transfection: implications for intracellular signalling in health and disease?" (oral presentation).
33. Nanobio Europe, Münster, Germany 15.-17.06.2010, S. Neumann, V. Sokolova, A. Kovtun, S. Chernousova, I. D. Meyer, M. Epple, R. Heumann, "Transfection with calcium phosphate/DNA nanoparticles – impact on intracellular calcium level and further improvements by PEI functionalization" (poster, in preparation).

7.4 Patents

M. Epple, A. Kovtun, V. Sokolova, H. Urch, Deutsche Patentanmeldung DE 10 2007 048 591.5, "Implantat und Verfahren zu seiner Herstellung" (angemeldet 05.10.07).

7.5 Awards

- May 2000 Third place on the regional Biology Olympiad, Kharkiv, Ukraine.
- June 2008 Young Researcher Travel Award of International Symposium on "Nanotoxicology Assessment and Biomedical, Environmental Application of Fine Particles and Nanotubes" (ISNT 2008), Hokkaido University, Sapporo, Japan.
- July 2008 DAAD Award for foreign students, University of Duisburg-Essen, Essen, Germany.
- November 2008 CeNIDE Best Paper Award 2008, Center for Nanointegration Duisburg-Essen, University of Duisburg-Essen, Duisburg, Germany.

7.6 Curriculum vitae

Name: Anna Kovtun

Date of Birth: 02.08.1983

Place of Birth: Kharkiv, Ukraine

- 1990-2000: Middle School Nr. 62, Kharkiv, Ukraine.
 2000-2004: V.N. Karazin Kharkiv National University, Ukraine.
Qualification: B.Sc. in Biology. *Speciality:* Physiology of Animals and Humans.
Title of Diploma thesis: “Modification of cytoskeleton’s proteins spectra of erythrocytes under the influence of cryoprotector PEO-1500, temperature, the variation of ionic power of solutions, and the maintenance of bivalent cations“.
- 2004-2005: V.N. Karazin Kharkiv National University, Ukraine.
Qualification: M.Sc. in Physiology, Teacher. *Speciality:* Physiology of Animals and Humans.
Title of Diploma thesis: “Evaluation of haemolysis changes and state of erythrocytic transport system under the hypertonic conditions“.
- May 2005: Participant of student exchange program at the University of Duisburg-Essen, Essen, Germany (Leonard-Euler program).
- Sept. 2005-
 Dec. 2005 Grant in Institute of Inorganic Chemistry, University of Duisburg-Essen, Essen, Germany.
- Since Jan. 2006: PhD-student in Institute of Inorganic Chemistry, University of Duisburg-Essen, Essen, Germany.

Acknowledgments

I am very grateful to

My supervisor Prof. Dr. Matthias Epple for welcoming me into his group, his guidance and for providing excellent working facilities and fascinating scientific activities,

Prof. Dr. Rolf Heumann for outstanding collaboration and great ideas,

Prof. Dr. Manfred Köller for the assistance with FACS measurements and his critical views,

Dr. Nadia Benkirane-Jessel for a productive collaboration,

Dipl.-Biol. Sebastian Neumann for an excellent collaboration and many conversations and advice,

Dr. Wolfgang Meyer-Zaika for providing TEM images,

Dipl.-Ing. Smail Boukercha for SEM images and friendly conversations,

Dipl.-Chem. Thorsten Peitsch for his help with computer problems and his readiness to correct my German grammar,

Dr. Viktoriya Sokolova for her advice and many friendly conversations,

Dipl.-Chem. Stefanie Kittler for her helpfulness, especially while sharing the office,

Dipl.-Biol. Svitlana Chernousova for critical reading of this work,

All my colleagues in the department for useful advice, helpfulness, friendly conversations and wonderful pastime in and out of the office,

And last but not least, I would like to thank my family and my best friend Olga for being always on my side, for their love, helpfulness and great support.

Hiermit versichere ich, die vorliegende Arbeit mit dem Titel

„Calcium phosphate nanoparticles as carriers of nucleic acids“

selbst verfasst und keine außer den angegebenen Hilfsmitteln und Quellen verwendet zu haben.

Zudem erkläre ich, dass ich die Arbeit in dieser oder ähnlicher Form bei keiner anderen Fakultät eingereicht habe.

Essen 12.10.2009

Anna Kovtun